UNIVERSITY OF NAIROBI

PREDICTING SERVICE LIFE OF PLASTIC LINING FOR WATER RESERVOIRS USING VISCOELASTICIY

By

Duncan Onyango Mbuge, B.Sc., M.Sc. (Agricultural Engineering)

A thesis submitted in partial fulfilment of the requirement for the degree on Doctor of Philosophy, University of Nairobi

August 2008

DECLARATION

I declare that this is my original work and has not been presented for a degree at any other University

Duncan Onyango Mbuge _____ 26th March 2009

(Signature) (Date)

This thesis has been submitted for examination by our approval as University Supervisors

Prof. L.O. Gumbe _____ 26 March 2009

(Signature) (Date)

Prof. G.O. Rading _____ 01-04-2009

(Signature) (Date)

ABSTRACT

The use of High Density Polyethylene (HDPE) lining in seepage prevention in small ponds had previously been identified as having potential to drastically reduce the cost of water storage. However, in order to be able to make it acceptable to end users, it is necessary to determine its lifespan when exposed to tropical climates with high day and low night temperatures as well as other degrading agents. The main objective of this research study was therefore to determine the service life of HDPE lining when exposed to natural degradation in tropical climates using viscoelastic models. The basic material properties were determined for fresh and naturally degraded specimens exposed to natural degradation for three, four and seven years. The tensile strength, density and maximum strain ranged from 12 MPa, 1290 kg/m3 and 3.5 mm/mm respectively for fresh specimens to 25 MPa, 1070 kg/m^3 and 1.3 mm/mm respectively for specimens degraded naturally for 7 years. A test rig for determination of tensile creep was developed for use in an oven to allow readings to be taken without opening the oven in the course of experimentation. Accelerated techniques of predicting the long term properties of the material were identified. In particular, incubation of specimens in Igepal® and exposure to low wavelength light (254nm) to simulate the effect of hydrolytic degradation and photo-degradation respectively was analysed. The Findley Power Law was used to build a model for prediction of the material behaviour at elevated temperature in both short term and long term applications. Time-Temperature Superposition (TTSP) was also used to develop master curves for prediction of long term properties at a reference temperature of 30°C. Micrographs were also presented to track the changes that took place in the

material during the aging process under different conditions. Naturally degraded specimens were collected from the field and tested in tensile creep. From the results, a simple model was developed on the basis of specimens collected from the field that had a well documented history. This model allows for estimation of the service life of the HDPE lining, and only requires the determination of maximum strain at a given temperature. From this model, being an exponential decay equation, it was also concluded that the degradation of the material takes place in the first few months of installation and any shading needs to be done in the initial stages otherwise, it may not be viable in the latter stages of use after exposure to the degradation agents. It was further concluded that the welded joint was the most serious factor undermining the service life of the lining material under tensile creep and that welding of this particular material needs to be carried out above 176°C for hot air welding and at a knife temperature of 400°C for knife welding at a pressure of 0.3 MPa for a dwell time of 10s, for the weld to achieve the highest level of bonding. It was also concluded that alternating temperature had a more damaging effect on the lining material than elevated temperature in the same range and this showed that the lining is likely to suffer more damage in the tropics than in other climates.

ACKNOWLEDGEMENT

First and foremost, I give thanks and honour to God through whom everything is possible. The completion of this work has also been the consequence of voluntary investment of resources by many dedicated people. For those who spent their time and mental resources on this project, I would like to say a special thank you.

I would like to thank my supervisors Prof. L.O. Gumbe and Prof. G.O. Rading for their willingness to assist me with the ideas, critique and encouragement necessary to undertake this work. It is impossible to thank these gentlemen enough in a few paragraphs.

I would also like to thank the University of Nairobi for offering me a fees waiver and DAAD for offering me a scholarship to undertake research.

I am grateful to the Department of Environmental and Biosystems Engineering, particularly the Chairman Prof. E.K. Biamah for his encouragement and accepting to host me. Special thanks go to the Department of Mechanical Engineering and Manufacturing Technology where I carried out most of the lab work. I should like to single out Messers Kahiro, Njue and Aduol from Department of Mechanical Engineering and Manufacturing Technology as well as Mwachoni, Kariuki, Muliro, AnnRose and Mathenge from Environmental and Biosystems Engineering without whom I may not have obtained any data.

DEDICATION

This work is dedicated to my wife Nereah and Children Rebecca and Mark, for their support and understanding

TABLE OF CONTENTS

LIST OF TABLES

LIST OF FIGURES

LIST OF PLATES

LIST OF ABBREVIATIONS

ASTM	American Society for Testing Materials
DSC	Differential Scanning Calorimeter
EMMA	Equatorial Mount with Mirrors for Acceleration of solar degradation
EMMAQUA	Equatorial Mount with Mirrors plus water spray for Acceleration of solar degradation
ESC	Environmental Stress Cracking
HDPE	High Density Polyethylene
LDPE	Low Density Polyethylene
LLDPE	Linear Low Density Polyethylene
PE	Polyethylene
TTSP	Time-Temperature Superposition
UHMWPE	Ultrahigh Molecular Weight Polyethylene
UV	Ultraviolet radiation

LIST OF SYMBOLS

A	Area
a_T	Shift factor in Time-Temperature Superposition
D	Creep compliance
E	Energy of activation of the reaction in the Arrhenius equation
$\varepsilon_e(\sigma, T)$	Elastic (instantaneous) deformation
$\varepsilon_p(t, \sigma, T)$	Plastic (irreversible) deformation
$\varepsilon_v(t, \sigma, T)$	Viscoelastic (reversible) deformation
$\varepsilon(T,t)$	Total time and temperature dependent strain
ε_c	Creep strain
$\varepsilon_c(T)$	Creep strain at the end of creep period
ε_{max}	Maximum strain
ε_o	Stress-dependent initial elastic strain
$\varepsilon_r(t)$	Residual strain
ε_t	Total time-dependent strain
ε_T	Tensor of thermal expansion
F_r	Fractional recovery,
I	Average intensity of the light source
k	Rate of reaction in the Arrhenius equation
m	Stress-dependent and temperature-dependent coefficient
m_{RT}	Stress-dependent and temperature-dependent coefficient at reference temperature

m_T	Stress and temperature-dependent coefficient at elevated temperature
n	Stress-independent and temperature independent material constant
n_{RT}	Stress independent material constant at reference temperature
n_T	Stress independent material constant at elevated temperature
P	Load
r^2	Coefficient of Determination
R	Gas constant
T	Temperature
t	Time
T_g	Glass transition temperature
t_d	Expected lifetime
t_p	Period of each loading cycle
T_{ref}	Reference temperature
σ	Stress
Z	Constant in the Arrhenius equation

CHAPTER 1: INTRODUCTION

1.1 Background

It has been predicted by UNEP (2003) that the next world war will be over water. In the world today, "two billion people are dying for water" - the theme for the year 2003 World Environment Day (UNEP, 2003). That is, two billion people worldwide are searching for potable water. It is estimated that water use has more than tripled since 1950. However, there is adequate water in the world. As a matter of fact three quarters of the world is covered by water, yet potable water is in shortage. As a consequence, one person in six lives without access to safe drinking water. Water related diseases kill a child every eight seconds and are responsible for 80 percent of illnesses and deaths in the developing world (UNEP, 2003; Tolba et al, 1992). Many farmers in the world are unable to break-even from rain-fed agriculture and do not engage in irrigated agriculture because of the high cost of water supply. The world needs to learn how to value water since water problems are related more with mismanagement rather than scarcity (UNEP, 2003).

The most important factor that undermines the availability of water is the prohibitive cost of water storage structures. In systems that depend on rainwater harvesting for example, water security and availability lies squarely on how much water one can store (Onyango, 2003). This is because rainfall patterns are such that it rains unexpectedly, and the total seasonal rainfall is concentrated in two to three week episodes. Also, the commencement of the rains is unpredictable. It is therefore important for water users to collect as much water as they can during these short rainy seasons and store it for use in times when there is no rainfall. This calls for large water storage structures, which most water users cannot afford due to their high costs (Onyango, 2003).

It is in recognition of this that there is need to develop cheaper alternatives for water storage. Already a lot of work has been done in this line which has led to the development of new products such as plastic tanks. A more recent introduction to Kenya is the plastic lined water reservoir for storage of water for both domestic and agricultural use. Using this technology, it is possible to store water at about one tenth of the cost of the conventional water storage structures such as ferro-cement tanks and plastic tanks. It also offers a unique opportunity to make collapsible tanks, which are vital in refugee camps and other conditions, which involve temporary settlement (Onyango, 2003).

1.1.1 Introduction to Polyethylene

Polyethylene (PE) is a semi-crystalline thermoplastic material that results from the polymerization of ethylene. Hence the monomer has the formula of ethylene (C_2H_4), although the double carbon to carbon bond (C=C) in an ethylene monomer is transformed into a single bond single carbon to carbon bond (C-C) in the polymer. The polymerization of ethylene results in a straight chain, high molecular weight hydrocarbon with the formula $(-CH_2-CH_2-)_n$ which can be represented as in Figure 1.1 (Earthodyssey, 2007; Crawford, 1998)

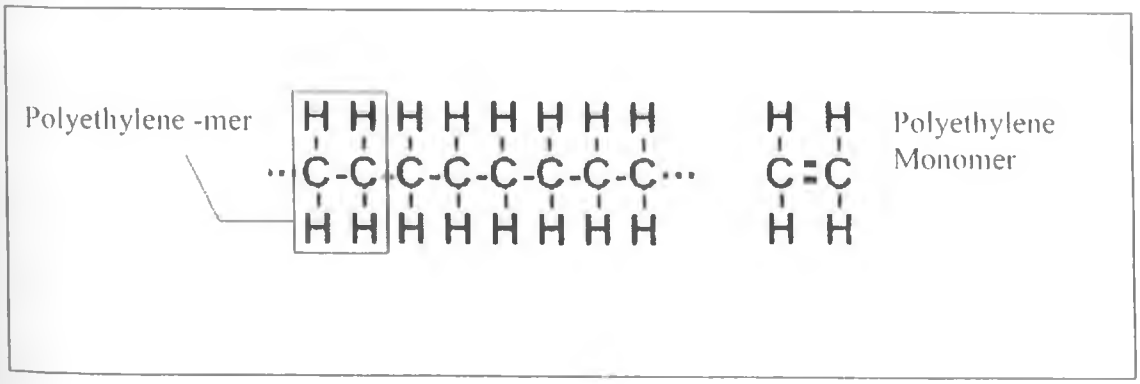

Figure 1.1: Structural formula of Polyethylene

The polyethylenes are classified as follows, according to the relative degree of branching (side chain formation) in their molecular structures, which can be controlled with selective catalysts.

1. Ultra High Molecular Weight Polyethylene (UHMWPE)
2. Low Density Polyethylene (LDPE)
3. Linear Low Density Polyethylene (LLDPE)
4. High Density Polyethylene (HDPE)

The mechanical and thermal properties of polyethylene significantly depend on the degree of crystallization, molecular weight and branching. The melting point and glass transition point vary strongly with the polyethylene type. Like other polyolefins, the polyethylenes are chemically inert. Strong oxidizing agents will eventually cause oxidation and embrittlement. They have no known solvent at room temperature. Aggressive solvents will cause softening or swelling, but these effects are normally reversible (Netzsch Applications Laboratory Newsletter, 2005).

Low-density polyethylene (LDPE) has more extensive branching, resulting in a less compact molecular structure. High-density polyethylene (HDPE) has minimal branching, which makes it more rigid and less permeable than LDPE (Netzsch Applications Laboratory Newsletter, 2005).

1.1.2 High-Density Polyethylene (HDPE)

A linear polymer, High Density Polyethylene (HDPE) is prepared from ethylene by a catalytic process. The absence of branching results in a more closely packed structure with a higher density and somewhat higher chemical resistance than LDPE. HDPE is also harder and more

opaque than LDPE. It has a melting point that ranges from 130°C to 137°C, a maximum continued use temperature of 65°C and a glass transition temperature of between -120°C to -125°C. It has a density of about 0.941 - 1.45 g/cm^3, a coefficient of thermal expansion of 100 - 220 x 10^{-6} per °C, a tensile strength of 15 - 40 MPa, a flexural modulus of 1.2 GN/m^2, Young's modulus of 0.7 GN/m^2 and Brinnel hardness of 2 and an elongation of 150%-500% at failure (Sigmaaldrich, 2008; Netzch, 2005; Corneliussen, 2002; Crawford, 1998; Idol and Lehman, 2004).

Traditionally, Ziegler-Natta catalysts have been used to produce polyethylene. These catalysts have the disadvantage of being multi-sited and produce polymers with short, medium and long molecules. With the advent of new catalysts called metallocenes, which are single-site catalysts, the polymer molecules produced tend to be all the same. This results in a narrow melting range and free flowing material even at low densities (Crawford, 1998).

1.1.3 High Density Polyethylene (HDPE) Sheeting

This is the material under study in this research study. It is used for lining water reservoirs in permeable soils. It is black in colour, mainly due to additives. High density polyethylene sheeting does not require soil cover unlike the other materials which are readily degraded if not covered. Installation is generally undertaken using fusion-weld joining equipment. Thickness range is 0.4 to 2.5 mm. It would be used on sites where puncturing of cheaper products cannot be avoided or where steep slopes (steeper than 2:1) preclude the use of other products (Swann, 1996).

HDPE is the most widely used geomembrane in the world and is used more commonly internationally due to its availability and relatively low material cost. HDPE is an excellent product for large dam applications that require UV and Ozone resistance, chemical resistance or high-quality installations. This product is delivered in large rolls and may be heat welded in the field by trained technicians. This product has been used in landfills, waste water treatment lagoons, animal waste lagoons, mining applications and for water storage (Swann, 1996).

1.2 Problem Statement

The use of plastic lined reservoirs has not achieved the intended impact due to scepticism as to how long the plastic can last when installed in the sunny tropical climate, with high day temperatures and low night temperatures and considering the susceptibility of plastics to solar and thermal degradation. Many would-be users of this technology would like to know its service life when used in tropical conditions before investing in it. Also, it is necessary to determine the strength of the product so as to set safety factors for its use under tropical conditions. This problem calls for a method that can be used to determine the expected service life of the plastic liner under load using relatively short experiments. It is for this reason that this research study investigated the service life of HDPE plastic lining.

1.3 Justification

This research study was a response to the need to determine the factors that limit the lifespan of the material under study when exposed to tropical climate. This research study contributed in part to the development of a model to determine the effect of factors that limit the service life of the plastic liner, such as solar radiation, hydrolytic degradation, alternate heating and cooling

(which simulates the high day temperatures and low night temperatures in the tropics) and elevated temperature. Being a polymer, it was also expected that the plastic liner would be subject to creep and recovery due to alternate filling and emptying of the reservoir. Therefore the effect of creep and recovery was also investigated. The study was expected to develop a model that would predict in a short time and using simple measurements the service life of HDPE plastic liner. This would not only contribute to the quick and easy determination of the properties of the material under study but would also provide the basis for testing other materials used in a similar manner.

1.4 Objectives

The broad objective of this research study was to determine the long term properties of High Density Polyethylene (HDPE) lining material so as to estimate the useful lifespan of the material under natural tropical conditions.

The specific objectives were:

1. To determine the basic properties and the creep rupture curves for the plastic lining material.
2. To model the service life of the material in creep and recovery using Time-Temperature Superposition for elevated temperature and also to model the effect of alternating temperature, aging by hydrolytic degradation and degradation under UV radiation.
3. To verify the models using naturally degraded specimens including comparison of microscopic surface images.
4. To determine the effect of welding HDPE on the expected lifespan.

CHAPTER 2: LITERATURE REVIEW

2.1 Aging

When polymers are exposed to the environment, the original properties of the material change in a process called aging. Material aging may translate to changes in components, which may weaken the material and cause the component in which the material has been used to be removed from service. Therefore, studying and understanding the aging process in polymeric materials is critical to their proper design, construction and safe operation, (Gates and Grayson, 1998).

Polymers with a carbon-carbon backbone (such as polyethylene) are easily and readily degraded by hydrolysis and through biodegradation than those that contain functional groups in the polymer chain notably polyesters, polyamides and polyurethanes. Polymers with a carbon-carbon backbone begin to degrade once they are oxidized (Grassie and Scott, 1985).

The potential long-term serviceability of materials refers to the maintenance of performance above a threshold level that is regarded as acceptable. Two aspects can be distinguished with regard to long term serviceability of materials:

(i) Stability of a material or composite of materials, that is, their resistance to environmental factors such as oxygen, ozone, moisture, heat and light, which primarily bring about chemical changes.

(ii) Durability which is largely the physical resistance to change with respect to the stress and strain of use (Feller, 1994).

The phenomenon of aging described above is different from what is called physical aging in many references that deal with viscoelasticity. However, these two phenomena are often confused and it is important to distinguish between them. Normally plastics exhibit rubbery behaviour during which they are flexible and tough. However, there is a certain temperature called the glass transition temperature (T_g) below which the material behaves like glass and becomes hard and rigid (Crawford, 1998).

When a polymeric material is annealed above its glass transition temperature (T_g) and then quenched below T_g, it does not immediately achieve thermodynamic equilibrium. Instead the material evolves towards thermodynamic equilibrium (see Figure 2.1).

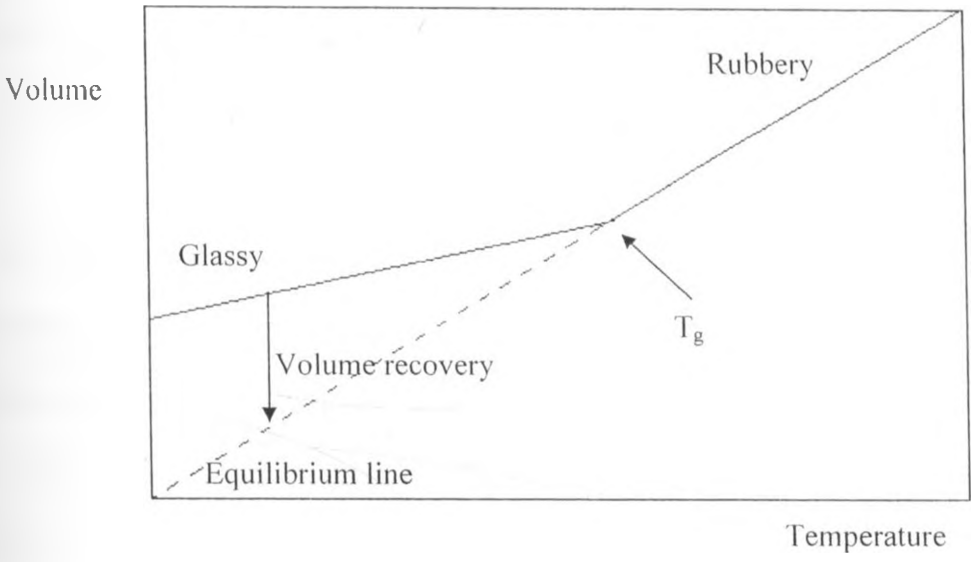

Figure 2.1: Schematic illustration of the volume-temperature response of a polymer (O'Connell and McKenna, 1997)

This phenomenon is known as physical aging and it is accompanied by an increase in stiffness, yield stress, density, and viscosity. Also there is a decrease in creep and stress relaxation rates and flexural strength (Barbero and Michael, 2003). The modelling of properties below the glass transition temperature (T_g) is done by use of Time-Aging Time Superposition, where aging time refers to the time a material exists below the glass transition temperature (O'Connell and McKenna, 1997).

Aging as a result of degradation on the other hand involves external natural or environmental factors acting on the material while physical aging is an internal change in material properties as the material attempts to regain equilibrium. Physical aging only occurs below the glass transition temperature T_g. Above the transition temperature polymers do not exhibit this phenomenon. The aging that is used in this research study is aging due to environmental factors only since the T_g temperature for polyethylene is -120°C and is way below the temperatures at which the product is normally used (Beckmann *et al*, 1997; Veazie and Gates, 2004)

2.1.1 Accelerated Aging

Most of the material degradation takes place over long periods of time and it is not feasible to wait many years for materials to be degraded so as to study the mode of degradation. Therefore, to investigate material properties associated with aging calls for accelerated testing methods (Gates and Grayson, 1998). Accelerated aging is the process required to accelerate a specific mechanism or mechanisms relative to a baseline aging condition; thereby resulting in the material reaching the same aged end-state as a real-time aged material, but in less time (Gates and Grayson, 1998).

Verified accelerated aging methods are needed to provide guidance for materials selection and to accurately assess aging of new materials. The following three terms are of particular importance in defining accelerated testing (Feller, 1994):

1. Environmental stress factor: Specific environmental conditions to which a material is exposed such as heat, moisture and mechanical load.
2. Critical degradation mode: The degradation mechanism that results in a significant loss in any important bulk physical property of the material system when exposed to environmental stress factors inside the limits of the use-environment.
3. Accelerated aging: As previously defined.

Only by understanding how each aging mechanism affects a given material system can it be determined if that aging mechanism can be properly accelerated. In the simplest case, aging is associated with a single mechanism, in which case acceleration of this mechanism will allow meaningful accelerated aging methods to be developed. However, in real life, the aging process normally involves several different mechanisms that may or may not act synergistically, complicating the problem significantly (Gates and Grayson, 1998).

Accelerated-aging tests, cited in the approximate order of the ease with which they can be achieved are carried out for three major purposes (Feller, 1994):

1. To establish in a conveniently short time the relative ranking of materials, or physical combinations of materials, with respect to their chemical stability or physical durability.

2. To estimate or "predict" potential long-term serviceability of material systems under expected conditions of use.
3. To elucidate the chemical reactions involved (the "mechanism" of the degradation) and the physical consequences thereof. An important facet of this effort is the disclosure of the overall pattern of deterioration, that is, whether the processes accelerate in time, whether there is an induction period, or whether a number of distinct stages are observable before failure occurs. The ultimate objective of this third area of investigation is the development of techniques that can monitor the extent of degradation and methods by which the useful lifetime of materials can be extended.

2.1.2 General Procedures for Conducting Degradation Analysis

The suggested procedure for conducting degradation analysis is outlined in Gates and Grayson, (1998) as follows:

a. Identify material by class (such as thermoplastic, thermoset)
b. Identify mechanism to evaluate (such as thermal stability and cracking)
c. Choose an environmental stress factor for aging
d. Conduct aging experiment within limits of the chosen environmental stress factor using established methods
e. Perform post-aging tests with indicators sensitive to changes in material performance and compare results to un-aged values

This is the procedure that was followed in this research study.

2.1.3 Mechanical Degradation

Mechanical degradation mechanisms are irreversible processes that are observable on the macroscopic scale. These degradation mechanisms include surface cracking, delamination, and inelastic deformation; and thus have a direct effect on engineering properties such as bulk stiffness and strength (Gates and Grayson, 1998).

2.1.4 Aging by Thermal Degradation

Feller (1994) observes that thermal degradation needs oxygen to proceed. This is because, the highest temperature to which a plastic material may be exposed outdoors (76°C) does not supply sufficient thermal energy (280–360 kJ mol^{-1}) to cause bond cleavage in commercial polymers. The strengths of C-C and C-H bonds that make up most polymers are approximately 420 and 340 kJ mol^{-1} respectively. Thus, although temperature is important as a rate-controlling parameter in many of the degradative processes (such as oxidation and hydrolysis), polymer degradation by pure thermal energy is not a critical factor in weatherability studies. Purely thermal degradation is often called thermolysis, thermolytic, or pyrolytic degradation and in these processes, oxygen is not involved.

However, in ordinary thermal aging tests, one usually has in mind thermo-oxidative deterioration; that is, reactions induced by thermal energy in the presence of and with the participation of oxygen but in the absence of visible and near-ultraviolet radiation. This is the meaning of thermal degradation that was adopted in this research study.

Inevitably, the samples are almost always also exposed to atmospheric humidity during testing. As noted by Feller (1994), in such tests there is always a question concerning whether water partakes in the process or whether water is absolutely necessary for a particular reaction to take place. However, Feller (1994) notes that, in the practical world of thermal accelerated-aging testing, it has often been the case that the concentration of water in the system is not monitored. Instead it is usually allowed to seek some ill-defined level dependent upon the temperature of the sample or physical system and upon the condition of humidity in the ambient atmosphere. In this research study, the humidity during the period of tests was recorded for the sake of repeatability of thermal degradation tests in future. However, the role of water, acting singly is discussed under hydrolytic degradation.

In precise studies, a distinction has to be made between three processes: purely thermal (pyrolytic), thermo-oxidative, and thermo-hydrolytic degradation. These aspects of deterioration can be isolated by carrying out studies under a vacuum (or inert gas), in oxygen (or air), and in the presence or absence of water vapour. Such practice can lead to valuable insights. For example, Hsuan (2003) compared the results of environmental stress cracking in water and in air and obtained a significant difference between the two degradation environments.

Grassie and Scott (1985) have presented two ways by which thermal degradation reactions normally occur:

1. De-polymerization – Breaking of the main polymer chain backbone so that the resulting products are similar to the parent material in the sense that the monomer units are still distinguishable (and similar to the parent chain).

2. Substituent reactions – Here the substituents attached to the backbone of the polymer molecules (and not the backbone itself) are altered so that the chemical nature of the repeat unit (-mer) is changed although the chain may remain intact. The volatile products formed are quite different from the monomer.

Elevated temperature aging in polymers in the absence of oxygen can also lead to changes in material properties due to additional cross-linking and/or chain scission. Generally, thermoset systems initially tend to embrittle during purely thermal aging. Depending upon thermoset chemistry, these systems may either continue to embrittle or start to degrade significantly. Indicators that are useful for tracking thermal degradation are much the same as for thermo-oxidative degradation. These include initial weight loss of a polymer exposed to a purely thermal environment, changes in colour, surface texture, and crack density, changes in the glass transition temperature and changes in mechanical properties such as tensile strength, compressive strength, and stiffness (Gates and Grayson, 1998).

2.1.5 Aging by Photo-degradation

In the absence of light, most polymers are stable for very long periods of time at ambient temperatures. Sunlight accelerates the rate of oxidation. The rate of oxidation may also be increased by industrial pollutants such as nitrogen oxides as well as sulphur oxides (Gates and Grayson, 1998).

The wavelength of radiation from the sun which reaches the earth's surface extends from the infra-red (greater than 700 nm), through the visible spectrum (400 – 700 nm) into the ultra-violet

(less than 400 nm) with a minimum value of about 300nm depending on atmospheric conditions. The energies of 700, 400 and 300 nm photons are approximately 170, 300 and 390 KJ mol^{-1} respectively. The strengths of C-C and C-H bonds are approximately 420 and 340 KJ mol^{-1} respectively. Thus, the energy of the quanta of the ultraviolet (UV) and of the visible light is sufficient to break chemical bonds and shorter wavelengths will be more effective (Grassie and Scott, 1985).

Light acts on plastic in two distinct ways namely photolysis and photo-oxidation. The first step in both cases is the photolytic formation of free radicals by bond scission. In the second step, photolysis leads to the un-saturation in the polymer while photo-oxidation leads to the production of aldehydes, ketones and carboxylic acids (Grassie and Scott, 1985).

2.1.6 Aging by Hydrolytic Degradation

The degree of plasticity in a polymer will increase due to long-term exposure to moisture. Exposure to moisture has two important effects:

1. Diffusion of water into the sample

Water is absorbed, usually according to Fick's law and firstly, occupies the voids of the material and finally causes changes in the resin (Eleni, 1998). Gates and Grayson, (1998) add that depending upon the diffusion coefficient of water in the polymer system, significant differences in water concentration can exist from one region of the sample to the next, imposing additional stresses on the system.

2. Effects of hydrolysis on polymers

The diffusion of water into resin leads to a distribution of swelling stresses that can crack and fail the resin, or cause hydrolysis and physical aging. Changes in the resin can be either reversible (plasticization and swelling) or irreversible (too much swelling, hydrolysis and micro-cracking). The chemical composition appears to influence the equilibrium content of water; the larger the content of water, the greater can be the hydrolysis and the swelling stresses (Eleni, 1998).

Moreover, another irreversible effect of water is the creation of a secondary cross-linking in the matrix, due to a specific kind of hydrogen bond that takes place between resin and water molecules. This phenomenon depends on the chemical structure of the resin, the temperature and the time the material is exposed to water and makes the material stiffer. Finally, the diffusion of water into materials may lead to the leaching of some resin molecules of low molecular weight which also leads to an irreversible stiffening of the polymer. In addition, salted water has been shown to have similar effects as distilled water, although molecules of salt inhibit its diffusion by blocking the paths in the polymer which would allow water get into the material. That is why distilled water is absorbed to a greater extent compared to salted water (Eleni, 1998).

Hsuan (2003) compared the results of environmental stress cracking in water and in Igepal® and obtained a good correlation between the two degradation environments. Igepal® is a non-ionic surfactant that acts on plastic in a similar manner as water, except that it does so at an accelerated rate. The slopes of the brittle curves in 10% Igepal® and water were very similar, suggesting that test specimens failed under a similar mechanism. The 10% Igepal® solution can shorten the failure time by a factor of 0.58 in comparison to water.

ASTM D1693 (2007a) uses Igepal® in stress cracking to accelerate hydrolytic degradation. It is for this reason that in this research study, accelerated hydrolytic degradation was effected by incubation in Igepal® as explicitly explained in the materials and methods section.

McKenna, (2003) and Gates and Grayson, (1998) suggest that the net result of the various aging agents acting on the material under study should be established by performing individual aging tests separately and obtaining the net effect by modeling. These results are then compared with materials of the same type collected from the field so as to validate the model produced.

2.1.7 Effect of Alternate Heating and Cooling

Kay *et al*, (2007), have given a detailed account of the influence of alternating temperature on polymeric materials. A temperature increase usually leads to a dilation of the material and chain reorganization processes such as chain relaxation, while a temperature decrease leads to a contraction. If the material deformation is restrained, thermal stresses are then built. In monolithic sheet-like geosynthetic materials (such as the type of material used in this research study) thermal contraction or dilation typically leads to a change in the overall dimension of the panel, creating wrinkles when the temperature increases, or creating a stress when the temperature decreases.

This problem may be handled at the construction stage by installation and welding of the geomembrane panels at relatively low temperatures. Other materials with a higher wall thickness, when exposed to sudden changes in temperature, can also be exposed to a temperature

gradient within their thickness. Depending on the thermal dilation coefficient of the polymer and its stiffness, this can lead to the introduction of a stress profile in the material. Ultimately, these stresses can influence aging of the material using one of the other degradation processes described in this section.

The junction of two different materials (that is, old / new geomembrane or prefabricated penetration structure / geomembrane) have to be considered as critical locations on a construction project with regard to a thermally induced failure, especially if the materials are expected to be directly exposed to thermal cycles (such as hot weather during the day and cold weather during the night) on a long term basis. One of the key items to be considered is the coefficient of thermal expansion of materials (Kay *et al*, 2007).

2.1.8 Environmental Stress Cracking (ESC)

Crawford (1998) defines environmental stress cracking as brittle cracking which occurs when a material is in contact with certain substances (or in a specific environment) whilst under stress. The stress may be applied externally, in which case it can be controlled. However, the more common source are internal or residual stresses introduced during processing. Most organic liquids promote ESC in plastics and sometimes even liquids that may not be chemically aggressive can promote it.

Peggs and Kanninen (1995) offer a more insightful account and assert that environmental stress cracking is a lubrication effect allowing the tie molecules to become disentangled more easily. Stress cracking is a synergistic function of applied stress, temperature and many material

parameters (e.g. molecular weight, molecular weight distribution, comonomer type and content, and crystallinity) and cannot yet be predicted. Peggs and Kanninen (1995) add that stress cracking occurs in many plastics but does not occur in polyethylene (the subject of this study) and polyvinyl chloride. In HDPE components, although the stress crack is not associated with any apparent adjacent material deformation, the fracture face itself provides evidence of ductility on a microscopic scale. It is important to recognize that under the conditions during which stress cracking occurs, and during subsequent room temperature testing, the material itself shows no conventional evidence of embrittlement. The material does not become brittle; it simply displays the appearance of brittleness (Peggs and Kanninen,1995).

Other specialized research studies have however shown that the first stress cracks in HDPE geo-membranes were observed along the edges of extruded fillet and lap seams, initiating in the top surface of the lower sheet. Cracking occurred predominantly in the upper half of side-slopes of uncovered liners used for impoundment of liquids. A number of factors were found to contribute to such failures:

- Use of resins with low resistance to cracking
- Stresses induced by restrained thermal contractions at low ambient temperatures
- Overheating seams (initially, or by repair seaming) or spot welding
- Mechanical damage
- Stresses induced by lack of support at corners
- Hard particle impingement
- Impact loading
- Chemical environment.

Problems are reported to have occurred from stones and other sub-grade debris pressing against the geo-membrane. Problems have also occurred when geo-membranes have been placed in 90° corners and against rough sub-grades. Stress cracking failures have occurred after 6 months to 10 years of service. Many of the seam cracking problems were simply solved by inserting a compensation panel of HDPE that eliminated the contraction stresses in the geo-membrane. Shattering failures in geo-membranes, unlike in pipes, have been frequently observed, and occur when the ambient temperature drops very quickly or when the liner suffers an impact force (Peggs and Kanninen, 1995).

2.1.9 Equatorial Mount with Mirrors for Acceleration

The British Plastics Federation (1981) describes two methods for determination of the progression of weathering of plastics under exposure to the sun called Equatorial Mount with Mirrors for Acceleration denoted as EMMA and one with mirrors plus water spray denoted as EMMAQUA. Both methods involve the selection of places with sunshine throughout the year such as Phoenix, one of the few areas in the world which receive on the average, more than 4000 hours sunshine a year (compared with the UK range of 1,000 to 1,400 hours). If specimens are so mounted on exposure that they are normal to the direct rays of the sun all day then they will receive more total solar radiation than statically mounted specimens.

The method of mounting specimens such that they follow the sun is known as an Equatorial Mount. The ten mirrors on the EMMA are a special finish aluminium and they are claimed to reflect from 70% to 80% of the ultra violet radiation and about 85% of the total solar radiation. Each machine has a guidance system, powered by solar energy, which keeps the mirrors facing

the sun at 90° all day. Blowers on each machine force air over and under the samples so that their surface temperatures are about the same as they would be if they were exposed on conventional racks at 45° facing the equator. In EMMAQUA, two spray schedules are normally used. Schedule A is the standard spray condition and schedule B is an experimental spray cycle which is claimed to provide a better correlation with weathering data obtained from exposure sites in Florida.

The specimens exposed on the "accelerating" machines (EMMA or EMMAQUA) are normally withdrawn from exposure after periods of 2, 4, 6, 8, and16 weeks. The specimens exposed on the static 45° racks were withdrawn after periods of 4, 7, 13, 26 and 52 weeks. These periods were based, in part, on the previous trial results and also in the expectation that the specimens on static exposure would take longer to show the effects of degradation. Specimens are normally examined for colour change, loss of gloss, cracking and chalking.

2.1.10 Analysis of Welded and Adhesive Joints

Welding in polymers is done in order to produce seals or joints of sufficient strength to survive the work environments. When these polymer surfaces are brought into intimate contact and are partially molten, a bond is achieved. In order to achieve a realistic bond, the surfaces are pressed together for a period of time sufficient for the polymer chains to diffuse across the interface and form connecting bridges. The formation of these bridges is a function of the material being welded and at a given thickness is a function of the material composition, average molecular weight, molecular weight distribution, and thermal conductivity (Aithani *et al*, 2006).

A weld seal is usually obtained by sealing like materials together. Weld seals are based on obtaining the strongest seal such that the material fails before the seal. The method of sealing, in particular how heat sealing is achieved, can be carried out by using different techniques like jaw-type bar sealers, rotary sealers, band rotary sealers, impulse sealers, bead sealers, hot knife, or side weld sealers. The basic process involves the welding of two polymer films when forced into intimate contact while they are in at least their semi-molten state. The two main sealing parameters that affect the heat seal quality are the interfacial temperature and sealing time. Therefore, in order to assess effectiveness of a welded joint in a polymeric material, it is very important to determine the interfacial temperature and heat sealing time that will result in a desirable seal. Many instruments have been developed, but no instrument or technique is capable of assessing these conditions yet (Aithani, *et al*, 2006).

The guiding principles of creating welded joints have been presented in part by Aithani *et al* (2006). They stated that when two pieces of a plastic film are heat sealed, there is an inflection point in the sealing time–temperature profiles of the materials. The inflection point occurs at a temperature below the melting point of the materials as measured by the Differential Scanning Calorimeter (DSC) technique. Aithani *et al* (2006) also found that pressure has limited effect on the sealing properties of the sealed films. The highest peel seal strength is achieved at a temperature near the fusion point. Seals made above the fusion point result in a weld seal that is not separable by the peel test.

Illinois Tool Works (2007) have presented three main design guidelines that should be considered when designing welded or adhesive joints as:

1. Maximize Shear and minimize peel and cleavage
2. Maximize compression and minimize tensile pull
3. Joint width is more important than overlap length and as a general rule it would be more feasible to increase the joint width rather than the overlap length.

Adhesives have been used successfully in joining plastics. However, the use of adhesives for joining HDPE sheets rather than welding is deemed by Illinois Tool Works (2007) and Salemi (2007) as difficult, unsuccessful or complicated. Because of their non-polar nature, polyethylene requires an oxidation treatment using flames, plasma treatment, or chemical etching to enhance the adhesive bond (Illinois Tool Works, 2007). Salemi (2007) has listed HDPE as one of the hard-to-bond plastics alongside LDPE, polypropylene and Teflon. The use of adhesives for joining HDPE was therefore not considered in this research study.

2.2 Long term performance of polymers

In the short term, the description of stress-strain behaviour is similar to that of metals, but a very important consideration for polymers is that the mechanical properties depend on the strain rate, temperature, and environmental conditions (Baragiola, 1999).

High Density Polyethylene (HDPE) was idealized as a homogeneous, isotropic and linearly viscoelastic continuum (Gumbe, 1993). As a homogenous material the material was considered to have uniform properties throughout. Hence, the properties are not functions of positions in the body. It was considered to be isotropic since it has properties that are the same in every direction

at a point within the body. Therefore, the properties are not functions of orientation at a point in the body, (Gumbe, 1993).

To obtain useful relationships, the small cube in Figure 2.2 was considered to be a point on which equal forces ΔP act in all directions, presented in the rectangular Cartesian coordinate system in three dimensions, (Chung, 1988)

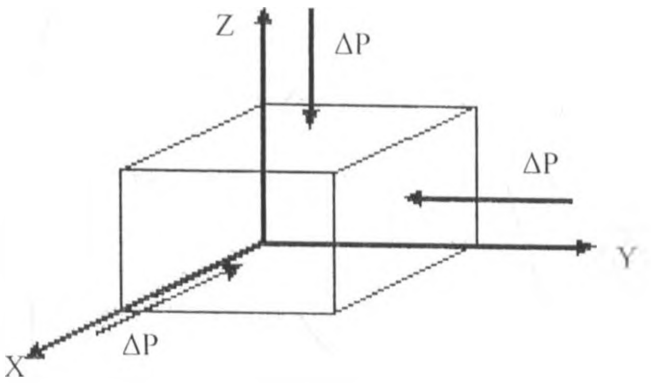

Figure 2.2: Forces acting at a point, equal in all directions

If a small area ΔA is taken in a plane and a force ΔP is the internal force acting on it activated from an external load P, then the unit stress at this point is defined as, (Chung, 1998)

$$\sigma = \lim_{\Delta A \to 0} \frac{\Delta P}{\Delta A} = \frac{dP}{dA} \qquad \text{.....[2.1]}$$

The stress may be resolved into two components:

1. Normal stress - Normal to the plane of reference.
2. Shear stress - Parallel to the plane of reference.

To completely specify the stress at point, it is necessary to specify the stresses at the point on three mutually perpendicular planes passing through the point. For each plane it is possible to specify one normal stress and two shear stresses. This yields a total of nine stress components at a point. If the three mutually perpendicular planes are perpendicular to the x, y and z coordinate axes, then the complete specification of the stress at a point is σ_{ij}, (Timoshenko and Goodier, 1983) where:

$$\sigma_{ij} = \begin{bmatrix} \sigma_{xx} & \sigma_{xy} & \sigma_{xz} \\ \sigma_{yx} & \sigma_{yy} & \sigma_{yz} \\ \sigma_{zx} & \sigma_{zy} & \sigma_{zz} \end{bmatrix} \qquad \text{.....[2.2]}$$

The first subscription denotes the normal to the plane under consideration and the second subscript designates the direction of the stress. Thus σ_{xy} denotes a shearing stress acting on the plane perpendicular to the x-axis and the stress acts in the y-axis. σ_{xx}, σ_{yy} and σ_{zz} are the normal stress components and the rest are shear stress components. Hence, the necessary and sufficient condition for state of pure shear exists when:

$$\sigma_{ii} = 0 \qquad \text{.....[2.3]}$$

Similarly, when an element body is deformed, the strain at a point on the element can be represented in a manner similar to equation 2.2 (Timoshenko and Goodier, 1983; Chung, 1988) as:

$$\varepsilon_{ij} = \begin{bmatrix} \varepsilon_{xx} & \varepsilon_{xy} & \varepsilon_{xz} \\ \varepsilon_{yx} & \varepsilon_{yy} & \varepsilon_{yz} \\ \varepsilon_{zx} & \varepsilon_{zy} & \varepsilon_{zz} \end{bmatrix} \quad \text{.....[2.4]}$$

Equation (2.4) can be reduced to obtain unidirectional strain. If there are no strains acting in z direction, but there are strains acting in x and y directions, the state of strain is called plane strain (Mase, 1990). Hence:

$$\varepsilon_{xz} = \varepsilon_{yz} = \varepsilon_{zz} = 0 \quad \text{.....[2.5]}$$

Then,

$$\varepsilon_{ij} = \begin{bmatrix} \varepsilon_{xx} & \varepsilon_{xy} & 0 \\ \varepsilon_{yx} & \varepsilon_{yy} & 0 \\ 0 & 0 & 0 \end{bmatrix} \quad \text{.....[2.6]}$$

In unidirectional strain, the elongation is in one direction only, say x-direction. Hence (Mase 1990)

$$\varepsilon_{ij} = \begin{bmatrix} \varepsilon_{xx} & 0 & 0 \\ 0 & 0 & 0 \\ 0 & 0 & 0 \end{bmatrix} = \varepsilon_{xx} \quad \text{.....[2.7]}$$

Equation [2.7] may be written as:

$$\varepsilon_{\eta} = \varepsilon_{xx} = \frac{(l_1 - l_0)}{l_0} \qquad \text{.....[2.8]}$$

in the x – direction.

Thermoplastic materials such as HDPE are viscoelastic, which means that their mechanical properties reflect the characteristics of both viscous liquids and elastic solids. Thus, when a polymer is stressed, it responds by exhibiting viscous flow (which dissipates energy) and by elastic displacement (which stores energy). The properties of viscoelastic materials are time, temperature and strain-rate dependent (Crawford, 2005).

Since polymers exhibit time dependent behavior, the stress and strain induced when a load is applied are functions of time. When a plastic material is subjected to a constant stress, it deforms continuously (Figure 2.3).

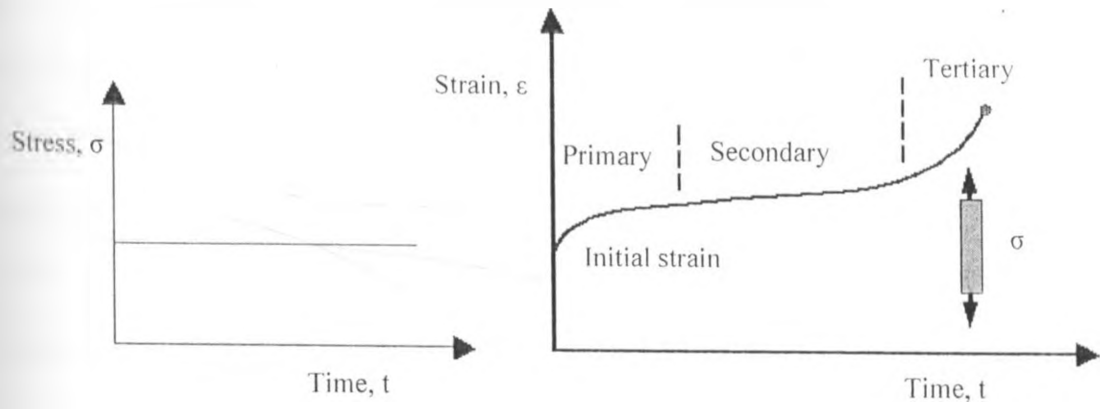

Figure 2.3: (a) When constant load is applied (b) Resulting creep curve for plastics (Wu, 2000)

The initial strain is roughly predicted by its stress-strain modulus. The material will continue to deform slowly with time indefinitely or until rupture or yielding causes failure. The primary region is the early stage of loading when the creep rate decreases rapidly with time. Then it reaches a steady state, which is called the secondary creep stage followed by a rapid increase (tertiary stage) and fracture. This phenomenon of deformation under load with time is called creep (Wu, 2000).

Reed (2003) adds that creep is the slow deformation of a material under stress that results in a permanent change in shape. Creep phenomena increase with stress, time and temperature. Creep is determined by a competition between recovery and work-hardening material properties. The term "recovery" describes all the mechanisms through which a material becomes softer and improves its ability to undergo additional deformation while the term "work-hardening" stands for all the processes that make the material more difficult to deform as it is strained.

Figure 2.3 is an idealized curve. Some materials do not have secondary stage, while tertiary creep only occurs at high stresses and for ductile materials. All plastics creep to a certain extent. The degree of creep depends on several factors, such as type of plastic, magnitude of load, temperature and time (Wu, 2000). The standard test method for creep characterization is ASTM D2990 (1995). In this test procedure, the dimensional changes that occur during time under a constant static load are measured.

Primary creep is characterized by the work-hardening behaviour of the material. As the strain increases, softening occurs and it leads to the steady state (secondary creep) in which recovery

and hardening processes balance one another. Tertiary creep is the result of micro-structural and mechanical instabilities such as cavities, cracks, grain-boundary separations, etc. that result in a local decrease in cross-sectional area and consequent higher stress levels (Reed, 2003).

2.2.1 Recovery

If the applied load is released before the creep rupture occurs, an immediate elastic recovery equal to the elastic deformation, followed by a period of slow recovery is observed (Figure 2.4) The material in most cases does not recover to the original shape and a permanent deformation remains. The magnitude of the permanent deformation depends on length of time, level of stress applied, and temperature. A detailed account of modelling of recovery in polymers is given in Section 2.4.

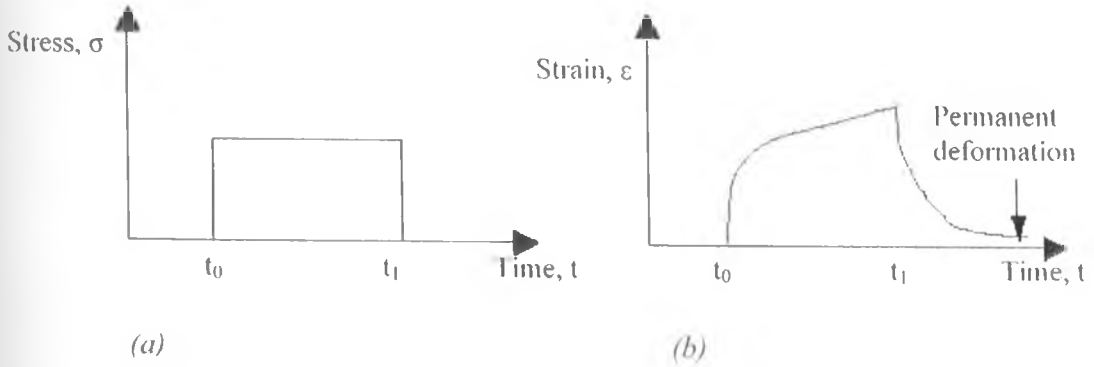

Figure 2.4: (a) When a constant stress level is applied at t_0 and removed at t_1 (b) Resulting creep curve with recovery (Wu, 2000)

2.2.2 Creep Rupture Test

The creep rupture test is basically similar to a creep test with the exception that it is continued until the material fails. Since higher loads are used, creep rates are higher and the material fails

in a shorter time, usually in less than 1000 h. This test is useful in establishing a safe envelope inside which a creep test can be conducted. The basic information obtained from the stress rupture test is the time to failure at a given stress. Based on this data, a safe stress can be determined below which it is safe to operate, given the time requirement of the end use application.

There are two ways in which creep rupture data may be presented. The first as seen in Wu (2000) is shown in Figure 2.5. The test is conducted under constant stresses and a curve of strain versus time is plotted. The points of the onset of tertiary stage are connected to form the creep rupture envelope.

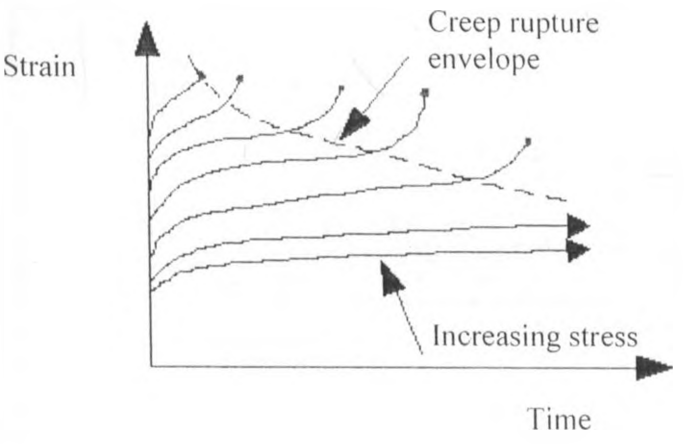

Figure 2.5: Illustration of Strain-Time to Failure Creep Rupture Envelope (Wu, 2000)

The second form of creep rupture envelope presented by majority of researchers including Hsuan (2003) and Plastics Pipe Institute (2008) is the relationship between tensile load (stress) and lifetime. There may be a characteristic envelope for a given set of conditions of temperature and environment. The applied stresses are below the yield stress of plastics (measured by the short-

term tensile test). The time required for each specimen to fail is recorded. By testing specimen at various conditions, creep rupture curves are generated. The time for specimen failure to occur increases as applied stress decreases (Plastics Pipe Institute, 2008).

It is possible to plot both types of creep rupture curves on a log-log scale, in which case, the strain-time to failure family of curves evolve into straight line curves which are easier to analyse. However, the onset of the tertiary stage may not be easily seen. An example of this is seen in Figure 2.6.

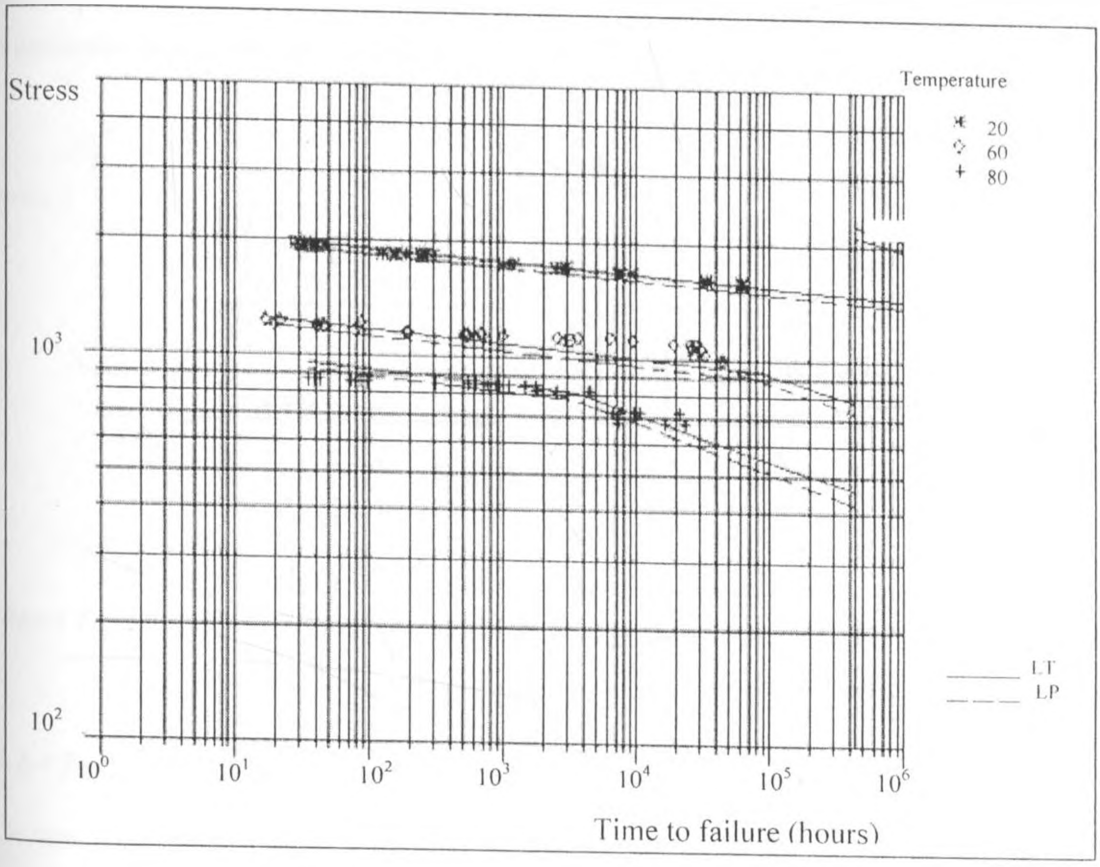

Figure 2.6: Example of a stress-failure time creep rupture envelope for PVC (Plastics Pipe Institute, 2008)

2.2.3 Stress relaxation, constant strain

Stress relaxation is defined as a gradual decrease in stress with time under a constant deformation or strain (Fung, 1972). This behaviour of polymers is studied by applying a constant deformation to the specimen and measuring the stress required to maintain that strain as a function of time as illustrated in Figure 2.7.

Stress relaxation test can be used for some practical applications. For example, low stress relaxation is desired for threaded bottle closures. The stress data obtained from stress relaxation test can be used to calculate transient modulus for plastics design by simply dividing the stress at a particular time by the applied strain.

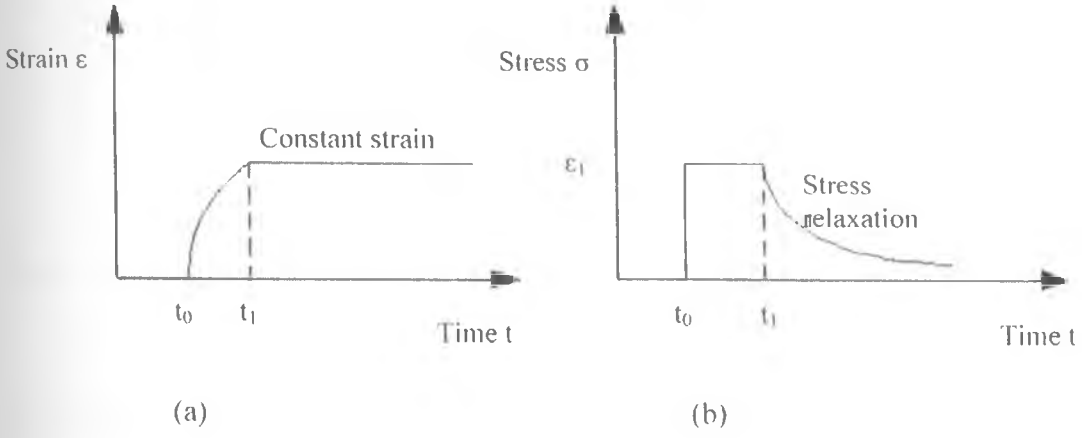

Figure 2.7: (a) As a result of constant strain (b) Stress relaxation of plastics results (Wu, 2000)

2.2.4 Design with plastics

Design with plastics can be divided into two categories, design for strength and design for stiffness (Wu, 2000). The strength of a component is limited by the yield strength and rupture resistance of the material from which it is made. As shown in Figure 2.8, a creep rupture

envelope can be obtained from creep test. For an expected life-time, the maximum stress allowed (σ_4) can be decided from the creep rupture envelope line. Design for stiffness with creep curves proceeds by establishing the maximum strain acceptable ε_{max}, thereby establishing a horizontal line on the creep diagram correspondingly. The expected lifetime t_l of the part is also determined, and the maximum stress permissible is found on the creep curve at the intersection of these two lines (Wu, 2000).

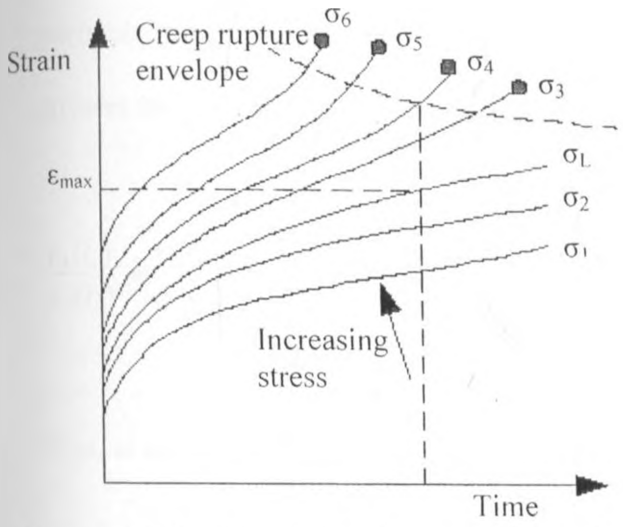

Figure 2.8: Design criteria by creep curves (Wu, 2000)

As shown in Figure 2.8, many combinations of ε and time will yield this maximum strain. For a desired lifetime t_L, however, there is one maximum level σ_l which satisfies the maximum strain. Design basis selection depends on the specific application. Usually, strain or dimension requirement is more critical, and design for stiffness is favoured in this case. If the dimension precision of the component under discussion is not so important compared to strength, design for strength is then used accordingly. For complicated structures, both can be used as design criteria to ensure successful material performance during service time (Wu, 2000).

2.2.5 Linear and nonlinear viscoelasticity

The time dependent material behaviour is often referred to as viscoelasticity. If a constant stress σ_1 is applied to a viscoelastic specimen, the time dependent strain is recorded as ε_1 as shown in Figure 2.9(a).

After some period of time, the load is removed. Suppose the specimen is allowed to recover and a larger stress σ_2 is applied. The time dependence of the strain ε_2 is shown in Figure 2.9(b). If at particular times t_1 and t_2 after loading, ε_1 and ε_2 are linear with the magnitude of correspondent stresses being σ_1 and σ_2, the stress strain relationship can be given by

$$\frac{\varepsilon_1(t_1)}{\sigma_1(t_1)} = \frac{\varepsilon_2(t_1)}{\sigma_2(t_1)}, \quad \frac{\varepsilon_1(t_2)}{\sigma_1(t_2)} = \frac{\varepsilon_2(t_2)}{\sigma_2(t_2)} \qquad \text{.....[2.9]}$$

Thus, at an arbitrary time t, the strains at the two stresses can be expressed as

$$\frac{\varepsilon_1(t)}{\sigma_1(t)} = \frac{\varepsilon_2(t)}{\sigma_2(t)} \qquad \text{.....[2.10]}$$

The strains in the two experiments are proportional to the imposed stresses. In general, for stress σ, the creep compliance D(t) can be given as the ratio of strain to stress at a certain time.

$$D(t) = \frac{\varepsilon(t)}{\sigma} \qquad \text{.....[2.11]}$$

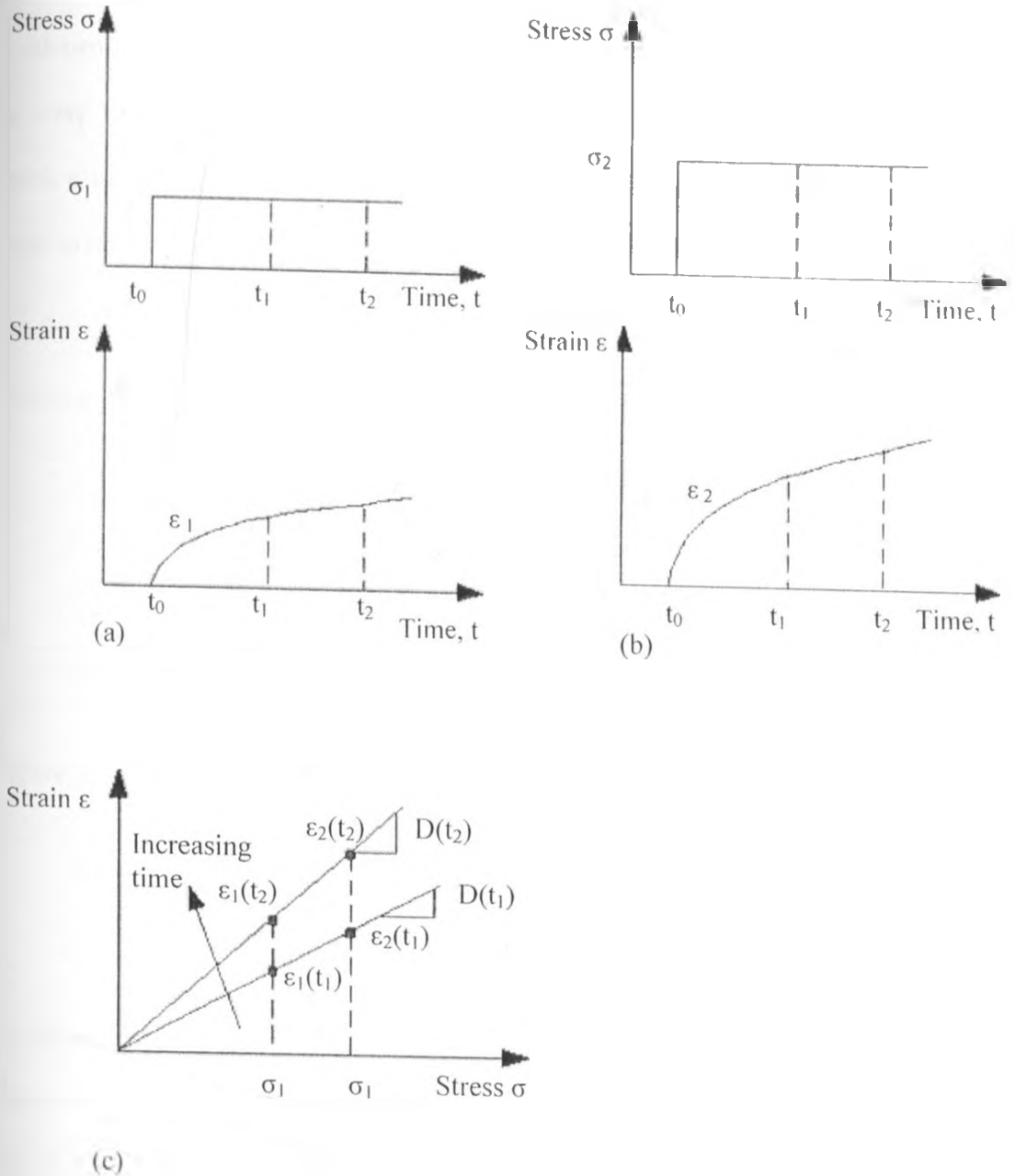

Figure 2.9: Linear viscoelastic creep: (a) constant stress σ_1 applied at time t_0 leads to time dependent strain $\varepsilon_1(t)$; (b) a higher stress applied at t_0 leads to time dependent strain $\varepsilon_2(t)$; (c) from (a) and (b) the strains at t_1 and t_2 are linear in the stress (Wu, 2000)

This property is often characterized as linear viscoelasticity. In the linear range, the compliance is independent of stress, which means that the compliance is the same whether stresses used in the creep test are σ_1, σ_2 or other stress levels as illustrated in Figure 2.8(c). The strain range in which a specimen is linear viscoelastic can be determined by a creep test. A transition from linear to nonlinear viscoelasticity is shown in Figure 2.10.

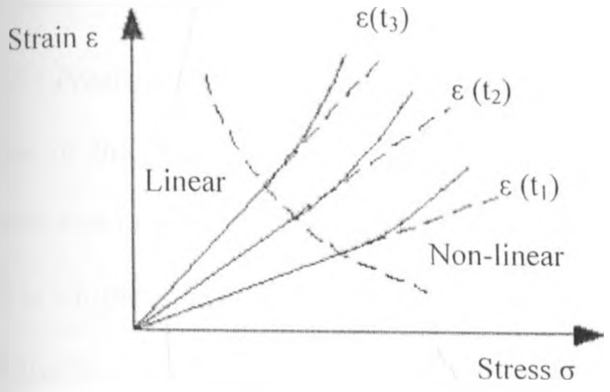

Figure 2.10: Linear-nonlinear transition of stress strain relationship with respect to different time levels (Isochronous creep curve, data are taken from creep test at different stresses) (Wu, 2000)

However, polymers generally exhibit linear viscoelastic property only at low stresses such that the corresponding strain is below 5×10^{-3}. At higher stress levels, the material will assume *nonlinear viscoelastic* behaviour which will not obey the linear relation between stress and strain described by equation (2.3). Since nonlinear behaviour is very important to determine material behaviour at moderate or higher stress levels, some models have been suggested for different kinds of polymers (Wu, 2000).

2.3 Modeling the Behaviour of Plastics

Experimental creep results are usually presented in graphical form. These curves are then fitted by an equation. From these equations creep rate may be calculated and interpolation and extrapolation of creep deformation may be done for extra-experimental conditions (Feller, 1994). This section considers the various approaches that have been used to describe creep curves of polymers, depending on the objectives of different researchers.

2.3.1 Prediction of Useful Lifetime

One of the important applications of models depicting the behaviour of plastics is in the prediction of useful lifetime. According to Feller (1994), there is no agreement among scientists as to whether it is possible to predict useful lifetime of products. While admitting that there are difficulties, he has reviewed three approaches that chemists and engineers have regularly employed in the effort to meet the objective of predicting long-term behaviour and time to failure. These approaches are:

2.3.1.1 Change According to Laws of Chemical Kinetics

If it can be shown on the basis of accelerated-aging tests that the observed change in chemical properties tends to follow one of the principal kinetic processes (zero-, first-, or second-order individually, sequentially, or reversibly), then the pertinent equations are often applied to predict the progress of additional accelerated aging as well as the course of aging under normal conditions. Such equations are theoretically based rather than empirical, conforming to a model of what must be taking place. Predictions regarding the effect of temperature may be based on the Arrhenius equation (Feller, 1994).

According to Feller (1994), the effect of temperature on the rate of chemical reactions can usually be expressed by a relationship proposed by Arrhenius in 1889 as follows:

$$\ln k = -\frac{E}{RT} + Z \qquad \text{.....[2.12]}$$

Where:

k is the rate of reaction

E the energy of activation of the reaction

R the gas constant (8.314 Joules per mole degree Kelvin)

T the temperature in degrees Kelvin

Z is a constant.

The ratio of the specific rates of reaction, k_2/k_1, at two temperatures, T_2 and T_1, is customarily calculated by the following form of the Arrhenius equation using logarithms to the base 10:

$$2.303 \log \frac{k_1}{k_2} = -\frac{E}{R}\left(\frac{1}{T_1} - \frac{1}{T_2}\right) \qquad \text{.....[2.13]}$$

The Arrhenius equation is normally used in accelerated thermal aging tests as follows: Some measure of the rate of reaction is determined at several temperatures (at least three, preferably more) and the logarithm of those *rates* is plotted versus $1/T$, the inverse of the absolute temperature (degrees Kelvin). The data can be used to estimate the rate that would be

experienced at other temperatures. The slope is extrapolated to predict the rate at room temperature, or extrapolated to some temperature at which a material will be used or stored.

There are two key limitations to the use of the Arrhenius equation:

a) Linear specific rates of change must be obtained at all temperatures used. By this it is meant that the rate of reaction, however this is measured or represented, must be constant over the period of time at which the aging process is measured. If the apparent rate should vary over the time of the test, then one would not be able to identify a specific rate that is assignable to a specific temperature. If the mechanism of the reaction at higher or lower temperatures should differ, this, too, would alter the slope of the curve.

b) Another source of error would be that the mode of physical failure of a system would differ at the two temperature extremes. Hence, the temperatures should not be so high that the mode of physical failure changes from that exhibited at the temperatures of normal usage.

2.3.1.2 Sizmann and Frank Method

During accelerated tests it has often been the custom to age two materials for a given length of time and then to compare their relative loss of strength. A more fundamental approach is to compare the length of time to reach the same degree of change as presented by Feller (1994).

2.3.1.3 Empirical Equations

These equations are based purely on observations from experiments. Past researchers have proposed the following empirical equation to calculate the change in thirteen different properties (P) in ten different plastics during exposure in xenon-arc radiation:

$$\text{Log } P = b_0 - b_1 (t - 250) + b_2 (I - 0.710) \quad \text{.....[2.14]}$$

Where:

t is time (hours)

I is the average intensity of the light source (cd)

b_0, b_1 and b_2 are constants.

Outdoor exposure has been used to confirm the effectiveness of the equation. Several other types of equations of this nature also exist and computer programs exist that allow one to develop equations that best fit a curve of the change in properties over time. However it has been pointed out that polynomial equations are often adequate for interpolation but may not be as accurate for extrapolation (Feller, 1994)

2.3.1.4 Semi-Empirical models

These models have a theoretical basis but certain sections are explained from practical experimental observations. Creep deformation (ε), depends mainly on time (t), stress (σ) and temperature (T). Different researchers have modelled these properties or combinations of the properties variously as follows:

Kolarik *et al* (2003) expanded the creep expression ε(t,σ,T), which consists of three components of time (t), stress (σ) and temperature (T) as follows:

$$\varepsilon(t, \sigma, T) = \varepsilon_e(\sigma, T) + \varepsilon_v(t, \sigma, T) + \varepsilon_p(t, \sigma, T) \quad \text{.....[2.15]}$$

Where:

$\varepsilon_e(\sigma, T)$ represents elastic (instantaneous) deformation

$\varepsilon_v(t, \sigma, T)$ represents viscoelastic (reversible) deformation

$\varepsilon_p(t, \sigma, T)$ plastic (irreversible) deformation

In practice, conditions where $\varepsilon_p(t, \sigma, T) > 0$ are avoided since plastic deformation represents irreversible damage to an end product (Kolarik *et al*, 2003). The corresponding tensile creep compliance, arising from equation [2.15] is:

$$D(t, \sigma, T) = \varepsilon(t, \sigma, T) / \sigma \quad \text{.....[2.16]}$$

By equation [2.15], it is represented as:

$$D(t, \sigma, T) = D_e(\sigma, T) + D_v(t, \sigma, T) + D_p(t, \sigma, T) \quad \text{.....[2.17]}$$

Another example of the use of this type of model is the Leaderman model. Beijer and Spoormaker (1997) used the Leaderman model with a plastic strain term added for higher stresses to determine the viscoelastic behaviour of HDPE under tensile loading. The Leaderman model was found to be applicable for stresses upto 14 MPa and is stated thus:

$$\varepsilon = \varepsilon_p + \varepsilon_v = D_p(\sigma)\sigma + g(\sigma)D(t)\sigma \quad \text{.....[2.18]}$$

The first term in Equation 2.10 is the plastic response power law described by Lai and Bakker

(1995) and the second for the viscoelastic response (the generalized Kelvin-Voigt model).

However, to simplify the description of creep under various conditions, it is the general practice to express compliance as a product of independent functions of time or stress or temperature. That is:

$$D(t, \sigma, T) = C_p\, f(t)\, g(\sigma)\, h(T) \qquad \text{.....[2.19]}$$

The parameters of such empirical equations are determined *a posteriori* by fitting experimental data (Kolarik *et al*, 2003).

The Findley equation for total strain ε under a given temperature T, and a given stress σ is presented by Smith (2005) by:

$$\varepsilon = \varepsilon_T + \varepsilon_t \qquad \text{.....[2.20]}$$

Where ε_t is the strain due to stress over time and ε_T is the tensor of thermal expansion. Therefore the time-dependent and the temperature-dependent behaviours are modelled separately and then summed with the strain due to thermal expansion to reach the total creep strain.

The time-dependent behaviour of materials to provide an accurate approximation of the creep deformation data may be modelled using the power law developed by Findley presented in Smith (2005) as:

$$\varepsilon_t = \varepsilon_0 + mt^n \qquad \text{.....[2.21]}$$

Where:

ε_t = total time-dependent strain

ε_0 = stress-dependent initial elastic strain

m = stress-dependent and temperature-dependent coefficient

n = stress-independent and temperature independent material constant

t = time after loading

Since the total viscoelastic model has been separated into two distinct parts, time-dependent behaviour and temperature-dependent behaviour, the room temperature creep tests may be used to model the time-dependent behaviour only. This may be done by considering ε_T in Equation (2.20) to be zero and therefore the total strain would be equal to the time-dependent strain. The empirical constants, m and n, needed to formulate the power law can be found from the experimental creep data, rearranging Equation [2.21] and taking the logarithm of both sides:

$$\log[\varepsilon_t - \varepsilon_0] = \log(m) + n\log(t) \qquad \text{.....[2.22]}$$

Plotting Equation [2.22] on a log-log scale yields a straight line from which the empirical constants can be calculated. From the resulting line, the y-intercept at t = 1 hour is equivalent to the value of m and the slope of the line is the material constant n. The Findley equation is then obtained by substituting for n and m in Equation [2.21]. Using this equation and the time range of the experiments, it is possible to generate values of creep strain from which a curve of creep

strain versus time may be plotted. A comparison is then made between the theoretical curve and the curve drawn from actual experimental data. A close relationship between the two curves denotes that the model is accurate and that it can be used to predict experimental data.

Using the average values of the empirical parameters m and n, the Findley power law model using Equation [2.21] is equated to the time-dependent behaviour of the material. Due to the relationship shown in Equation [2.20], the temperature-dependent behaviour of the material can be found by subtracting the time-dependent strains from the total strain recorded in the experimental data as follows:

$$\varepsilon_T = \varepsilon - \varepsilon_t \qquad \text{.....[2.23]}$$

Using the results of Equation [2.23], a secondary Findley power law can be used to express the temperature-dependent behaviour of the material. To accomplish this, the results of Equation [2.23] are found using the recorded strains at the elevated temperatures as ε and the recorded strains at a reference temperature as ε_t. These results are then plotted on a logarithmic scale and the values for m and n are taken in the same manner as described earlier, where m is the y-intercept at t = 1 hour and n is the slope of the resulting straight line. For the temperature-dependent model, these parameters will be designated as m_T and n_T. Using the empirical constants m_T and n_T, the temperature-dependent creep strains can be modeled using a power law model as:

$$\varepsilon_T = \varepsilon_0 + m_T t^{n_T} \qquad \text{.....[2.24]}$$

Thus, the strain as a function of time and temperature can be modelled by summing the results of the room temperature and the temperature-dependent Findley power law models (Smith, 2005):

$$\varepsilon(T,t) = \varepsilon_0 + m_{RT} t^{n_{RT}} + m_T t^{n_T} \quad \text{.....[2.25]}$$

Where:

$\varepsilon(T,t)$ = total time and temperature dependent strain

ε_o = stress-dependent initial elastic strain

m_{RT} = stress-dependent and temperature-dependent coefficient at reference temperature

n_{RT} = stress independent material constant at reference temperature

m_T = stress and temperature-dependent coefficient at elevated temperature

n_T = stress independent material constant at elevated temperature

t = time after loading

2.3.2 Time – Temperature Superposition

Leaderman was the first to observe that the creep compliance versus log (time) curves for different temperatures for various (polymeric) materials are of the same shape, but increasing temperature has the effect of contracting the time scale. Many researchers were subsequently able to make use of Leaderman's observations to superimpose the individual curves into a single reference curve (Johnson *et al*, 1996; Kwan *et al*, 1993 and Pioleti *et al*, 1996).

To perform time-temperature superposition, experimental curves of creep or creep compliance D $= \varepsilon / \sigma$ versus time are first obtained at a series of temperatures over a specific time period. Then a curve at some temperature is chosen as reference. The curves are then shifted one by one, using

the shift factor in equation 2.18 until they superimpose. The nature of the shift factor is such as to shift the curves above the reference temperature to the right and those below to the left (Wu, 2000). Subsection 2.3.2.1 is dedicated to the discussion of shift factors. One of the important considerations is the smoothness at the overlap where two different individual curves meet. If the Time-Temperature Superposition (TTSP) method is valid, the master curve represents the true behaviour of a long-term test at the reference temperature. It is recommended, though, that the master curve be shifted only to temperatures in the range in which the data was collected. This ensures a valid extrapolation of data (Thermal Analysis and Rheology, 2007).

According to Alwis and Burgoyne (2006), it is generally difficult to obtain a smooth match at the overlapping region. However, partial matching of the two curves is possible. A small change at the overlap may lead to erroneous predictions of the rupture times. The error in time may be as large as ten years as the shifting is performed along the log (time) scale and the error may accumulate if multiple tests are used. If it is possible to generate a smooth master curve by applying a horizontal shift along the log (time) axis, the material is classified as a thermorheologically simple material (TSM). However, for some materials a vertical shift factor may be needed to obtain a smooth master curve and they are classified as thermorheologically complex materials (TCM).

2.3.2.1 Shift Factors

There are two types of relationships for shift factors:

1. Empirical relationships for horizontal shift factor

The term h(T) from (2.11) is usually identified with the Williams-Landel-Ferry (WLF) or Arrhenius equation, represented by Donald (2004) as:

$$Log\ (a_T) = \frac{-C_1(T - T_{ref})}{C_2 + (T - T_{ref})} \qquad \text{.....[2.26]}$$

Where:

a_T is the shift factor

T_{ref} is the reference temperature

C_1 and C_2 are approximately universal constants for many polymers with C_1 = 17.4K and C_2 = 51.6K if T_{ref} is chosen as the glass transition temperature

Equation [2.19] as implied by the expression h(T) is a function of temperature only. It is also the equation that is applied to data for different viscoelastic properties at different temperatures to shift curves onto a single curve at a single temperature to create a master curve during time-temperature superposition. The WLF equation is therefore very useful as it enables the response of a system to be described from limited experimental data. The resulting master curve also covers a large range of times (Donald, 2004; Wu, 2000).

The use of WLF equation is restricted to materials above the glass transition temperature (Alwis and Burgoyne, 2006) or in the glass transition region (Thermal Analysis & Rheology, 2007). The equation is based on the assumption that, above the glass transition temperature, the fractional free volume increases linearly with respect to temperature. The model also assumes that as the

free volume of the material increases, its viscosity rapidly decreases (Thermal Analysis & Rheology, 2007).

However, some materials do not display a glass transition, but remain crystalline at all temperatures. The relationship between the temperature and the horizontal shift factor, log (a_1), for materials that do not display glass transition or for those that are being studied below the glass transition temperature is based on the Arrhenius equation. This relationship derives from Equation [2.13] and is presented by Alwis and Burgoyne (2006) as:

$$\log(a_T) = \frac{E}{2.303R}\left[\frac{1}{T} - \frac{1}{T_R}\right] \qquad \text{.....[2.27]}$$

Where:

Log (a_T) is the shift factor and is the ratio of the rates k_1/k_2 in Equation [2.13]

E is the activation energy for creep

R is the universal gas constant

T is the absolute temperature replacing T_1 in equation [2.13]

T_R is the reference temperature replacing T_2 in equation [2.15]

The superposition theory (with regard to the Arrhenius equation) is only valid if the same mechanism is present at all the temperature levels and this can be checked by determining the activation energy of the process which should be independent of temperature (Alwis and Burgoyne, 2006).

2. Empirical relationships for vertical shift factor

For thermorheologically complex materials the visco-elastic properties do not superpose completely if only horizontal displacements are performed. Vertical shift factors are needed to account for change in material density, hygrological effects, and thermal expansion and contraction. When the specimens were loaded after heating, no adjustment may be needed (Alwis and Burgoyne, 2006; Morgan *et al*, 2003 and Thornton *et al*, 1997).

2.3.3 Application of the Master Curve

The master curve can be used to determine the time at which a particular viscoelastic quantity reaches some critical value. For example, a geo-membrane under load may rupture after months or years of use when it achieves a certain compliance value. The time that it takes to achieve this particular critical compliance at a given temperature can be easily established from the master curve.

The versatility of the Time-Temperature Superposition (TTSP) can be seen in a research conducted by Smith (2005) which shows that accelerated test durations of 1,000 hours produced an estimation of the creep strain over a period of 2,165 years. Analysis of the creep data in the investigation reveals that three creep tests of 120 hours (5 days) would be sufficient to provide an estimation of the strain response over a 50 year service life. It is for this reason that creep tests in this research study were limited to less than 200 hours.

Apart from creep compliance, TTSP has been used to obtain the master curves for several properties such as creep, and stress compliance against time (or log (time)) or dynamic modulus

against frequency (Alwis and Burgoyne, 2006; Fung, 1972; Lai and Bakker, 1995; Rowe et al, 2003).

The accuracy of the master curve is dependent on the following factors:

1. Variation of the shift factors with temperature.
2. Existence of the same creep mechanism under different temperatures.
3. The humidity.
4. State of the polymeric material (glassy, rubbery, or at the transition range).
5. The initial strain rate applied to the specimens in creep testing. Although the creep stress, σ_0 is assumed to be applied instantaneously, a finite time and a certain rate of strain are needed to reach the required stress level.
6. Initial preparation of the specimens, the type of the clamping system and the type of the testing machine.
7. Rate of application of heat to reach an isothermal temperature level.

2.3.4 Modeling Recovery

It was important to discuss and investigate recovery in this research study since the material used was expected to be loaded intermittently. The water reservoir is sometimes full of water in which case certain parts of the liner is exposed to high loads and is sometimes empty, in which case there would be no loading. This presents a case of creep in when the reservoir is loaded and recovery is assumed as it is emptied. For a linear viscoelastic material in which strain recovery may be regarded as the reversal of creep, then the material behaviour may be represented as in Figure 2.11. Thus the time-dependent residual strain, $\varepsilon_r(t)$ may be expressed as:

$$\varepsilon_r(t) = \varepsilon_c(t_c) - \varepsilon_c(t, t_c) \qquad \text{.....[2.28]}$$

Where:

ε_c is the creep strain during the specified period, denoted by (t) or ($t-t_c$).

t_c is the specific time when the material is unloaded at the end of the creep period

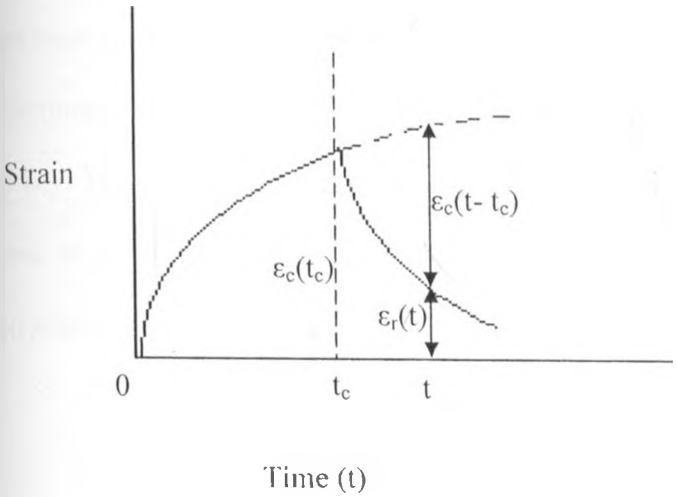

Figure 2.11: Typical Creep and Recovery Behaviour (Crawford, 2005)

There can be an infinite number of combinations of creep and recovery periods. It is therefore convenient to express this behaviour in terms of either fractional recovery or reduced time.

Fractional recovery, F_r, is defined as:

$$F_r = \frac{Strain\ recovered}{Max.\ creep\ strain} = \frac{\varepsilon_c(t_c) - \varepsilon_r(t)}{\varepsilon_c(t_c)} \qquad \text{.....[2.29]}$$

Where $\varepsilon_c(t_c)$ is the creep strain at the end of creep period and $\varepsilon_r(t)$ is the residual strain at any selected time during the recovery period.

Reduced time is a dimensionless variable defined as:

$$t_R = \frac{Recovery\ time}{Creep\ time} = \frac{t - t_c}{t_c} \qquad \text{.....[2.30]}$$

It has been shown that if the final creep strain is not large, then a graph of Fractional Recovery Vs Reduced Time is a master curve, which describes recovery behaviour with acceptable accuracy. The relationship between F_r and t_R may be derived as follows. When creep curves are plotted on logarithmic strain and time scales they are approximately straight lines so that the creep strain $\varepsilon_c(t)$ may be expressed as:

$$\varepsilon_c(t) = At^n \qquad \text{.....[2.31]}$$

Using the relationship in Equation [2.31],

$$\varepsilon_r(t) = At^n - A(t - t_c)^n \qquad \text{.....[2.32]}$$

Therefore, the Equation [2.29] for Fractional Recovery may be written as

$$F_r = \frac{At_c^n - \left[At_c^n - A(t-t_c)^n\right]}{At_c^n} = 1 - \left(\frac{t}{t_c}\right)^n + \left(\frac{t}{t_c} - 1\right)^n \quad \text{.....[2.33]}$$

Hence,

$$F_r = 1 + t_R^n - (t_R + 1)^n \quad \text{.....[2.34]}$$

The relationship in Equation [2.34] is only a good approximation since plastics are not linearly viscoelastic and do not completely obey the power law in Equation [2.31]. However, the equation is favoured on account of its simplicity and is sufficiently accurate for most purposes and allows the analysis of intermittent loading.

From Equation [2.34] and the definition of Fractional Recovery, F_r in Equation [2.29], the residual strain is given by:

$$\varepsilon_r(t) = \varepsilon_c(t_c) - F_r.\varepsilon_c(t_c) = \varepsilon_c(t_c)\left[\left(\frac{t}{t_c}\right)^n - \left(\frac{t}{t_c} - 1\right)^n\right] \quad \text{.....[2.35]}$$

If there are N cycles of creep and recovery, the accumulated residual strain would be:

$$\varepsilon_r(t) = \varepsilon_c(t_c)\sum_{x=1}^{x=N}\left[\left(\frac{t_p.x}{t_c}\right)^n - \left(\frac{t_p.x}{t_c} - 1\right)^n\right] \quad \text{.....[2.36]}$$

Where t_p is the period of each cycle and thus the time for which total accumulated strain is being calculated is $t = t_p N$.

It is also noted that that the total accumulated strain after the load application for the $(N+1)^{th}$ time will be creep strain for the load-on period, given by $\varepsilon_c(t_c)$ plus the residual strain $\varepsilon_r(t)$, that is:

$$(\varepsilon_{N+1})_{max} = \varepsilon_c(t_c)\left\{1 + \sum_{x=1}^{x=n}\left[\left(\frac{t_p x}{t_c}\right)^n - \left(\frac{t_p x}{t_c} - 1\right)^n\right] - \right\} \qquad \text{.....[2.37]}$$

Tests have shown that when total strain is plotted against the logarithm of the total creep time (that is, N_t or total experimental time minus the recovery time) there is a linear relationship. This straight line includes the strain at the end of the first creep period and thus one calculation, for say the 10^{th} cycle allows the line to be drawn. The total creep strain under intermittent loading can then be estimated for any combinations of loading/ unloading times.

In many design calculations it is necessary to have the creep modulus in order to estimate deflections and other parameters from standard formulae. These calculations are straight forward for steady loading. For a case of intermittent loading, the modulus of the material is effectively increased due to the apparent stiffening of the material caused by recovery during rest periods.

CHAPTER 3: MATERIALS, EXPERIMENTAL AND ANALYTICAL METHODS

3.1 Description of Test Specimens

The specimens used in this project were obtained from HDPE plastic dam liner manufactured by A-Plus Ltd. in Nairobi at different time and were classified in three categories:

3.1.1 Fresh specimens

The particular sheet used in this experiment was manufactured by the extrusion process on 3rd March 2006. They were then stored at room temperature with no exposure to light or other degrading agents such as humidity till the date of testing. Tests were conducted on the specimen between the date of manufacture and May 2008 in the Mechanical Engineering Laboratories, University of Nairobi. The material is available commercially in four classes with regard to the thickness ranging from 0.5 mm to 1.2 mm. The material used in the tests was 0.8mm thick. The rest of the dimensions are as shown in Figure 3.1, which is the recommended geometry proposed by ASTM D 638 (2003) for Type II specimens. The length of the specimen was changed to suit the design of the test apparatus as recommended by the standard. The other dimensions used in this research study were similar to those provided in the standard.

Specimens in both the axis parallel to the direction of extrusion and in the axis perpendicular to the direction of extrusion were used in the tests in equal proportions so as to cancel the effect of material orientation.

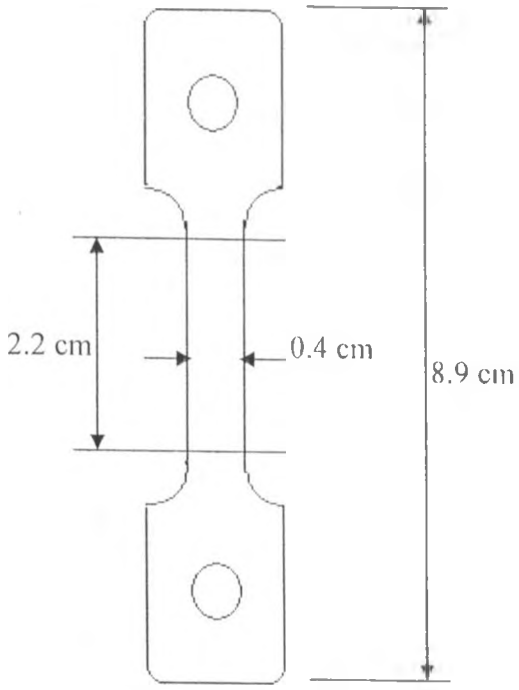

Figure 3.1: Specimen Geometry – Die Type II Dimensions used in the research study

3.1.2 Specimens Subjected to Accelerated Aging

These are the specimens that were exposed to UV radiation or treated in Igepal® as expounded in Sections 2.1.5 and 2.1.6 respectively (so as to achieve accelerated aging) and subsequently tested. Fresh specimens were incubated in 70% Igepal® for one and two weeks respectively,prior to testing so as to accelerate the effect of long term exposure to water. Fresh specimens were also exposed to artificial UV radiation using a UV bulb with a wavelength of 254nm for different durations for 40 and 80 hours respectively prior to testing to have the effect of accelerated UV radiation. The dimensions used for specimens subjected to accelerated aging were similar to those in Figure 3.1.

3.1.3 Naturally degraded specimens

To be able to monitor deterioration in real life and validate results from modelling, it was necessary to collect specimens that had been degraded naturally in the field. This enabled a comparison to be made between the properties of fresh specimens, specimens degraded in the laboratory and those degraded naturally in the field. Samples were collected from three different sites as follows:

1. Mwala, Machakos, where the plastic lined reservoir was installed in February 2000, hence the samples had been exposed to natural conditions for 7 years.
2. Ndeiya Karai in Kiambu where the plastic lined reservoir had been installed in June 2003 (4 years exposure).
3. Ndeiya Karai in Kiambu where the plastic lined reservoir had been installed in June 2004 (3 years exposure).

It was ascertained that the specimens had been supplied by the same manufacturer and under similar conditions from the same raw materials. The dimensions used for specimens subjected to accelerated aging were similar to those in Figure 3.1.

3.2 Experimental Setup

The test rig in Figure 3.2 was set up and used to collect data for the research study as stipulated in ASTM-D638 (2003). The whole setup, except the strain indicator was placed inside an oven where it was possible to control and vary temperature. Inside the oven, the specimen was gripped between a fixed jaw at the top and a moving jaw at the bottom. The actual grips were knurled to avoid slippage of the specimen. Weights were then suspended at the free end of the specimen.

The total friction resistance and initial force (before application of the dead load) of the system was determined and subtracted from the total dead weight applied.

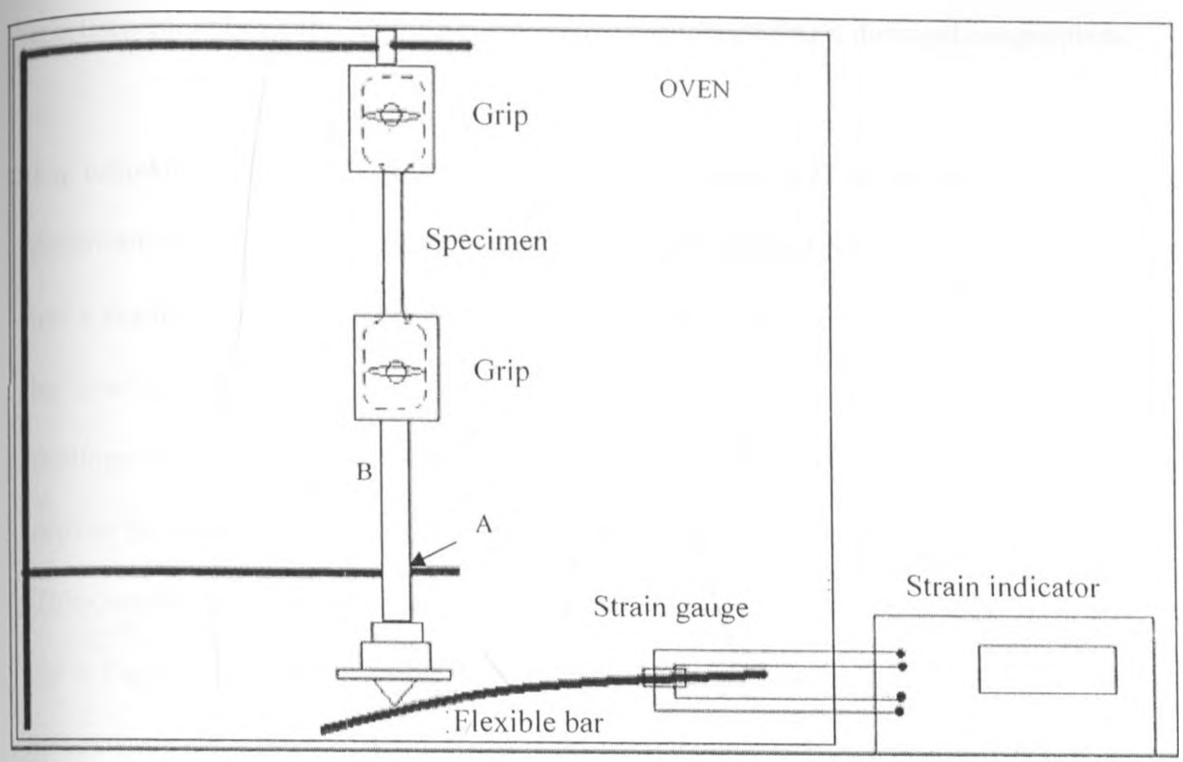

Figure 3.2: Test rig for the research study

The total friction resistance was determined as follows: The only source of friction in the set up was the guide at point A in Figure 3.2. Graphite was applied to the interacting surfaces to reduce friction. The arm B was then allowed to deflect the flexible arm without any specimen and the reading of deflection recorded. This initial reading constituted the net effect of friction resistance and the load applied by the arm. In the results presented, the net effect of friction and the additional load imposed by the arm B had been removed.

To keep the temperature in the oven constant, it was vital to keep the oven closed through the whole duration of a creep test. It had been noted that whenever the oven was opened, there

resulted in temperature as well as humidity fluctuations greater than 10°C and 20% respectively. It is for this reason that there arose a need to devise a system by which the extension of the specimen could be read from outside the oven, without opening it during the experiment.

The following system was devised as presented in Figure 3.2: As the specimen was stretched downward in tension, the pointer beneath the weights pushed the flexible bar. The flexible bar had a strain gauge along its length on either side so as to determine the extent of bending. As the bar was bent, readings of bending strain were recorded on the strain recorder. In this way readings were taken without opening the oven during the test. However, there was need to convert the readings of bending strain of the flexible bar into readings of extension during creep. This conversion will be presented in the section 3.3 on calibration of strain gauges. With the set-up in Figure 3.2, it was possible to run three tensile creep tests concurrently albeit at the same temperature since there were three rigs in the oven mounted side by side.

3.3 Calibration of Strain Gauges

There was need to establish a relationship between the actual extension on the specimen and the bending strain on the flexible flat bar shown in Figure 3.2. Since three tests were running concurrently, there were three strain gauges to be calibrated using one of the methods described in Dally and Riley (1985). These were named Strain Gauge 0, Strain Gauge 1 and Strain Gauge 2 respectively. For each strain gauge, the bar was bent without a load and the corresponding strain meter reading recorded. The corresponding vertical displacement (which represented extension) for each bending level was determined using vernier calliper and recorded. A curve was then plotted of extension versus strain gauge output.

For each curve, the equation relating the extension to the strain meter reading was obtained (using Microsoft Excel) as well as the coefficient of determination r^2, to give an indication of how well the actual line is estimated by the straight line equation. Using the equations, it was possible to convert any values of bending strain of the bar into values of extension of the specimen. From these readings of extension, it was possible to calculate strain values. For each flexible flat bar, three test runs were done, hence for every gauge there were three curves.

3.4 Tensile Testing

The tensile tests were carried out at the Kenya Bureau of Standards' Textiles Laboratory using the Testometric Tester M350-5kN type DBBMTCL made by SDS Atlas, Rochdale, England. The test was done with five replications at a speed of 500mm/min as per the standard ASTM D638 (2003) at an average temperature of 23°C and 50% relative humidity.

The initial purpose of tensile testing of the specimens was to determine the range of loads that may last long enough to achieve a considerable time for the creep test. However the more fundamental reason for carrying out the tensile test was to compare the change in the tensile strength and strain as the test material ages with time and under different conditions. In particular, tensile tests were carried out for fresh specimens and on specimens that had been exposed to natural degradation for 3 years and 7 years respectively. It was also conducted on specimens that had been incubated in Igepal® and those that had been exposed to UV radiation.

3.5 Tensile Creep Rupture

This set of experiments was performed to determine the short term creep properties of the material as per ASTM D 2990 (1995) standard. This was done to determine the range of loading

of the material for both long term and short term creep experiments. The results may also be used for design purposes, since the creep envelope determines the maximum loading range for the material. The specimens were stressed with dead loads to failure in relatively short time (longer than required for tensile test but shorter than required for creep tests, on average 24 hours). Specimens were tested at 20°C, 28°C and 48 °C. For each temperature, three specimens were tested at each of the following stresses induced by dead loads: 7.8, 8.1, 9.3, 10.2 MPa so as to achieve the range of loads and time to failure as specified in ASTM D 2990 (1995). The specimens were placed on the test rig, loaded with the weights and the timer started. Readings of elapsed time, temperature, relative humidity and extension were taken. The results of the creep rupture were presented graphically.

To obtain the creep envelope, individual curves of strain versus time for different loads at three temperature levels, 20°C, 28°C and 48°C were plotted. The creep rupture envelope was presented in two ways:

1. By joining the points on each creep curve where the onset of failure begins represented by a sudden increase in the steepness of the creep curve just before failure.
2. By plotting stress versus time to failure on a log – log scale

3.6 Tracking Progression of Aging by Light Microscope

In order to track the progression of aging, micrographs were taken by light microscope, to such a magnification as to be able to view the external changes taking place on the surface of the material under study in a manner similar to that employed in Kolarik *et al*, (2003). These micrographs were taken on specimens at magnifications of ×100 and ×200. The micrographs

were taken of freshly manufactured specimens, naturally degraded specimens (at 3, 4 and 7 years), specimens treated in Igepal® and those exposed to artificial UV radiation. The specimens were prepared and mounted on the microscope and the photographs taken by a digital camera from the eye piece of the microscope. An analysis of the pictures was then done.

3.7 Modelling Short-term Creep and Creep Compliance

This was done so as to determine the effect of temperature in the short term prior to performing the Time-Temperature Superposition as done by Smith (2005). The approach used in modelling short-term creep was by trying out different models such as the power law to see to what extent they would describe the data. In particular, this method was used to determine the effect of different levels of applied stress on the specimen as well as the effect of elevated temperature.

3.7.1 Determination of the Effect of Applied Stress

Creep curves were obtained by applying different stresses at constant temperature as suggested by Smith (2005). This was done at 30°C, 40°C and 50°C. For each temperature level, three different stress levels (0.78 MPa, 0.94 MPa and 1.56MPa) were applied and then the following was done. From total time dependent strain ε_t obtained from the strain experiment, the stress-dependent initial strain ε_o (the initial steep section of the creep curve) was subtracted. Curves were then plotted of Log(t) versus Log(ε_t- ε_o) and the y-intercept at Log(t) = 1 recorded as m and the slope recorded as n. These were then used to obtain the Findley Power Law Model as per Equation 2.13 for the creep at the constant reference temperature at which the creep readings had been obtained at three different stress levels. The results of this operation were then analysed.

3.7.2 Modelling the Effect of Temperature Variation

At temperatures 30°C, 40°C and 50°C, creep curves were obtained while holding the stress levels constant. The specimens were tested for durations of about 140 hours. The procedure used by Smith (2005) was then applied. From total time dependent strain ε_t obtained from the strain experiment, the stress-dependent initial strain ε_o was subtracted. Curves were then plotted of Log(t) versus Log(ε_t- ε_o) and the y-intercept at Log(t) = 1 recorded as *m* and the slope recorded as *n*. These were then used to obtain the Findley Power Law Model for the creep at the reference temperature.

3.8 Construction of Creep Master Curves (Time-Temperature Superposition -TTSP)

This was done so as to predict the long term creep behaviour of the material at a reference temperature of 30°C at which the material under study is normally used under tropical conditions.

3.8.1 Duration of Testing

Time Temperature Superposition (TTSP) was performed to obtain the long term creep properties of the material. It was determined from earlier work by Smith (2005) that to get reasonable TTSP results for predicting properties up to 50 years lifespan, 120 hours of loading is sufficient. Since the expected lifespan of the material under investigation is in the range 10 to 20 years, the duration of testing of about 140 hours that was used is deemed to be adequate.

3.8.2 Experimental Design for Creep Experiments

Creep curves were obtained for the following types of specimens using the set-up shown in Figure 3.2 by applying dead loads at different levels:

1. Fresh specimens at 30°C, 40°C and 50°C to serve as the reference point or control and to determine the effect of elevated temperature on the material. These specimens were also used to model the effect of load and temperature in the short run, including construction of the creep rupture curve as described in Section 3.7.
2. Fresh specimens exposed to alternating temperatures during loading at between 20°C – 30°C, 30°C - 40°C, 40°C - 50°C and 50°C - 60°C so as to determine the effect of material exposure to alternating temperature.
3. Specimens with welded joints tested at 30°C, 40°C and 50°C.
4. Specimens degraded naturally for 3 years tested at 30°C, 40°C and 50°C.
5. Specimens degraded naturally for 4 years tested at 30°C, 40°C and 50°C.
6. Specimens degraded naturally for 7 years tested at 30°C, 40°C and 50°C.

3.8.3 Shifting procedure

To obtain a master curve, the individual creep curve segments were shifted along the log time axis. Rapid changes of the creep gradient are normally seen in the early stages of straining (initial strain) but after 1 hour or so, the curves seem to be of fairly low gradient, which indicates the steady state of the creep process. An adjustment for initial strain was done before any shifting was carried out in the log time axis to obtain smooth master curves. For better matching of individual creep curves, the shifting was performed for the steady state regions of the creep curves, so the creep data up to maximum stress dependent strain (ε_0) was omitted when TTSP

was applied for 30°C, 40°C and 50°C. The upper tail of the master curve represents the rupture time of the specimen if the last creep segment was tested to failure. However, this stage was hardly reached for most of the specimens as the loads applied were generally low. Once the creep curves were obtained, they were plotted on semi-log scale, with the time (x) axis having the log scale. To make it easy to do this operation in Microsoft Excel®, it was found more convenient to convert all ordinary times to logs to the base 10 and then to plot the log time values against values of strain on an ordinary scale.

A temperature of 30°C was selected as the reference temperature, since most of the long-term applications of this material would be at this temperature. This is an average temperature in most of the places where the material is normally used. Hence the creep curve obtained by testing at 30°C was left in its original position while the curves obtained at 40°C and 50°C were shifted to coincide with the curve obtained at 30°C. To achieve this shift, a factor was added to the log time so as to map the shifted data on the reference curve. This was the horizontal shift factor, a_t and was recorded for each shifting operation.

3.9 Fitting a Curve to Creep Data

Various models were tried to describe creep data for the material, including power law variations, linear and semi-linear and hereditary type equations as presented in Chapter 2. The equation of the best fitting curve in each case was used to describe the creep data of the master curve. For each curve, the value of the shift factor as well as the other parameters of the best fit equation were determined and recorded.

3.10 Determination of the Effect of Welding Specimens

To determine the effect of welding on the material during operation, specimens were selected that included a welded joint in the narrow section of the dumbbell specimen. The specimens were then tested in tensile creep at temperatures of 30°C, 40°C and 50°C and stresses of 0.78MPa, 0.94MPa and 1.56MPa. The methods used in these test was similar to that described by Aithani *et al* (2006). This test was done so as to determine to what extent welding would limit the lifespan of the material during normal operation. All the welded joints were lap joints welded together by hot air fusion followed by application of pressure. In all cases, the welding had been done on site.

For comparison, welded joints (lap joints) were fabricated in the laboratory using the hot air and hot-knife techniques and tested using similar methods as those used for samples collected in the field. The pressure applied on the welded joint and the dwell time of the pressure were held constant at 0.3MPa and 10s respectively from Aithani *et al.* (2006). A variation was also made in the width of the welded joint from the field weld dimension of 1.3 cm to 2.6 cm. The peel, tensile and creep tests were done on the control specimens.

Hot air welding was simulated in the laboratory by heating the oven to the desired temperature. The specimens to be welded were prepared by covering the sections not to be melted with wood as insulation. The specimens were then placed in the oven for 10s. The sections to be joined were placed together and pressure applied.

The hot knife welding was done by incubating a flat bar of width 2.6mm in the oven at a given

temperature for 20 minutes. Two pieces of the material to be welded were placed to form a welded joint and the hot flat bar passed in the lap joint at the rate of 1cm/s for a weld piece of 10 cm. length. Pressure was then applied for 10 s. Specimens for subsequent tests were then prepared with a dumbbell cutter, with the welded section at the centre of the specimen.

3.11 Determination of the Effect of Alternating Temperature

In this experiment, the specimens were loaded at 0.78 MPa, 0.94 MPa and 1.56 MPa respectively in tensile creep. However during the course of the experiment, temperature was alternated between two temperatures with a difference of 10°C after every 24 hours. The temperatures were alternated between 20°C and 30°C, 30°C and 40°C, 40°C and 50°C, 50°C and 60°C. This experiment was done to evaluate whether stressing specimens in tension in alternating temperature has any effect different from similar tests carried out at constant temperature.

3.12 Constant Temperature Creep for Naturally Degraded Specimens

These specimens were subjected to tensile loading under constant temperature (first at 30°C, then at 40°C and 50°C) under the same load of 0.94 MPa as had been done for fresh specimens for comparison. This was done for specimens that had been exposed to natural degradation in the field for three, four and seven years. The creep curves obtained were then plotted alongside those that had been obtained for fresh specimens at the sae temperatures and the results analysed.

CHAPTER 4: RESULTS AND DISCUSSION

4.1 Calibration of Strain Gauges

The calibration curves are presented in Figure 4.1 (a) – (c) for Strain Gauge 0, 1 and 2 respectively. For each strain gauge, three trials were carried out and it is for that reason that there are three curves in each graph. Included in each curve are the equations for each curve and the value of coefficient of determination, r^2. The calibration had been carried out in line with Dally and Riley (1985).

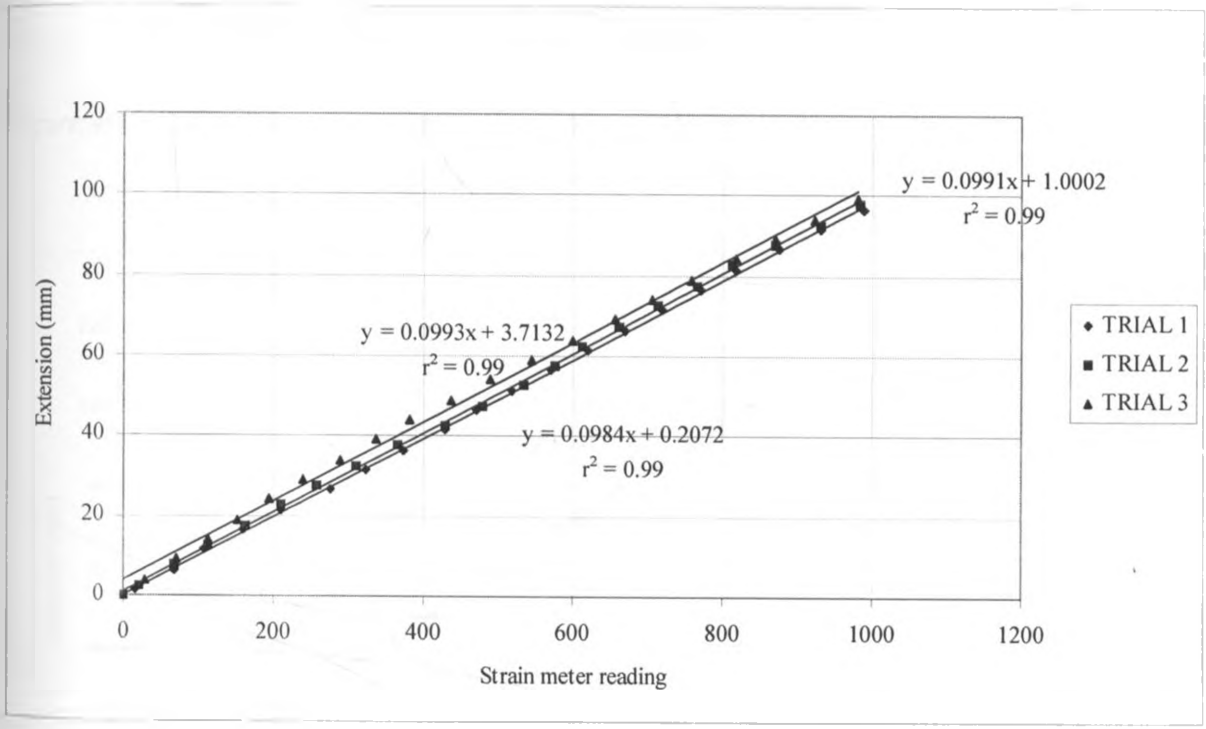

Figure 4.1 (a): Calibration curves for Strain Gauge 0

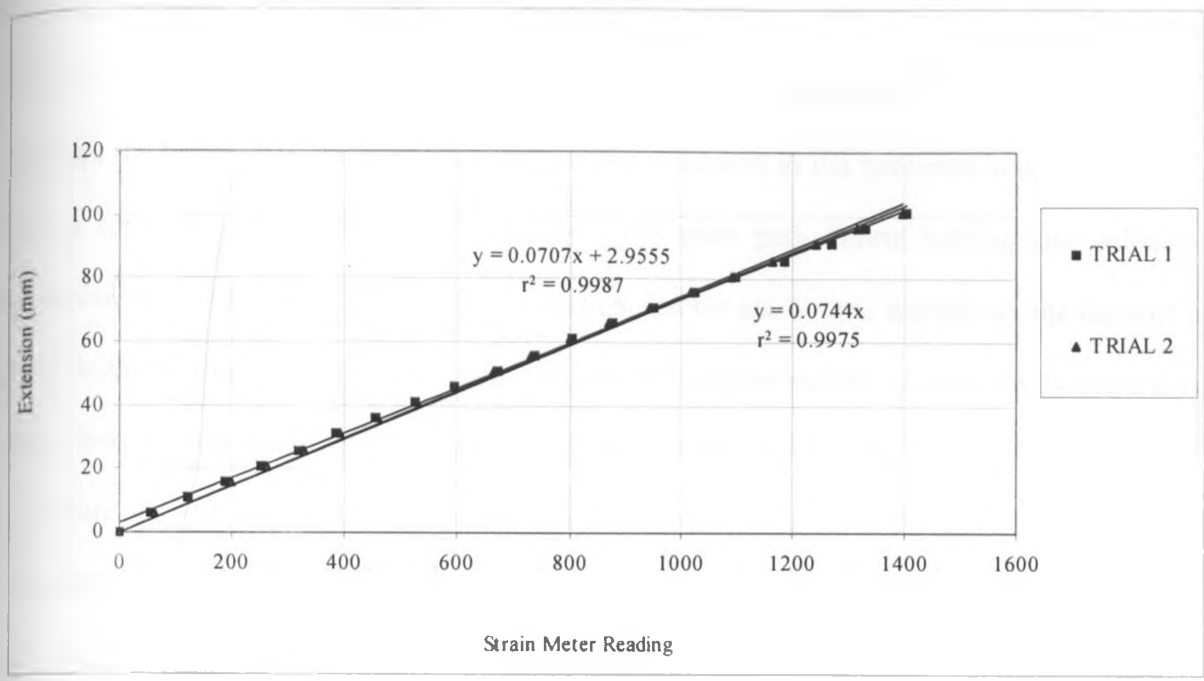

Figure 4.1 (b): Calibration curves for Strain Gauge 1

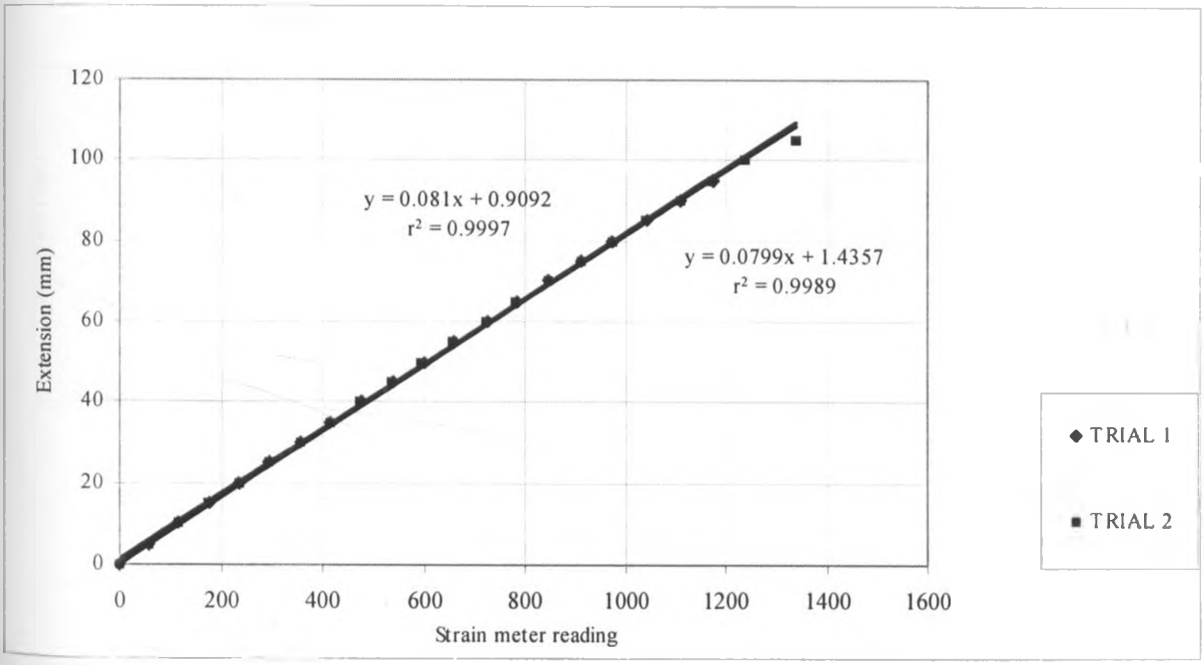

Figure 4.1 (c): Calibration curves for Strain Gauge 2

4.1.2 Combined Calibration Curves

From the calibration curves presented in Figure 4.1 (a - c), it was seen that that the relationship between the bending strain of the flat bar and the extension in the specimen was linear. All the curves for each gauge followed more or less the same path during loading and unloading. However, only one of the curves obtained was chosen for use in data analysis on the basis of the curve with the highest value of r^2 to represent the best approximation of linearity. Hence a set of three 'best' curves was selected for each of the three strain gauges and plotted on the same axes in Figure 4.1 (d). These are the curves that were used to convert all the values of bending obtained from the strain meter to values of extension that were used to calculate the strain resulting from creep experiments conducted.

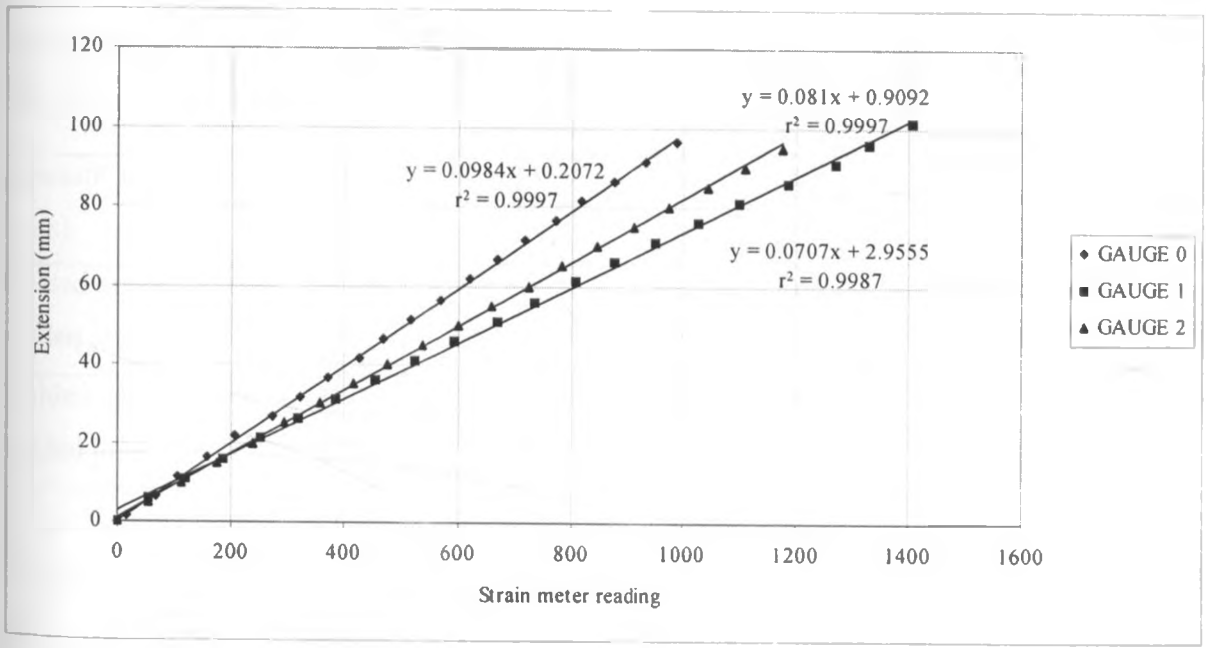

Figure 4.1 (d): Consolidated Calibration Curves

4.2 Tensile Test, Density, Shrinkage and other Observations

The tensile tests carried out on the various types of specimens yielded the results presented in Table 4.1.

Table 4.1: Results for tensile test

Specimen	Tensile strength (MPa)	Density (kg/m^3)	Maximum Strain (mm/mm)
Fresh	12	1290	3.5
3 year exposure to natural degradation	16	1240	2.2
4 year exposure to natural degradation	18	1220	2.0
7 year exposure to natural degradation	25	1070	1.3
Exposure to Igepal® (2 weeks)	12	1280	3.5
Exposure to UV radiation (80 hours)	12	1285	3.5
Welded specimen with 1.3 cm welded joint	5	1290	1.2
Welded specimen with 2.6 cm welded joint	11	1290	0.5

All the experiments were carried out at a room temperature of 23°C and relative humidity of 50%. As the first step to the research effort, the tensile test was useful in obtaining basic material properties especially the material strength at different stages of degradation and the maximum strain before material failure. The results obtained for tensile test were in the range 12 – 25 MPa,

while the results documented in literature (see section 1.1.2) were slightly higher (15 – 40 MPa). Hence the results obtained from tensile experiments fall within an acceptable range. The result of maximum strain was useful in designing the test rig used in subsequent experiments particularly those involving tensile creep since with this result it was possible to predict the expected elongation and be able to optimize test chamber dimensions.

By this test it was also possible to confirm the accuracy of the blanking die used to make the specimens. This was attributed to the failure at different positions along the length in the narrow section of the dumbbell specimens.

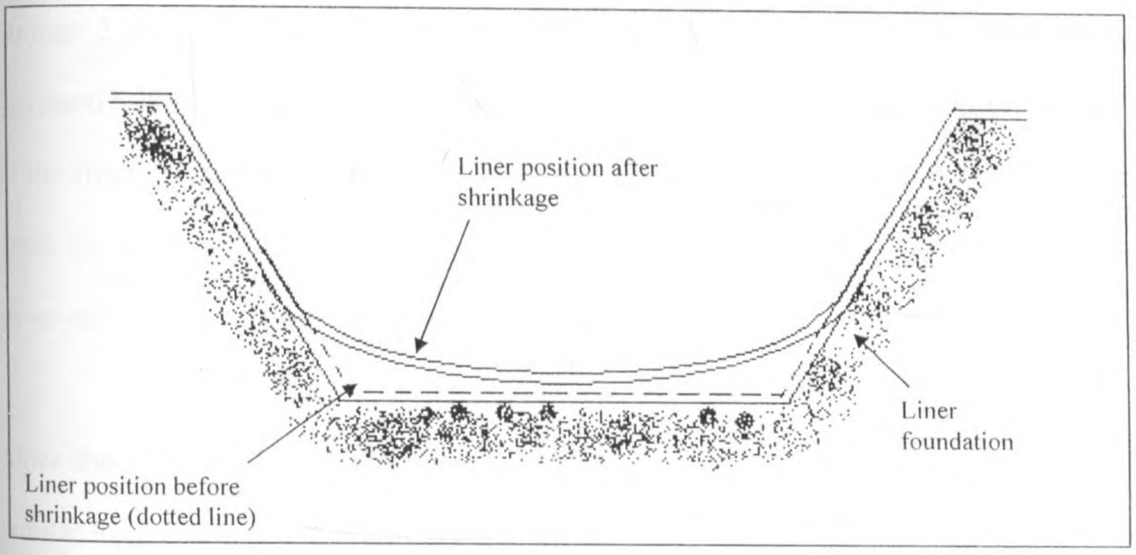

Figure 4.2 (a): Effect of shrinkage on dam liner (This is normally observed when no allowance is made for shrinkage during initial installation)

As can be seen in Table 4.1, the tensile strength increased with time of exposure to the natural environment. That is, the specimens that had been exposed to the natural environment for 7 years

were found to be strongest followed by those that had been exposed for 3 years and the fresh specimens were found to have the smallest tensile strength. There was need to provide an explanation for this phenomenon. It had been observed in Kenya Rainwater Association (2004) during field visits that the material actually shrunk over time as depicted in Figure 4.2 (a). Therefore, it was expected for the density to increase. Hence density was determined for each specimen with different exposure time to the natural environment.

It was found that the density of the material decreased with time of exposure to the natural environment as per Table 4.1. It was therefore concluded that the observed phenomena were the result of chemical activity associated with aging such as those discussed in Sections 2.1.3 through 2.1.8. This may be reinforced by the fact that the material was observed to have increased brittleness over time. The increase in brittleness over time was very pronounced since in the fresh samples there was absolutely no resistance to bending and it was not possible to break the material by bending. However it was possible to break the 7, 4 and 3 year old samples by several bending cycles.

Since the strength of the material was actually increasing over time, and the loads were of a similar nature and magnitude during that period of time, if the material failed then the failure would be due to another cause other than inadequate strength, otherwise it would have failed in the initial stages of loading when it had lower strength. However, the phenomenon of shrinkage depicted by Figure 4.2 (b) gives a clue as to the possible mode of failure of the degraded material that over time has become stronger but more brittle. If at one instant the reservoir had been empty and assumed the status in Figure 4.2 (a), where, the material was not in contact with the

bottom of the reservoir due to shrinkage, then during refilling, the sequence of activities will be determined by the age of the material. If the material is still flexible and elastic, it will creep to assume the shape of the reservoir and no failure will occur. On the other hand, if it has aged significantly, and is unable to creep sufficiently to cover the entire area of the reservoir bottom, then the overlying water will cause failure as shown in Figure 4.2 (b) since the un-reinforced plastic lining will be unable to support the massive weight of the water.

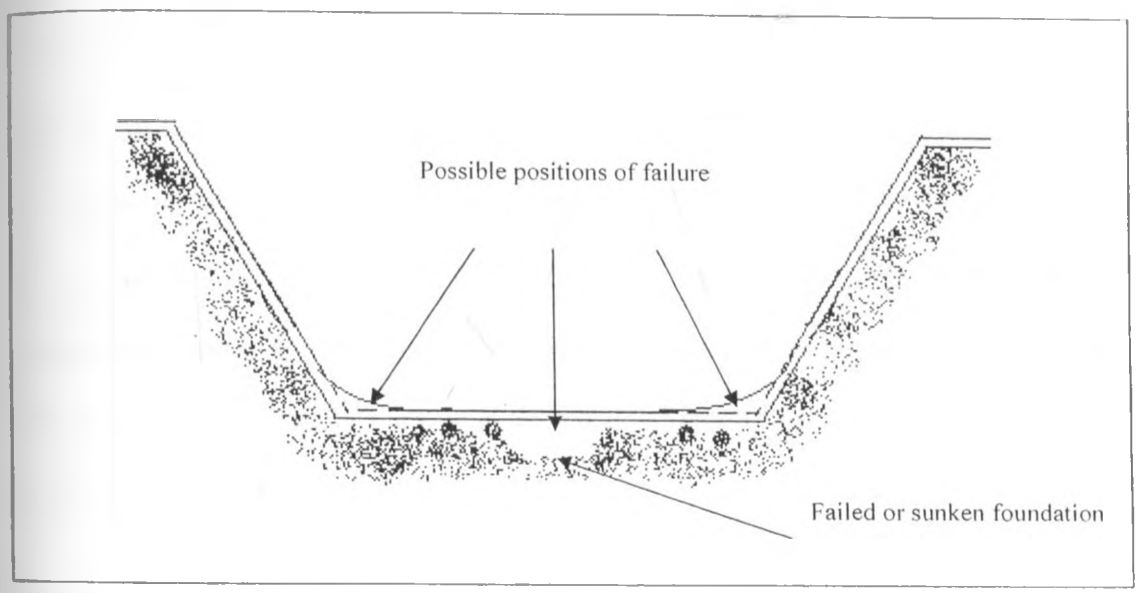

Figure 4.2 (b): Likely failure modes of a plastic liner in use

It was therefore concluded that one of the most important parameters determining whether the liner will fail or not is the strain achievable after exposure to natural degradation and not the strength. Hence, it was necessary to determine the maximum strain achievable for specimens exposed to thermal degradation for different durations as presented in Table 4.1. A detailed analysis is given of the effect of time of exposure on the maximum strain achievable in Section 4.11.

Field observations of failure were seen at points such as in Figure 4.2 (b) and the failures were round in shape, denoting punctures after sustained pressure (Kenya Rainwater Association, 2004). The best way to mitigate against such failures is to give an allowance of 10% extra material during the initial laying of the liner so that should there be any subsidence, the excess material would flow into the depressions, without requiring the material to deform to occupy the extra surface area. This would also guard against shrinkage of the liner, which was observed in the field to be the cause of some failures.

Table 4.1 also reveals that there was no change when the specimens were incubated in Igepal® for 2 weeks and also when the specimens were exposed to UV radiation for up to 80 hours. This can be explained by the fact that the product had been treated with carbon black and anti-oxidants which protected it against UV radiation and hydrolytic degradation respectively in the short term. For this reason, the values of tensile strength, maximum strain and density were similar to those of fresh specimens.

4.3 Creep Rupture

Figures 4.3 (a – c) represent the creep rupture envelope obtained by plotting strain versus time for fresh specimens. It was observed that the 20°C curve yields lower values of maximum strain than at 28°C and 48°C. Hence, the maximum strain in the material increases with temperature as can be seen more clearly by combining the three curves of rupture in Figure 4.3 (c).

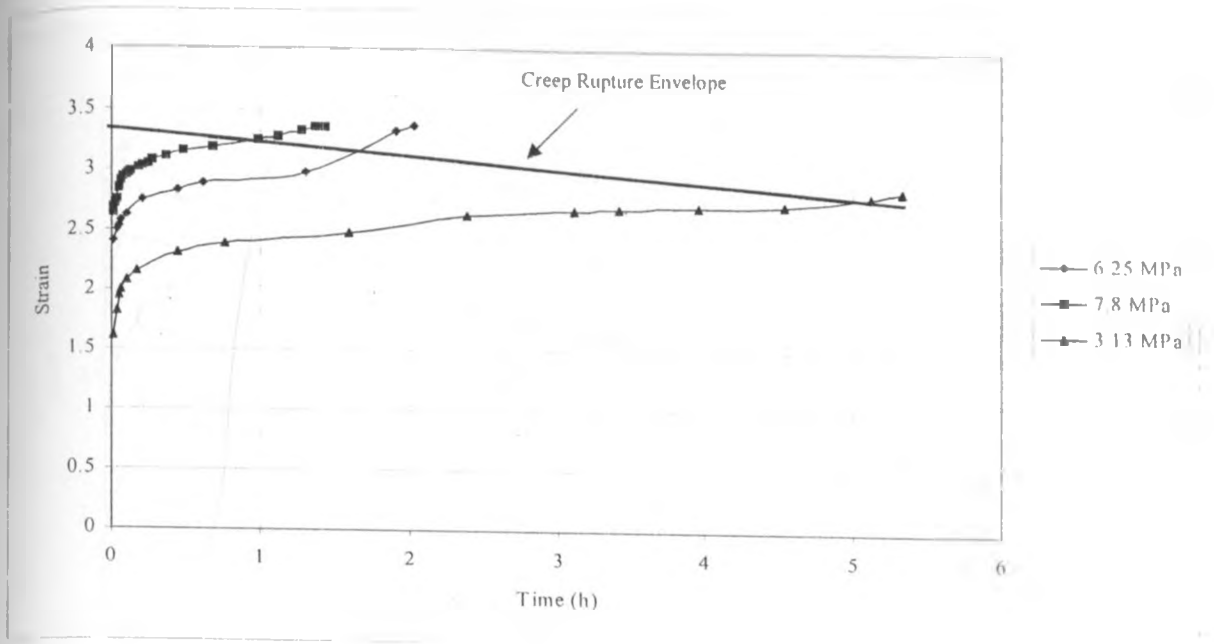

Figure 4.3 (a): Creep rupture envelope at 48°C

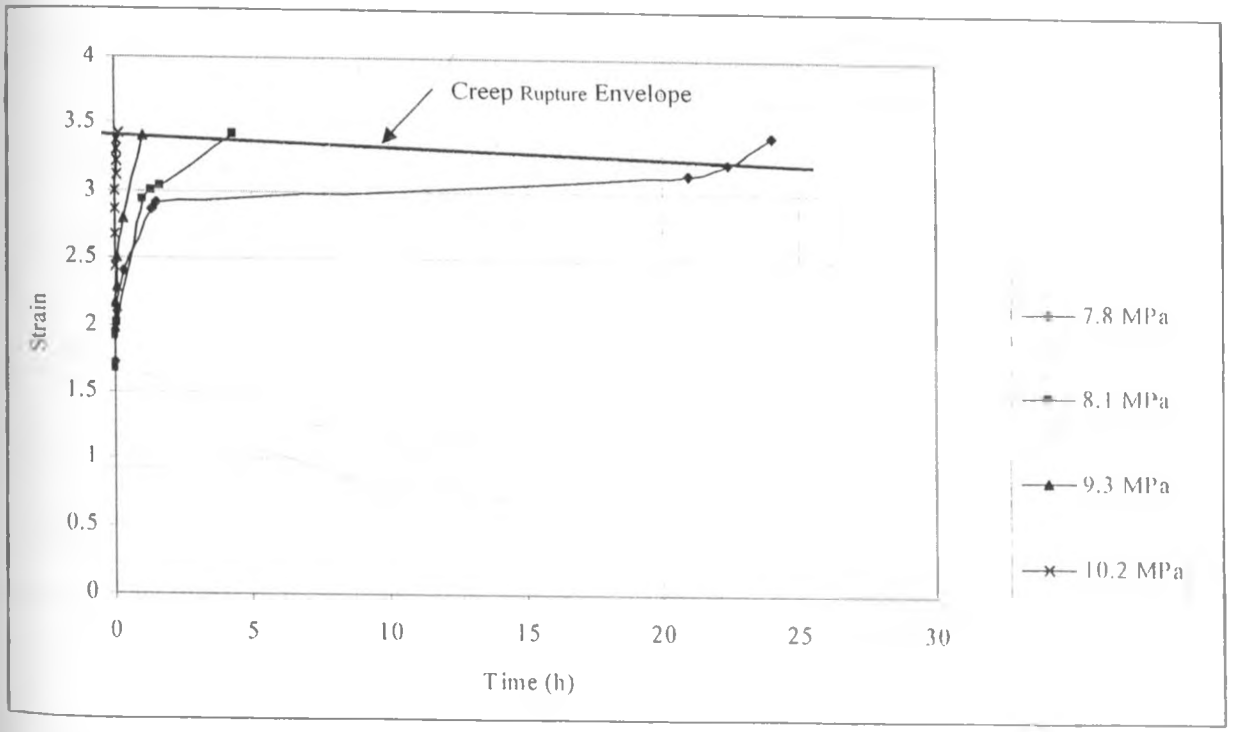

Figure 4.3 (b): Creep rupture envelope at 28°C

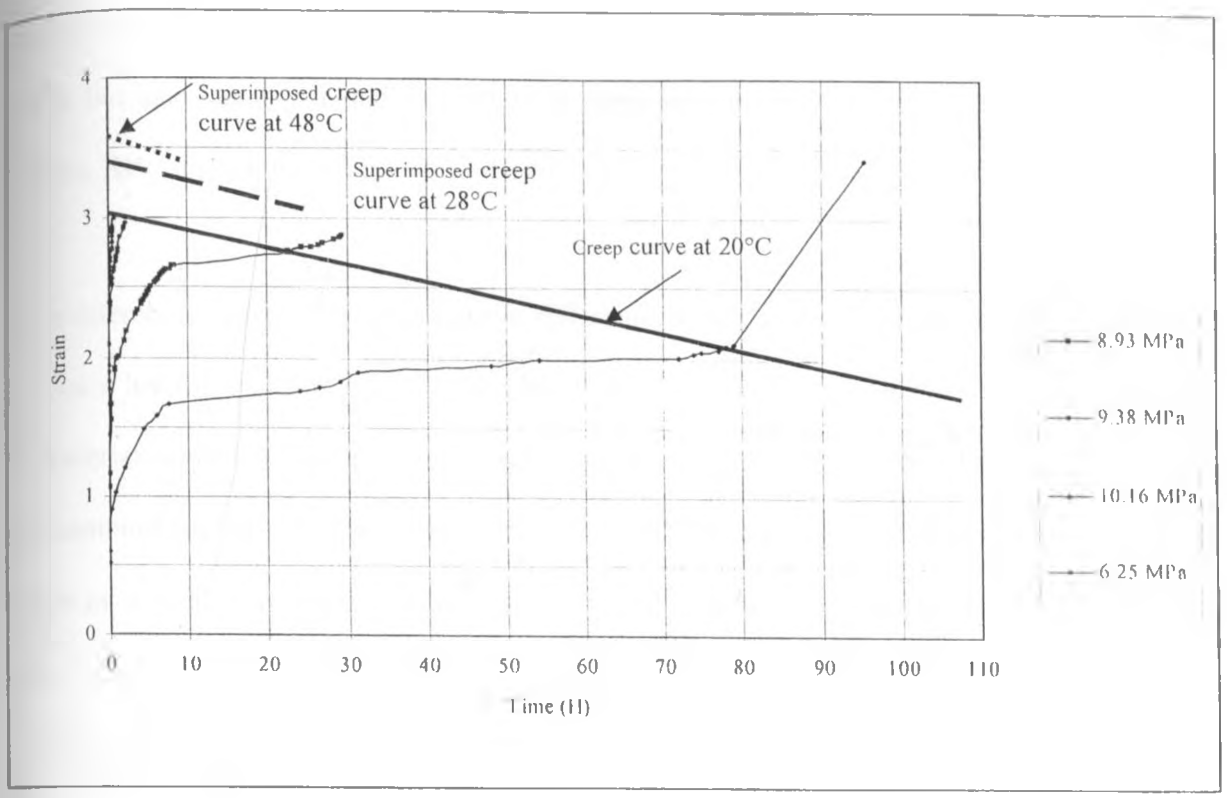

Figure 4.3 (c): Creep rupture envelope at 20°C

To obtain an accurate position of the creep rupture envelope different stresses were used all the time since the only important point was the inflection of the curve at the onset of tertiary creep. It is these points of inflection that were joined to form the rupture envelope. Since the construction of the creep rupture curve is a short term experiment, the dead loads used were much higher than those used during creep test so as to obtain tertiary creep in shorter times. However, the temperature was held constant during each experiment as the creep rupture envelope applies to a particular temperature.

A dramatic decrease was observed in Figure 4.3 (c) in the time taken to failure as temperature increased, from about 100 hours at 20°C to 20 hours at 28°C and below 10 hours at 48°C. This

result not only underscored the important influence of temperature on material properties of HDPE but also suggested that this effect is more pronounced between 20°C and 28°C than between 28°C and 48°C.

Other references define the rupture curve differently as the plot of applied stress versus failure time on a log-log scale (Hsuan, 2005). This curve would give an indication of how much time the material would last under a given load at a particular temperature before failure. In particular, any combination of load and time below the curve (creep rupture envelope) would not cause failure or would be safe to use at the particular temperature it represents. Hence the same data used in Figure 4.3 (a – c) was used to plot this second type of creep rupture curve and presented in Figure 4.3(d).

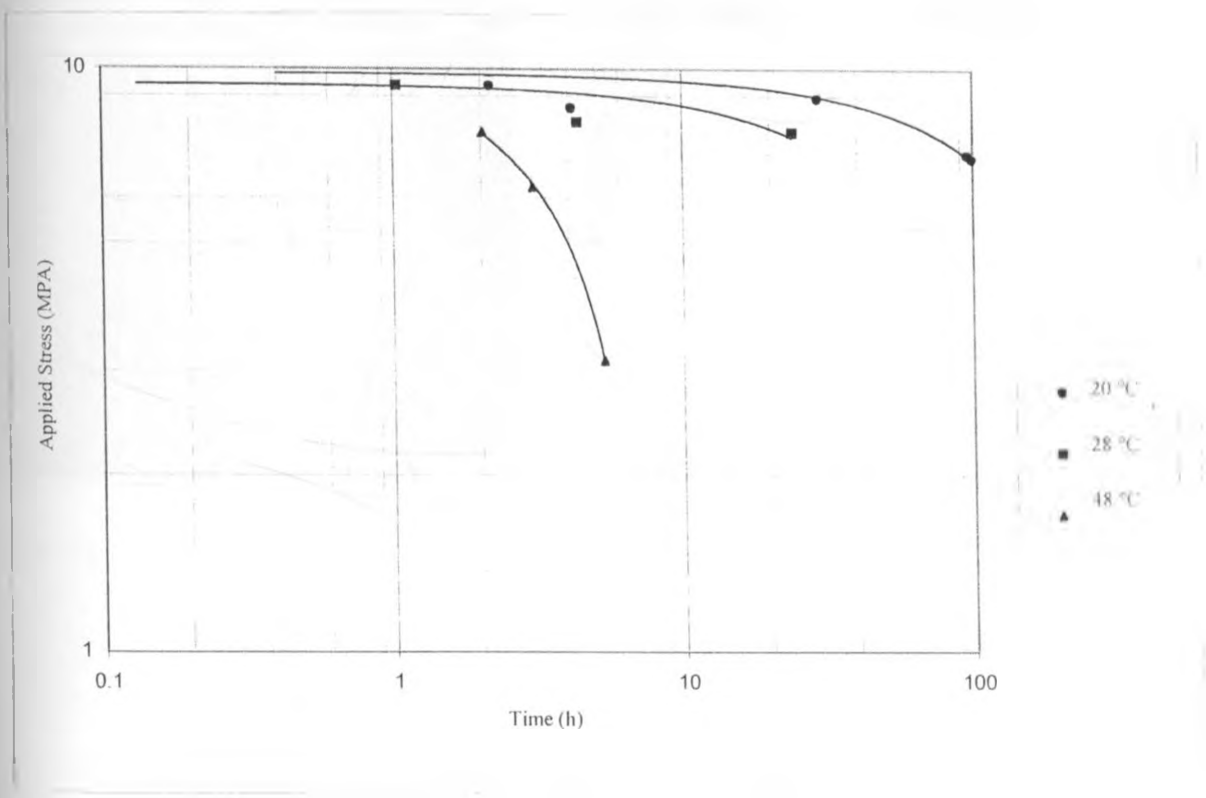

Figure 4.3 (d): Applied stress vs. failure time on a log-log scale

The curves obtained in Figure 4.3 (d) show a trend very similar to that in Figure 2.6 where, the trend line shows the curves bending downward as the time of loading increases (Plastics Pipe Institute, 2008).

4.4 Tracking Progression of Aging by Light Microscope

The micrographs that were taken using a light microscope were presented in Plates 4.1 – 4.9 beginning with fresh specimens followed by those with 3, 4 and 7 years of exposure to natural degradation respectively. All the units are in mm.

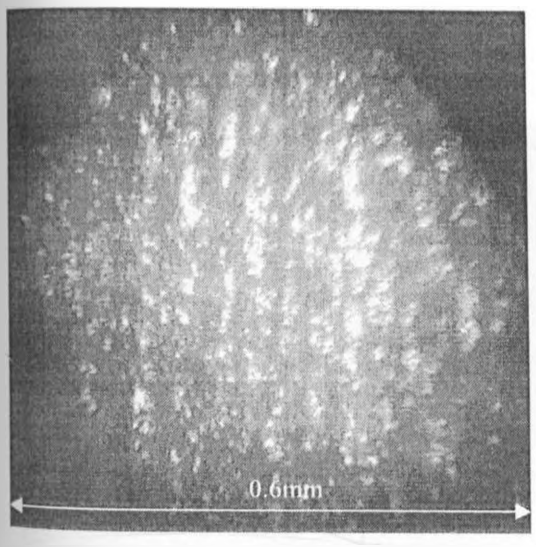

Plate 4.1 (a): Micrograph for Fresh specimens (×100 mag)

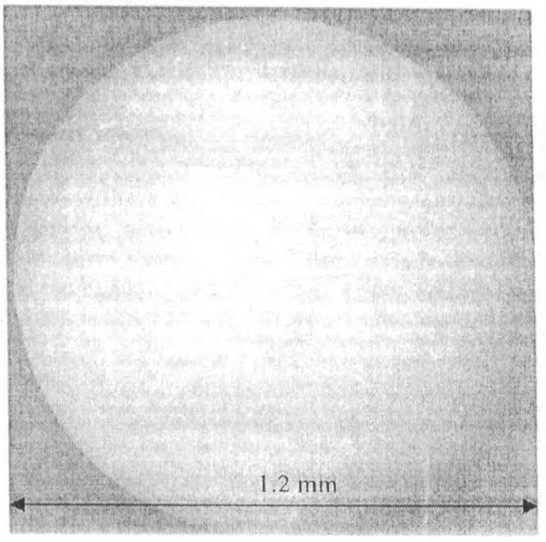

Plate 4.1 (b): Micrograph for Fresh specimens (×200 mag)

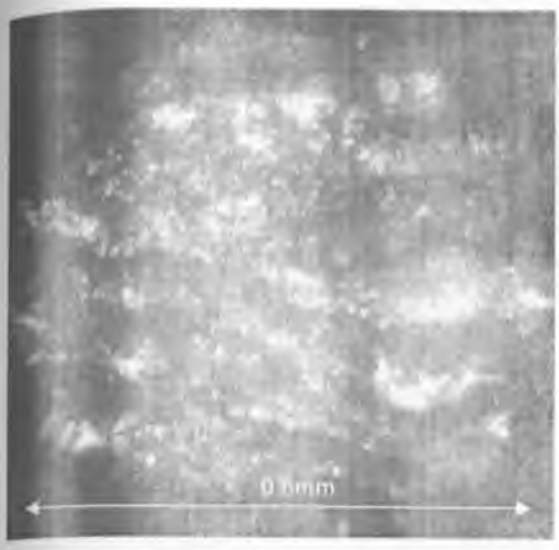

Plate 4.2 (a): Micrograph for specimen degraded naturally for 3 years (×100 mag)

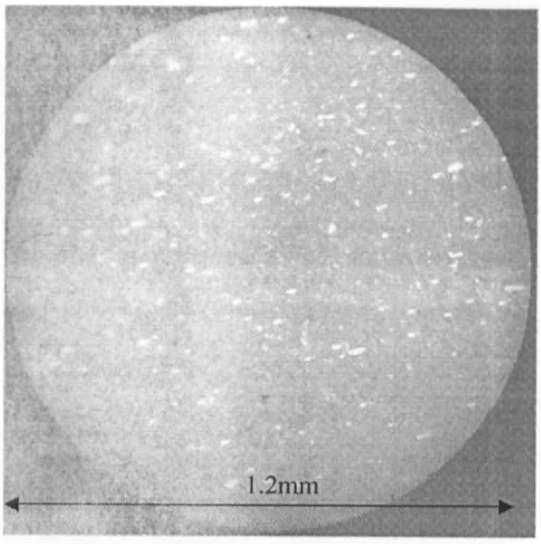

Plate 4.2 (b): Micrographs for specimen degraded naturally for 3 years (×200 mag)

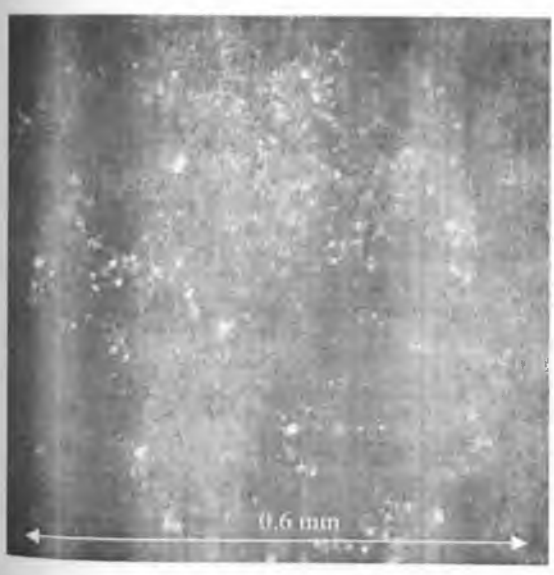

Plate 4.3 (a): Micrograph for specimen degraded naturally for 4 years (×100 mag)

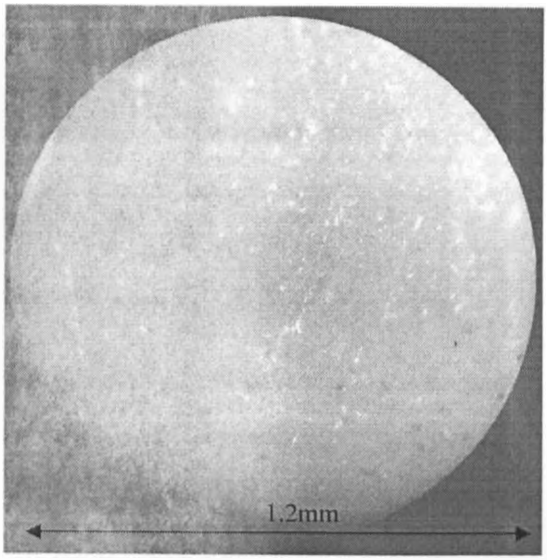

Plate 4.3 (b): Micrographs for specimen degraded naturally for 4 years (×200 mag)

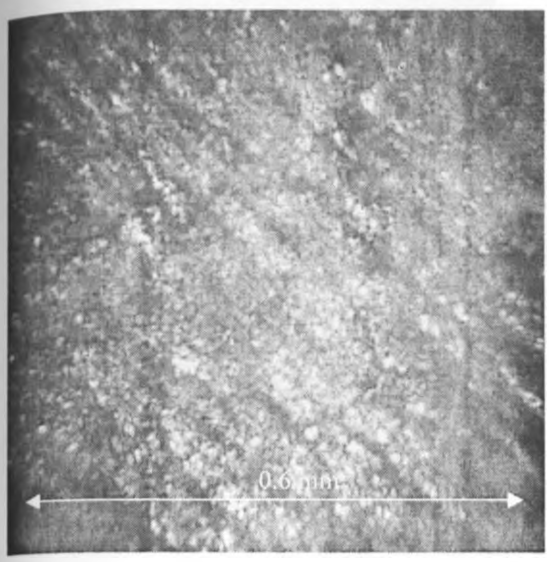

Plate 4.4 (a): Micrograph for specimen degraded naturally for 7 years (×100 mag)

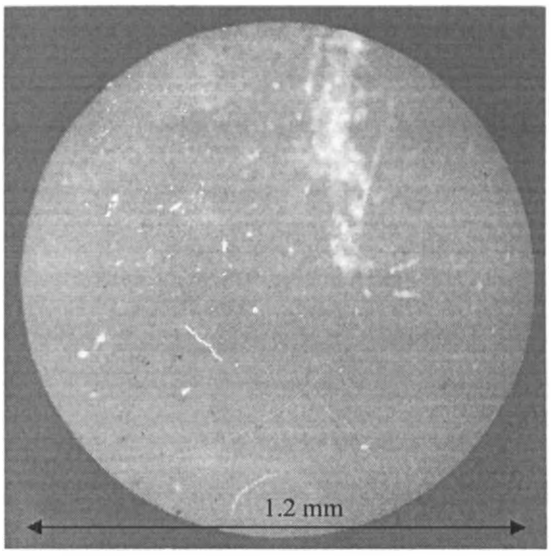

Plate 4.4 (b): Micrographs for specimen degraded naturally for 7 years (×200 mag)

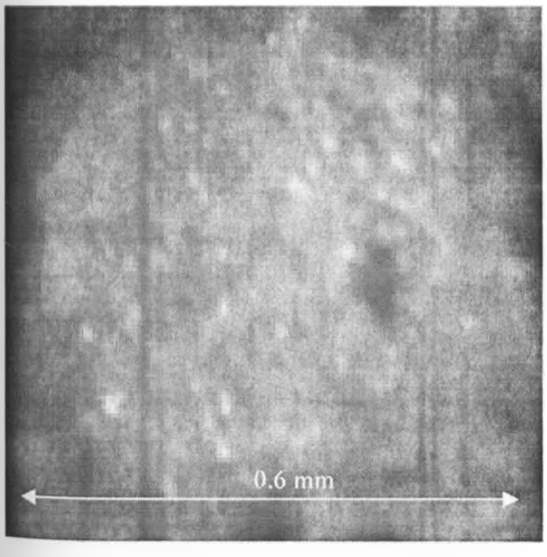

Plate 4.5 (a): Micrograph for specimen Incubated in Igepal® for 1 week (×100 mag)

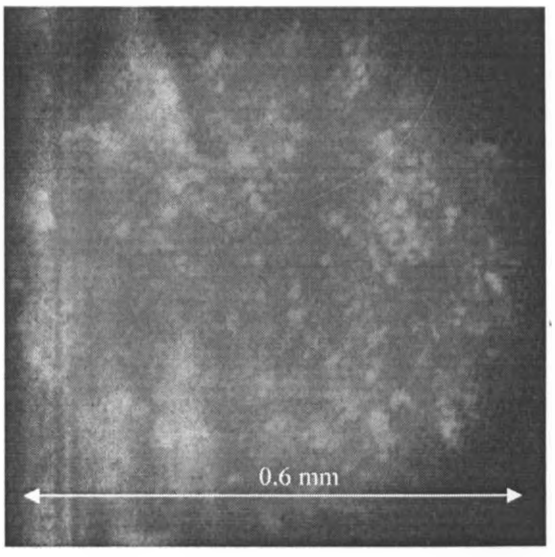

Plate 4.5 (b): Micrograph for specimen Incubated in Igepal® for 1 week (×200 mag)

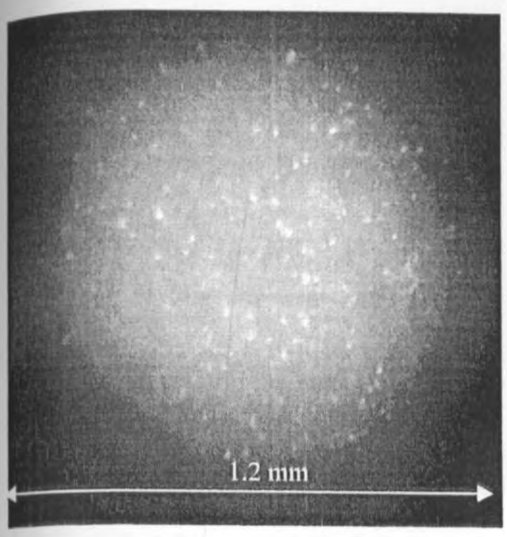

Plate 4.6: Micrograph for specimen Incubated in Igepal® for 2 weeks (×200 mag)

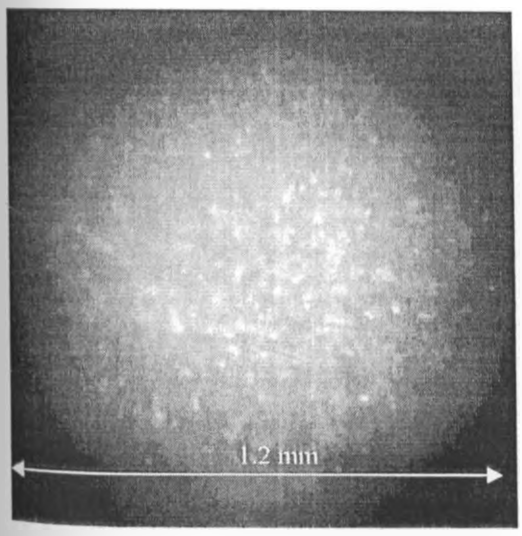

Plate 4.7: Micrograph for specimen exposed to UV radiation for 20 hours (×200 mag)

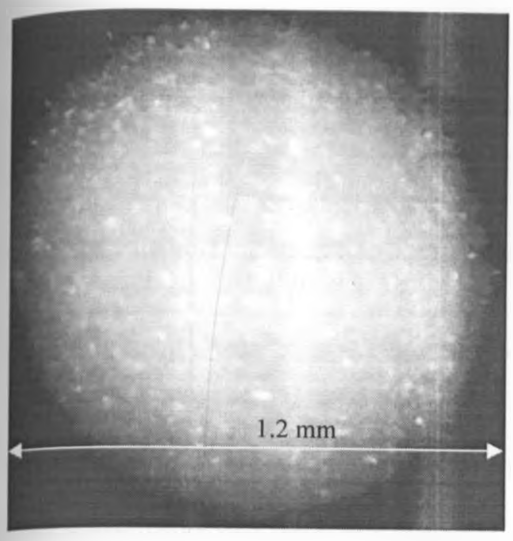

Plate 4.8: Micrograph for specimen exposed to UV radiation for 40 hours (×200 mag)

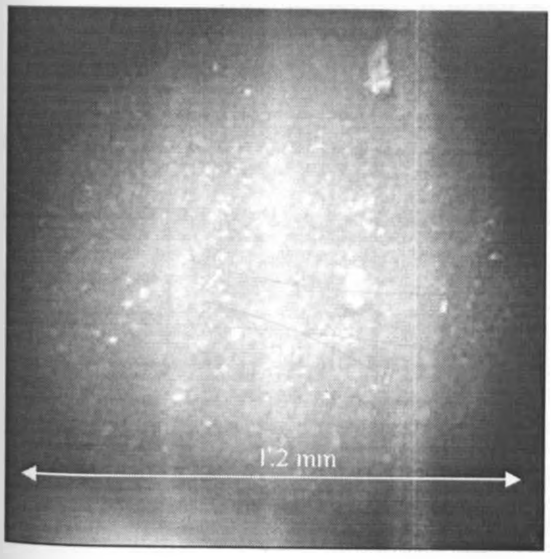

Plate 4.9: Micrograph for specimen exposed to UV radiation for 80 hours (×200 mag)

From the micrographs, it is clear that indeed there are profound physical aging processes that took place on the fresh specimen after exposure to the elements of degradation. In Plate 4.1 of fresh specimens, it was seen that the texture of the surface is smooth and even. However, as time progressed, the surface became rough, dented and scratched in many places as observed in Plates 4.1 through 4.5.

These dents and discontinuities become more visible in Plate 4.2, where it is possible to clearly see discontinuities that have formed on the surface of the material after 3 years and in Plate 4.3 after 4 years of exposure to natural degradation. It was observed that the 4 year specimen seemed less damaged than the 3 year specimen. This is attributable to the fact that the 4 year specimen was obtained from a shaded pond and may not have been subject to the full glare of the environmental degradation specifically elevated temperature, alternating hot and cold temperature and solar radiation. Hence, it was only subject to degradation by water and limited amounts of other degrading agents. It is not surprising therefore that the mode of degradation as seen in the size and shape of the white patches is very similar to the mode shown in Plate 4.5, that was only exposed to hydrolytic degradation as accelerated by incubation in Igepal® for one week. Plate 4.4 represents a specimen that was exposed to all the degradation agents for 7 years and the resulting damage is more pronounced than in the other micrographs. It is badly charred and cracks are clearly visible (see dark lines on the specimen). The material had by this time become brittle and stiff.

The specimens that had been incubated in Igepal® for 1 week in Plate 4.5 and two weeks in Plate 4.6 respectively as well as those exposed to UV radiation for 20 hours in Plate 4.7, 40 hours in

Plate 4.8 and 80 hours in Plate 4.9 show varying degrees of surface disruption. The micrographs of these specimens are closely related to the micrograph of the specimen exposed to natural degradation for 3 years by visual examination. However, this alone is not enough to make conclusions about mechanical properties.

4.5 Creep Data for Fresh Specimens

Curves in Figure 4.5(a) through Figure 4.5(c) are the creep curves obtained for material tested under three different stresses at three different temperatures of 30°C, 40°C and 50°C. These curves are presented on an ordinary scale and the initial one hour data (stress dependent strain, ε_o) normally removed during modelling is still retained. These curves represent the raw data obtained from the creep tests carried out.

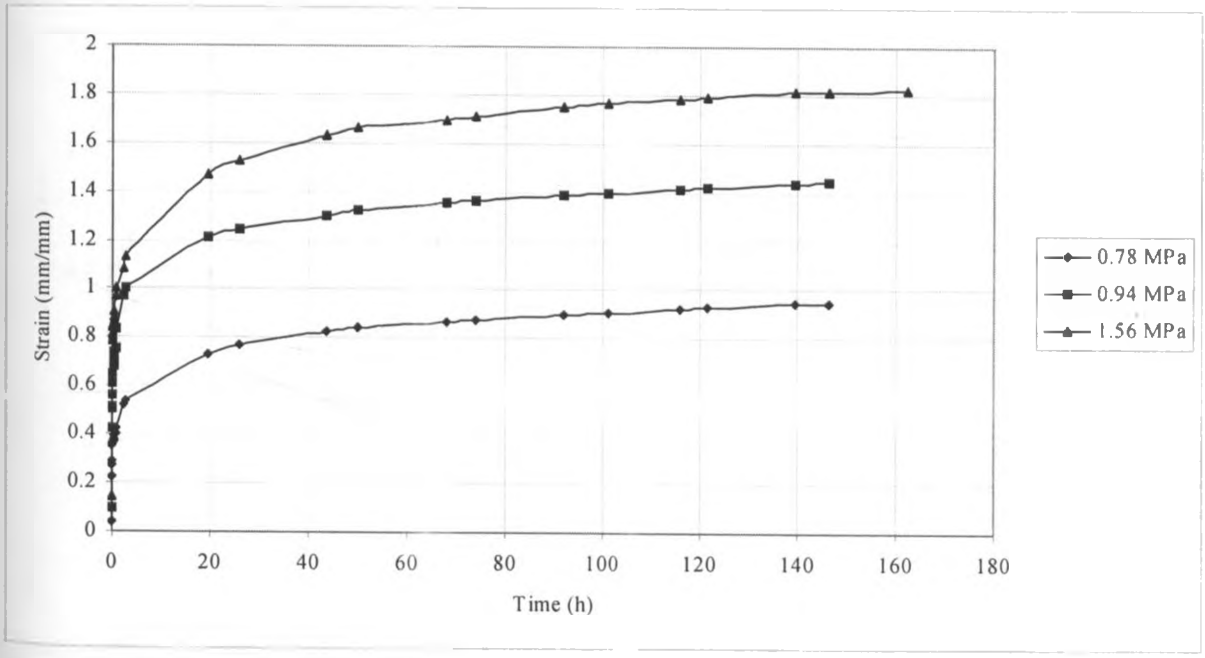

Figure 4.5 (a): Constant Temperature Creep Curves at 30°C

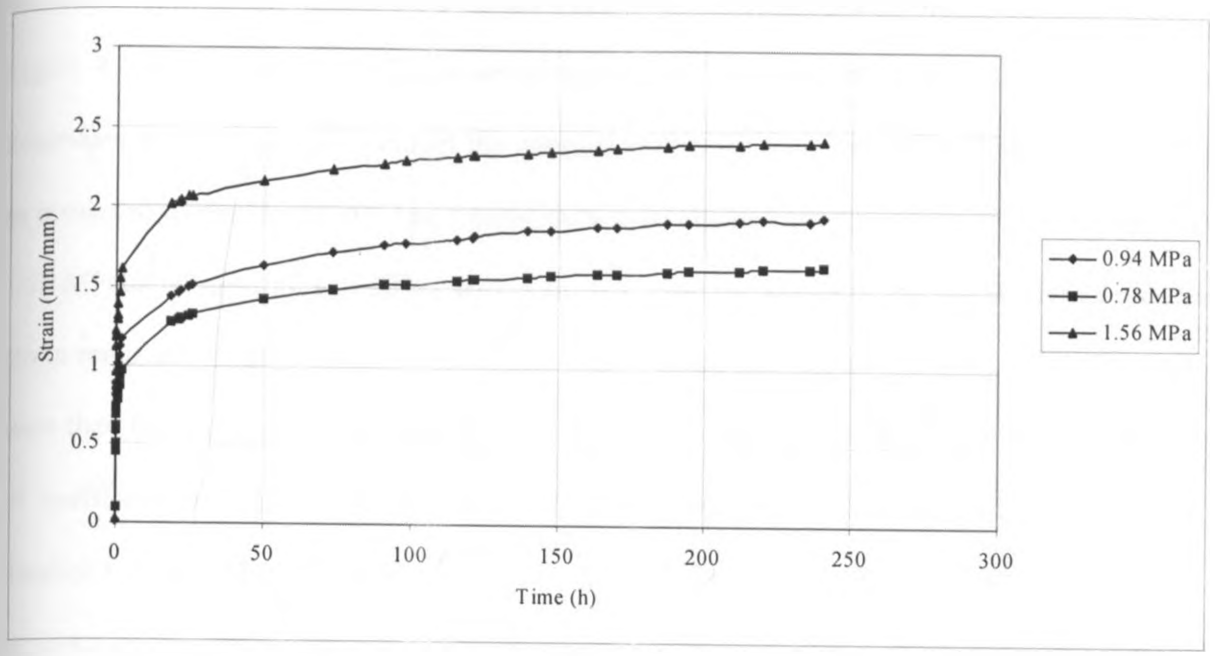

Figure 4.5 (b): Constant Temperature Creep Curves at 40°C

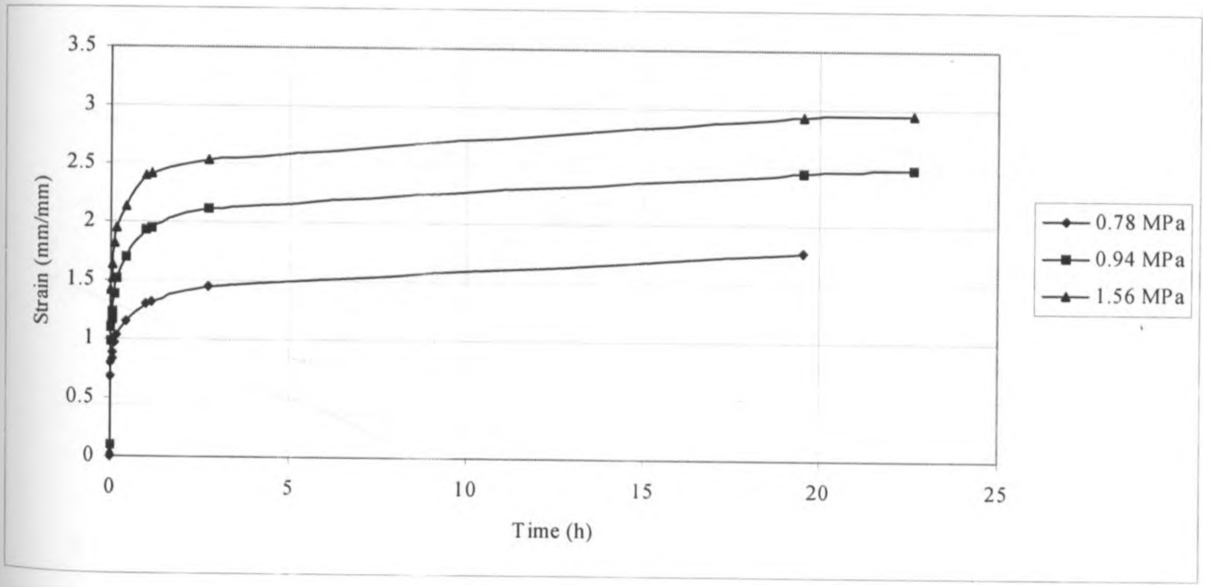

Figure 4.5 (c): Constant Temperature Creep Curves at 50°C

4.6 Determination of the Effect of Stress Variation on Fresh Specimens

Figure 4.6(a - c) are the modifications of curves in Figure 4.5 by removing the initial time-dependant strain (ε_o) so as to model the material behaviour according to the Findley Power Law as presented by Smith (2005). The figures show data at stress levels of 0.78 MPa, 0.94 MPa and 1.56 MPa at temperatures of 30°C, 40°C and 50°C with the values of the initial stress-dependent strain removed, so as to obtain plots of time versus strain ($\varepsilon_t - \varepsilon_o$) on a log-log scale. The curves were then fit by power law and the approximations were quite good as seen from the high values of coefficient of multiple determination, R^2. The curves were observed to be approximately parallel to each other. Since the curves are plotted for a constant temperature, the effect of temperature can be said to have been removed and any variation was attributed to change in stress.

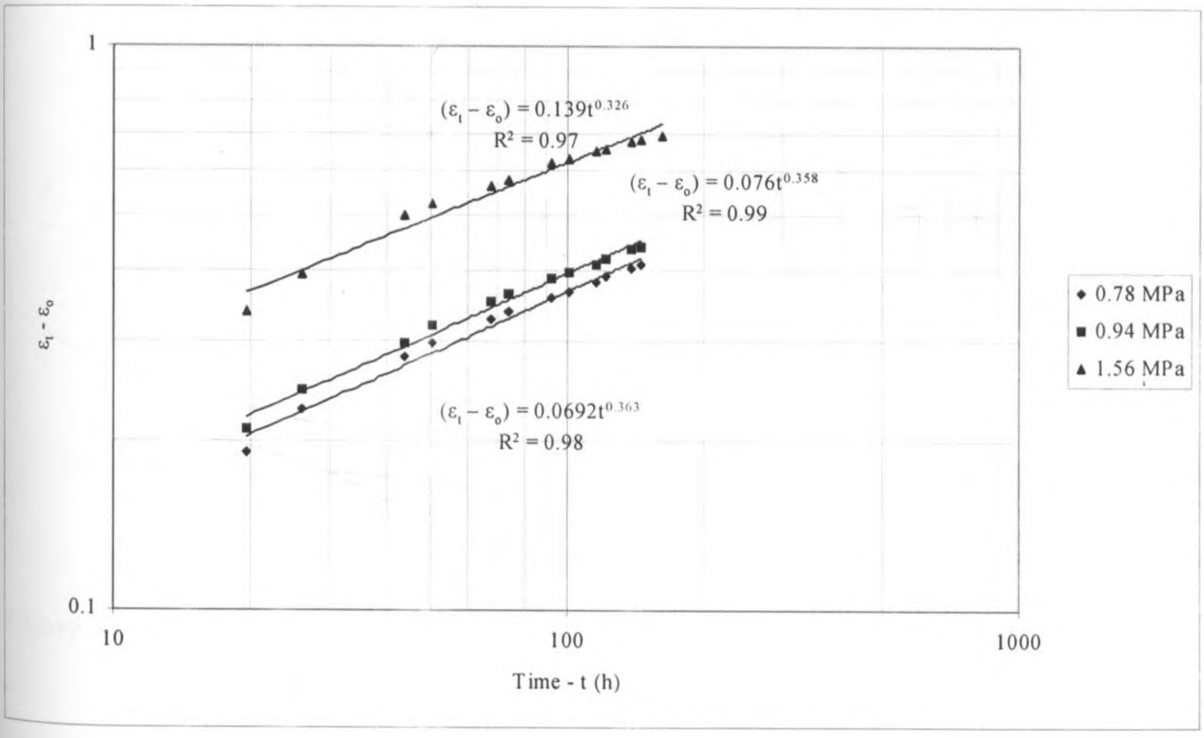

Figure 4.6 (a): Log-log curve of time versus strain ($\varepsilon_t - \varepsilon_o$) at the reference temperature of 30°C

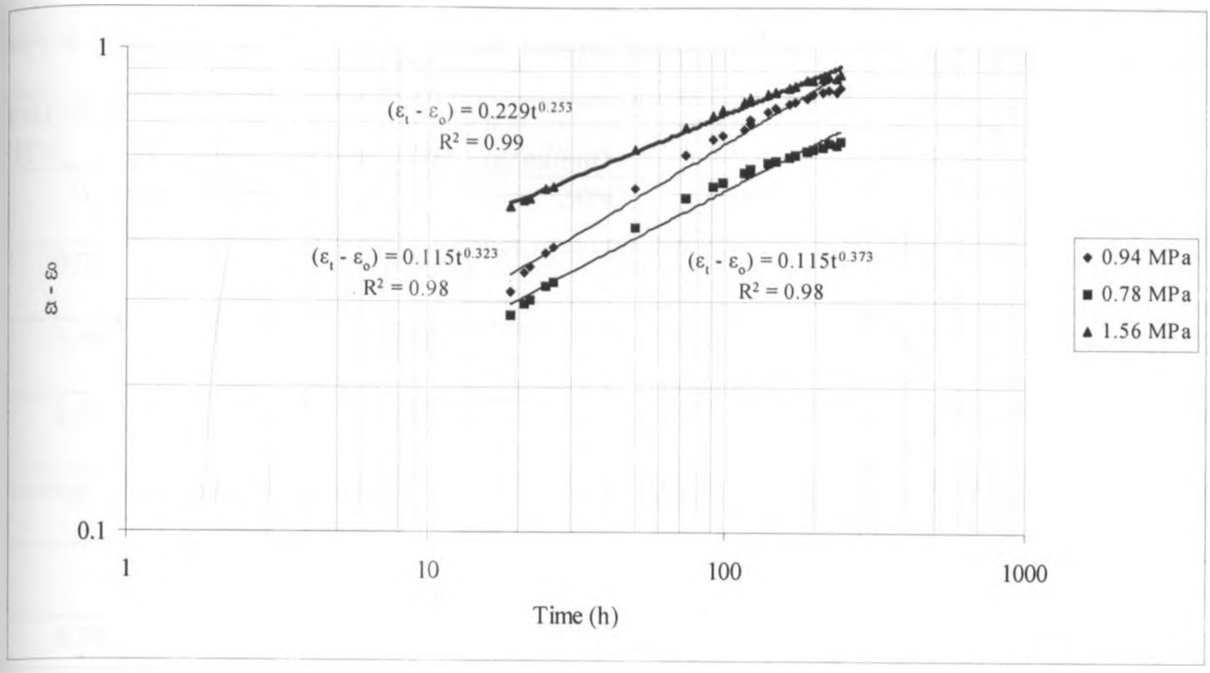

Figure 4.6 (b): Log-log curve of time versus strain ($\varepsilon_t - \varepsilon_o$) at the reference temperature of 40°C

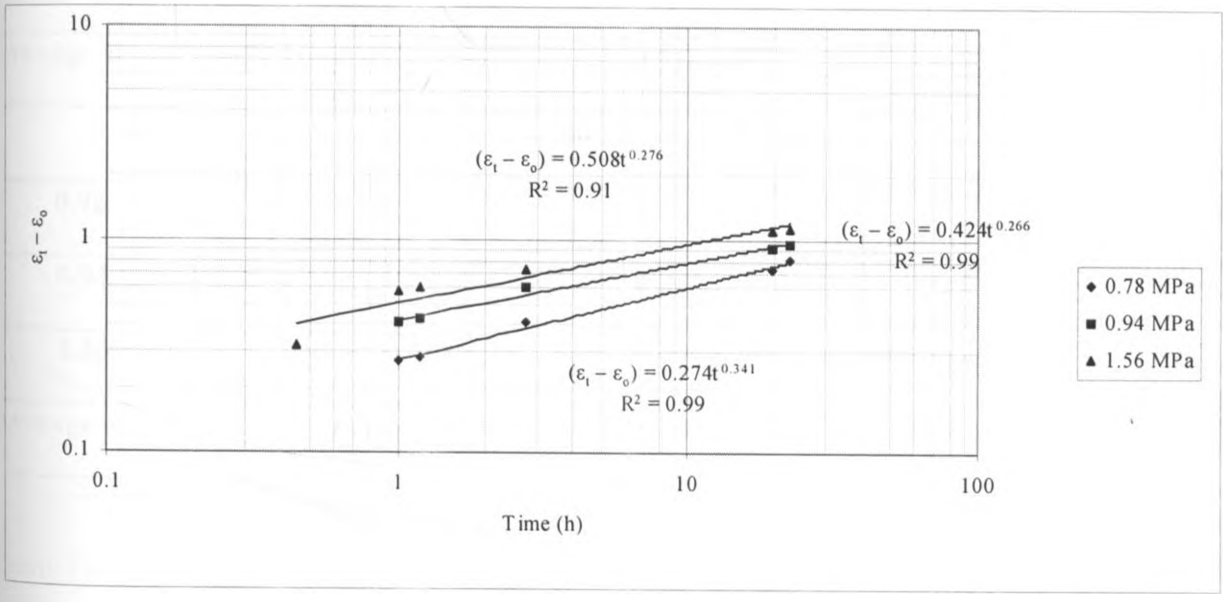

Figure 4.6 (c): Log-log curve of time versus strain ($\varepsilon_t - \varepsilon_o$) at the reference temperature of 50°C

A summary of the values of *m* (y-intercept), *n* (gradient), ε_o (initial stress dependent strain) and R^2 for the curves obtained at different stresses and temperatures is given in Table 4.2.

Table 4.2: Summary of the Findley Power Law parameters as stress and temperature are varied

STRESS (MPa)	*m* (*y-intercept at time =1h)*	*n* (*gradient)*	ε_o	R^2
30°C				
0.78	0.069	0.362	0.426	0.98
0.94	0.080	0.358	0.834	0.99
1.56	0.136	0.326	1.01	0.97
Average of *n* (Creep Exponent)		**0.349**	-	-
40°C				
0.78	0.115	0.373	0.968	0.98
0.94	0.115	0.323	1.168	0.98
1.56	0.229	0.253	1.607	0.99
Average of *n* (Creep Exponent)		**0.316**	-	-
50°C				
0.78	0.274	0.341	1.31	0.99
0.94	0.424	0.266	1.52	0.99
1.56	0.508	0.276	2.14	0.91
Average of *n* (Creep Exponent)		**0.299**	-	-

From Table 4.2, the exponent *n* was obtained by averaging the values of *n* for the different curves since this property does not change with increase of stress at the same temperature, according to various sources. This exponent has been called material constant by Smith (2005) and no detail has been given about its nature except that it is constant at a particular temperature. Reddy and Fluet, (1995) have also presented data modeled by the Findley Power Law showing

that the material constant n is independent of the applied stress and constant at a constant temperature. This was found to be true for the material under study. Since the curves at any temperature were found to be approximately parallel to each other, the gradient was taken as constant at a particular temperature and the average value was found at each temperature and stress level. From Table 4.2 it appears that exponent n decreases with increase in temperature. A firm conclusion may only be made with more temperature variations over a wide range of temperature since there is no clear stability of this exponent even at constant temperature and average values were only obtained on the strength of past work of similar nature.

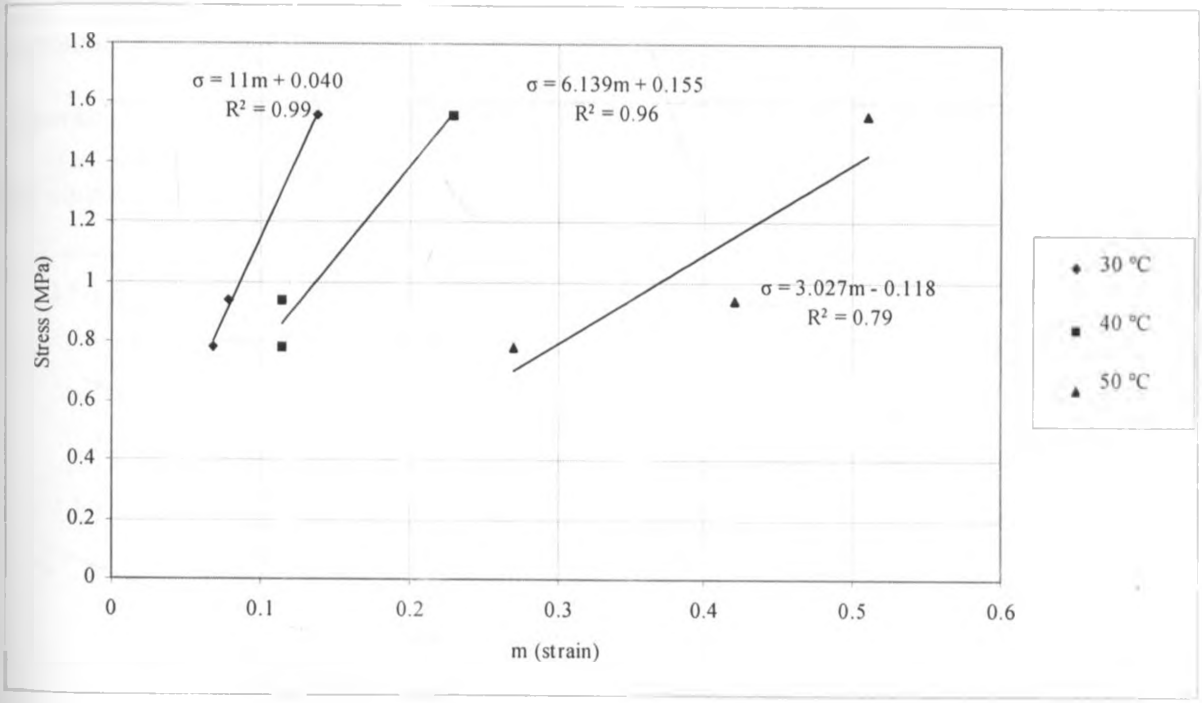

Figure 4.6 (d): Variation of m with stress at different temperatures

However, the y-intercept *m* (an expression of strain) was observed to increase linearly with the stress applied as per the curves in Figure 4.6 (d), drawn from the first two columns of Table 4.1 with *m* in the x-axis and the applied stress in the y-axis.

The values of coefficient of multiple determination, R^2 are quite high, indicating a strong case for linearity. Hence it is possible to predict the values of *m* induced by loads applied within the range (0.78 – 1.56 MPa), that is, by interpolation. The possibility of extrapolation could not be established due to the limited range of data. Once the values of *m* are known and the material constant *n* is also known, it is possible to predict the behaviour of this material at 30°C, 40°C and 50°C for any load applied within the specified range.

From Figure 4.6(d), it was also observed that the slope of the curves reduced as temperature increased. This serves to show that increase in temperature increases the strain levels at constant stresses. It was also observed that the curves had decreasing slope (moved from vertical to horizontal) as temperature increased. Therefore, from Figure 4.6(d) it may be suggested that as temperature increases, there may reach a certain temperature when the slightest stress applied may cause large strains or deformation.

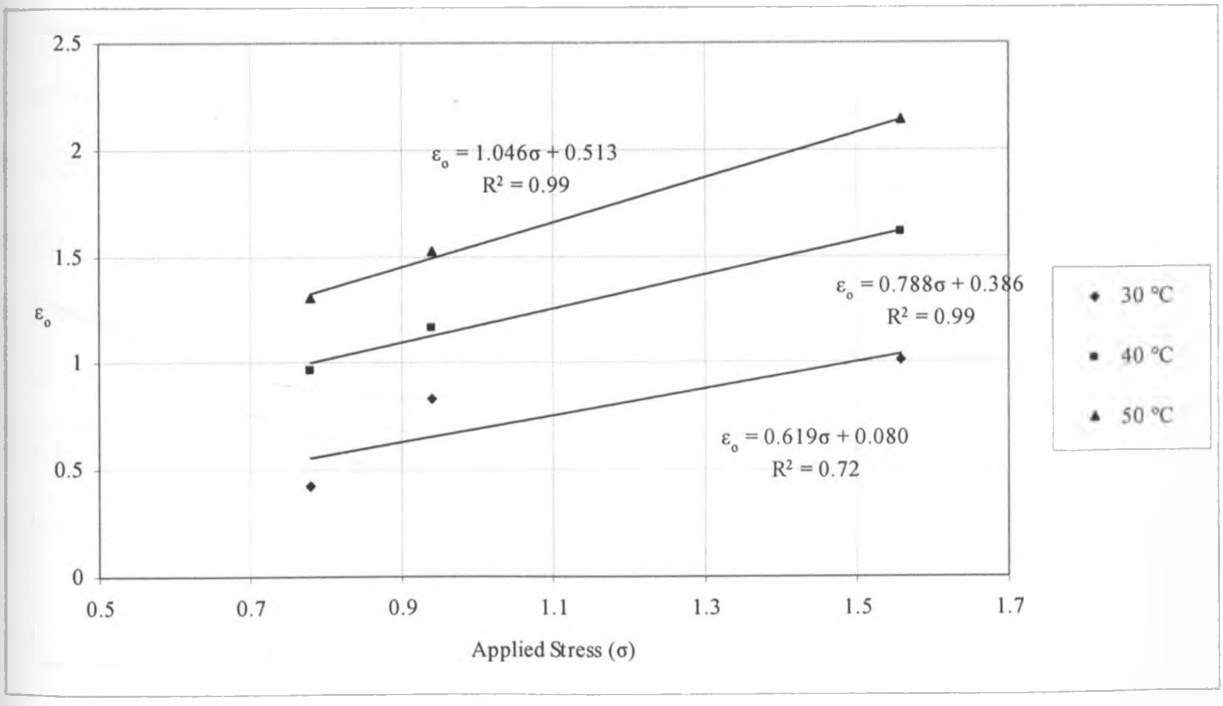

Figure 4.6 (e): Relationship between Applied Stress (σ) and initial strain (ε_o)

The maximum stress dependent strain, ε_o was found to increase as the applied stress increased. Since the ε_o occurs just at the end of the elastic phase of the stress-strain curve, a linear relationship was used to fit the curves as shown as shown in Figure 4.6 (e) with fairly high values of R^2.

Logarithmic relationships for the curves that had slightly better values of R^2 were rejected since there was no theoretical basis for adopting a logarithmic relationship for stress verses strain (ε_o) on the threshold of the elastic limit. The essence of relating m and ε_o with applied stress was to allow for the reconstruction of the creep curves when one only has the value of the applied strain.

This is due to the fact that from both Figure 4.6(d) and 4.6(e), when given only the value of the applied stress, one may obtain a good estimate of both ε_o and m and since n is constant at a particular temperature, it is possible to construct a creep curve for any temperature / stress combination desired within the range of the experimental data. This was deemed to be useful in predicting short term design data for low loads. Therefore the equation describing variation of creep strain with stress was summarized as per equation 2.13 of the Findley Power Law with the definitions of the variables as follows:

ε_t = Total time-dependent strain

ε_o = Initial elastic stress dependent strain, which was fully described in Figure 4.6 (e)

m = Stress-dependent coefficient, which may be obtained from Figure 4.6 (d) for a particular temperature

n = The exponent of the Findley Power Law, given as an average at a particular temperature

t = Time after loading

4.7 Determination of the Short–Term Effect of Temperature Variation on Fresh Specimens

To model the effect of temperature in the short-term, a form of Findley's Power Law was used similar to that used in modelling the effect of strain variation. To accomplish this, creep curves were plotted showing the variation of strain as a function of the time at the temperatures 30°C, 40°C and 50°C. In plotting each curve, the initial strain ε_o was deducted from the total strain. The resultant curves are shown in Figure 4.7 (a-c).

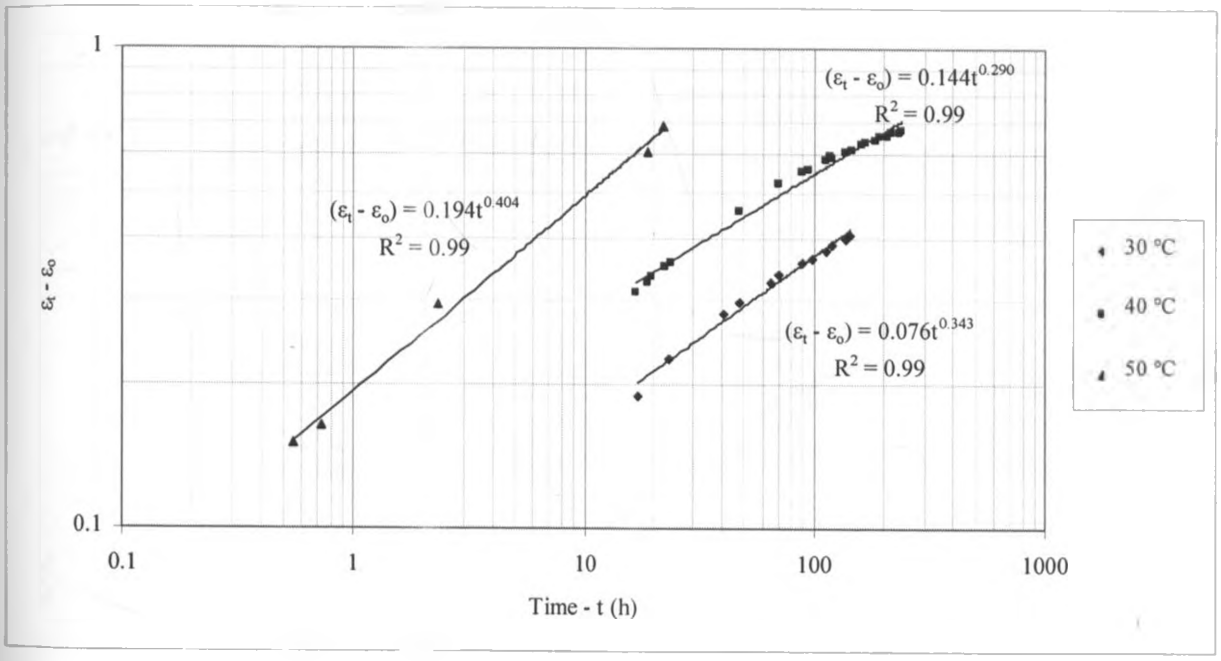

Figure 4.7 (a): Variation of strain with time at 0.78 MPa

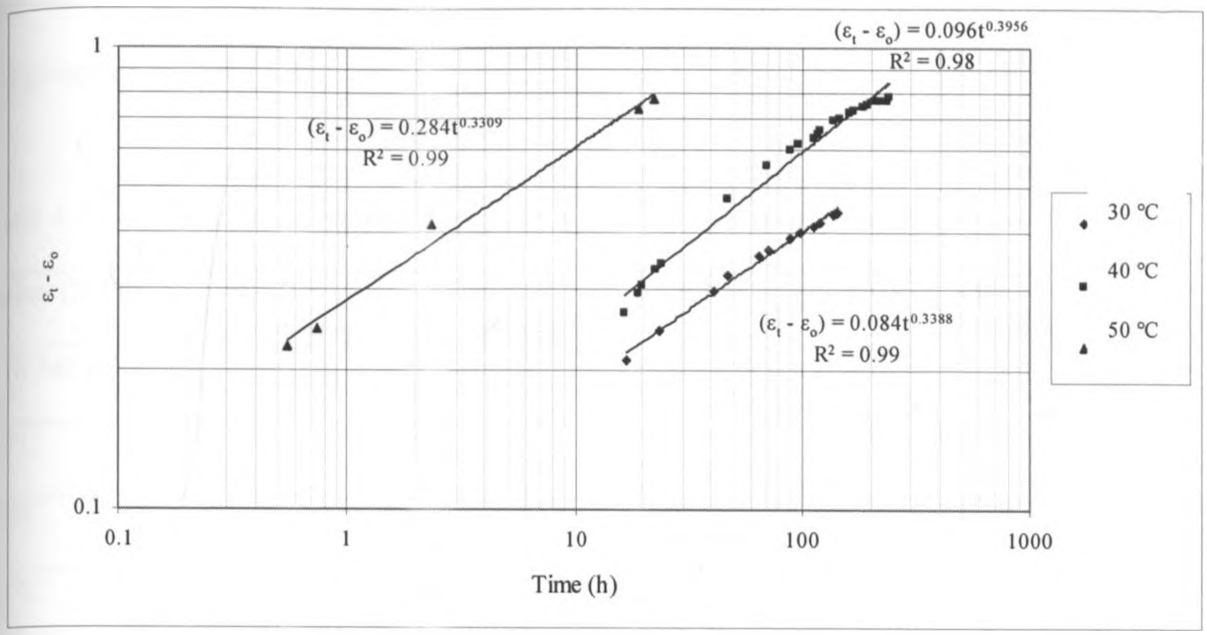

Figure 4.7 (b): Variation of strain with time at 0.94 MPa

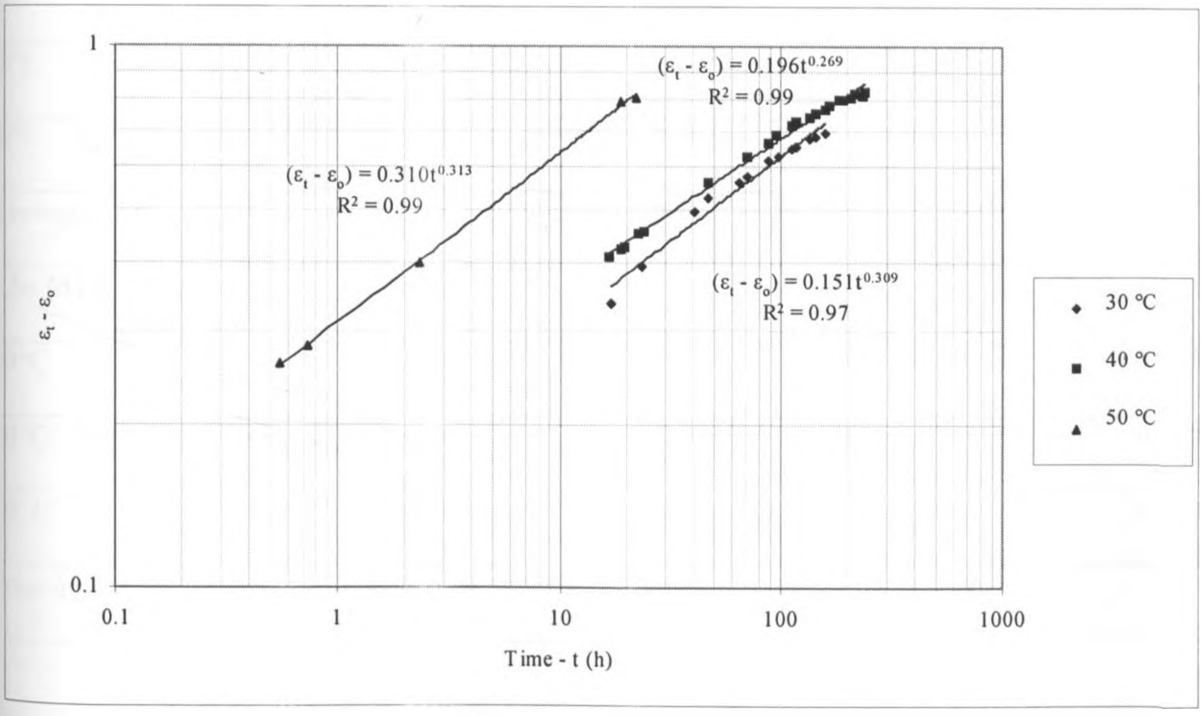

Figure 4.7 (c): Variation of strain with time at 1.56 MPa

From the curves in Figures 4.7 (a – c), values of the parameters m_T, n_T, ε_o and R^2 were obtained and presented in Table 4.3.

Table 4.3: Summary of the Findley Power Law parameters as temperature is varied

Stress (MPa)	m_T *(y-intercept)*	n_T *(gradient)*	ε_o	R^2 (Creep curve)
0.78 MPa				
30°C	0.076	0.343	0.542	0.986
40°C	0.144	0.290	0.968	0.986
50°C	0.194	0.404	1.306	0.995
Average of n_T		**0.346**	-	-
0.94 MPa				
30°C	0.084	0.339	1.001	0.992
40°C	0.096	0.396	1.168	0.983
50°C	0.284	0.331	1.934	0.990
Average of n_T		**0.355**	-	-
1.56 MPa				
30°C	0.151	0.309	1.135	0.973
40°C	0.196	0.269	1.607	0.993
50°C	0.310	0.313	2.139	0.999
Average of n_T		**0.297**	-	-

From Table 4.3., the curves were observed to have almost similar gradients. Hence the average value of the gradient, n_T was obtained at each stress level. The y-intercept (m_T), however was

observed to increase with temperature and the graphical presentation for this is given in Figure 4.7 (d).

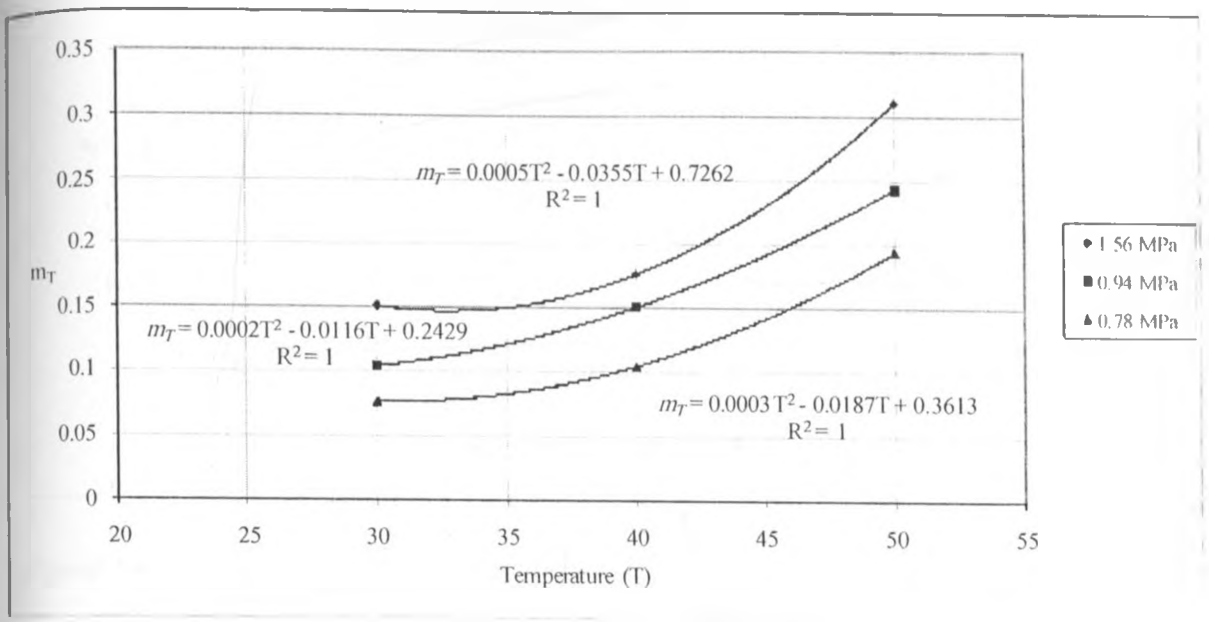

Figure 4.7 (d): Relationship between temperature (T) and the y-intercept (m_T)

The relationship between temperature and m_T was found to be more appropriately described by a second order polynomial relationship than a linear or other relationship. This was due to the fact that, between 30°C and 40°C, the difference in m_T is smaller than the difference between 40°C and 50°C. The values of R^2 are all unity but it must be emphasized that this accuracy may only be limited to the range of temperatures covered, that is, between 30°C and 50°C.

It was further noted that the time to attain ε_o increased with increase in temperature. It was therefore concluded that the best way in which the contribution both variables that feed into the constant ε_o could be captured was by plotting ε_o versus temperature divided by the time to attain the ε_o at the particular temperature as shown in Figure 4.7(e).

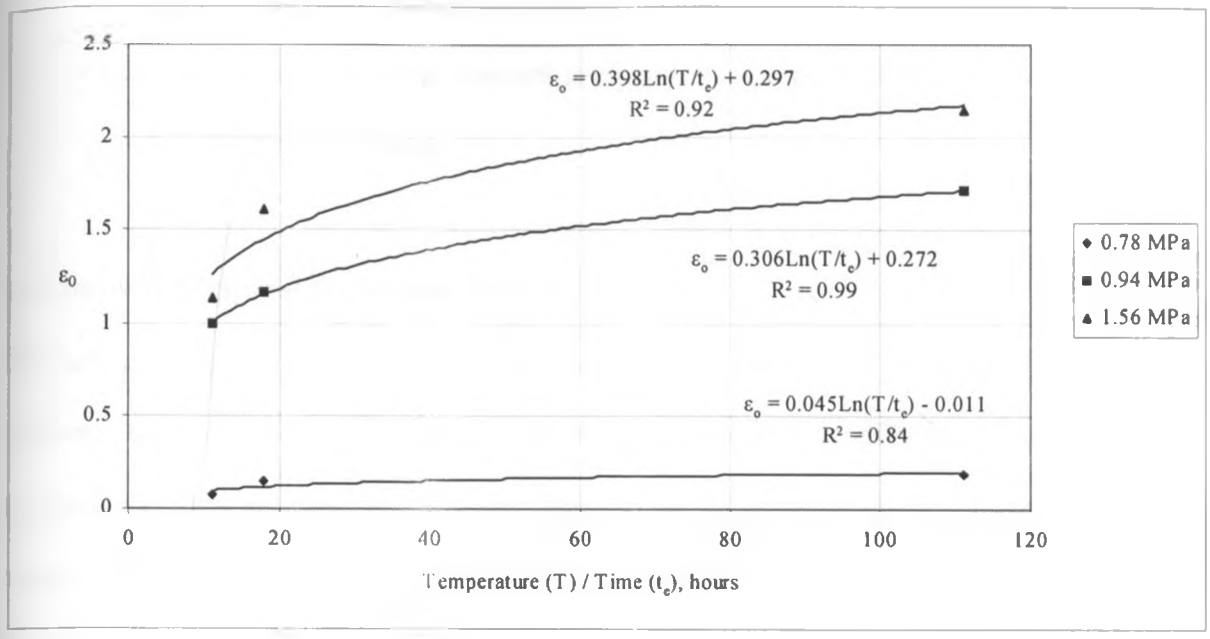

Figure 4.7 (e): Relationship between temperature/time and ε_o

Therefore, with the equation describing variation of creep strain with temperature and time presented in Equation 2.17, it is possible to predict the strain of the material at any temperature, and stress after a given length of time. To fully construct a creep curve from the model, the parameters in Equation 2.17 may be obtained and interpreted as follows:

$\varepsilon(T,t)$ = total time and temperature dependent strain

ε_o = stress-dependent initial strain which may be obtained from Figure 4.7 (e) given the temperature at which the creep is desired

m_{RT} = stress-dependent and temperature-dependent coefficient at reference temperature where the reference temperature is the expected temperature of operation. It may be obtained from Figure 4.7 (d) at the chosen reference temperature as a special case of m_T.

n_{RT} = stress independent material constant at reference temperature (obtained as n_T from

Table 4.2 as n_T at the reference temperature

n_T = stress independent material constant at elevated temperature obtained from Figure 4.7 (e) at the specific temperature

4.8 Constant Temperature Master Curves

The curves in Figures 4.7 (a – c) illustrate that once the initial strain in the first one hour was removed, the curves have a similar gradient and that it was possible to conduct Time-Temperature Superposition (TTSP) on them so as to obtain master curves. A reference temperature of 30°C was selected since the prevailing temperature to which the plastic lining material is normally exposed in the tropics is approximately 30°C. The curves obtained at 40°C and 50°C were then shifted to the 30°C curve and the resulting curves were the master curves at 0.78 MPa, 0.94 MPa and 1.56 MPa respectively presented in curves 4.8 (a – c).

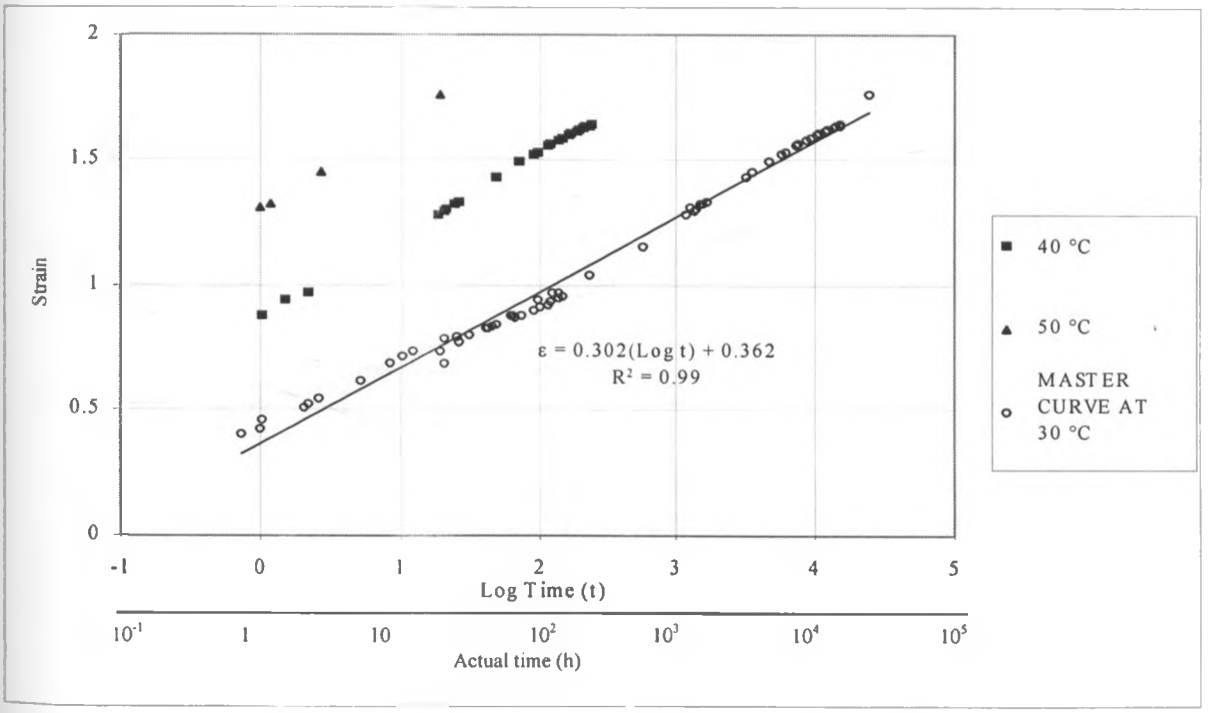

Figure 4.8 (a): Master curve at 0.78 MPa. at 30°C, shifting 40°C and 50°C creep curves

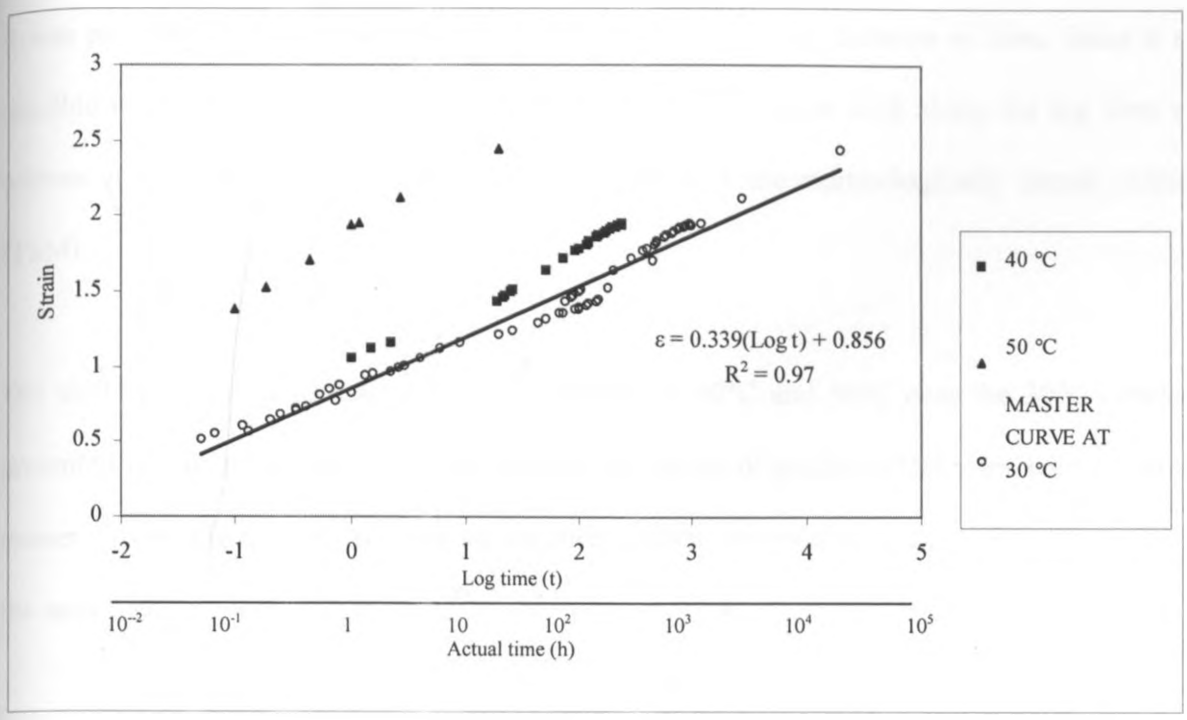

Figure 4.8 (b): Master curve at 0.94 MPa. at 30°C, shifting 40°C and 50°C creep curves

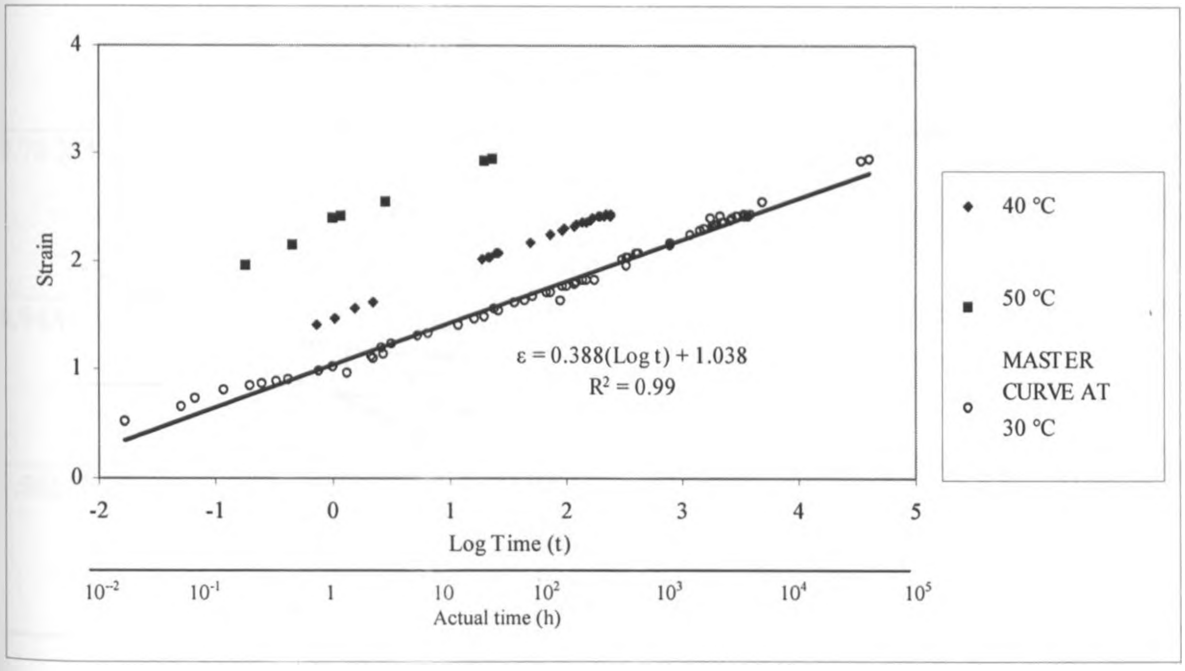

Figure 4.8 (c): Master curve at 1.56 MPa. at 30°C, shifting 40°C and 50°C creep curves

It was possible to predict properties of the material over a long duration of time. Since it was possible to generate master curve by applying only a horizontal shift along the log time axis without a vertical shift, the material is classified as a thermorheologically simple material (TSM).

The shift factors used to map the curves obtained at 40°C and 50°C onto the 30°C curve are presented in Table 4.4. The table also presents the values of gradients and y-intercepts from the master curves. Figure 4.8 (d) gives all the three master curves obtained at different stresses on the same axis.

Table 4.4: Summary of shift factors, gradients and y-intercepts from the constant temperature master curves

Applied Stress	**Property**	**Temperature**	
		40 °C	**50 °C**
0.78 MPa	Shift factor (a_T)	1.8	3
	Master curve gradient	0.302	
	Master curve y-intercept	0.362	
0.94MPa	Shift factor (a_T)	0.6	3
	Master curve gradient	0.339	
	Master curve y-intercept	0.856	
1.56MPa	Shift factor (a_T)	1.2	3.25
	Master curve gradient	0.388	
	Master curve y-intercept	1.038	

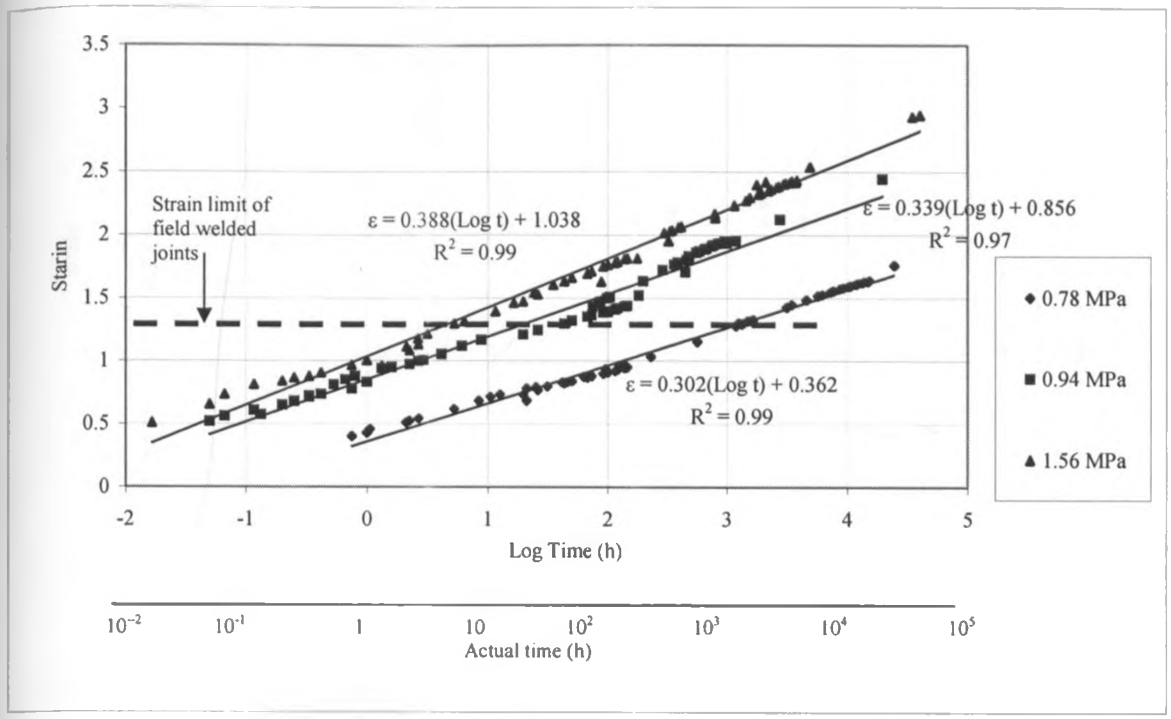

Figure 4.8 (d): Consolidated graph of master curves at 0.78 MPa, 0.94 MPa and 1.56 MPa.

Despite the possibility of predicting creep over long periods of time, the material may not last that long due to environmental factors that degrade the material. Also, the fact that the material is welded before use also causes further weakness in the material structure and may reduce its lifespan. In the proceeding sections, the various factors that limit the lifespan were analyzed so as to obtain a realistic lifespan when the material is exposed to all the degradation agents.

A comparison was made between the Findley Power Law and the master curve obtained from TTSP at 30°C and 0.94 MPa loading for a prediction of strain for about 50 years in Figure 4.8 (e). It was concluded that the two models were not very different. However, there was increased divergence for predictions over 10,000 hours. For prediction within 20 years, the expected service life of HDPE, the difference obtained is within acceptable limits.

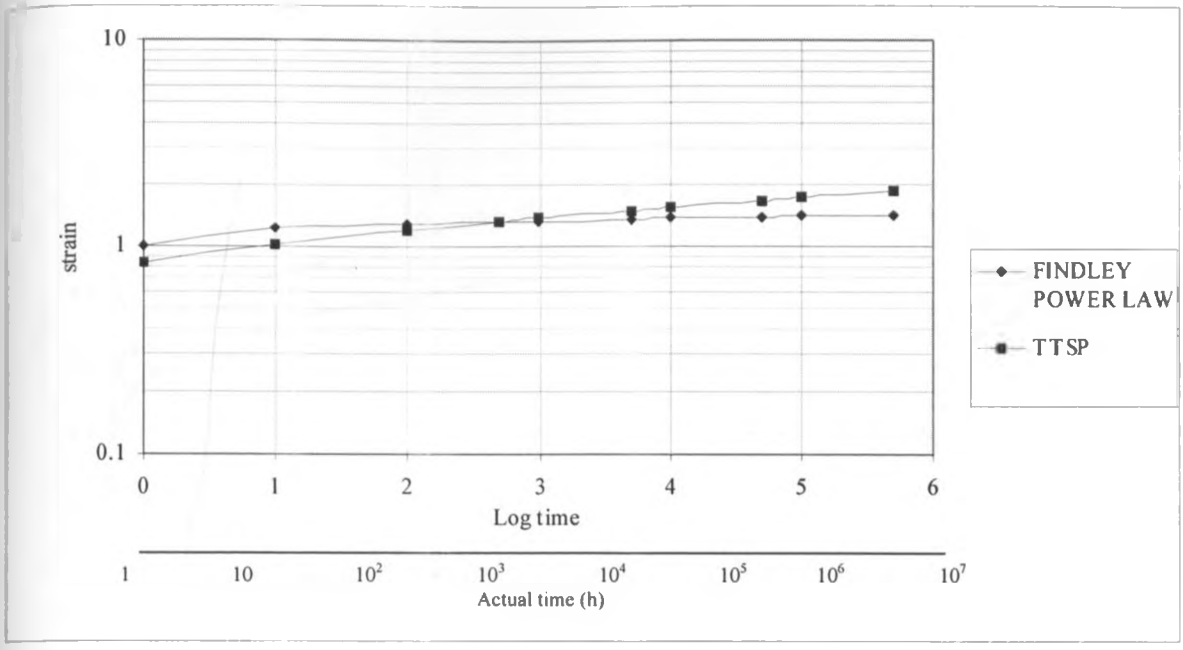

Figure 4.8 (e): Comparison of results obtained by Findley Power Law and TTSP

From Figure 4.8 (e), it was observed that for the short term, the Findley Power Law may be used to give better safety since it gives higher values of the predicted strain. For the long term, the TTSP curve gives higher values of predicted strain than those obtained from the Findley Power Law. Considering that recovery also plays a role in determining the strain over time, then the Findley Power Law may be giving more realistic values since the values of strain increase at a lower rate than those obtained by TTSP.

4.9 Creep Curves for Welded Specimens

Tests were done to determine the behaviour of test pieces with welded joints in tensile creep over time. In all instances the specimens obtained from the field failed at the welded joint. The failure was observed to result from shear between the welded surfaces. The curves of strain versus time for welded specimens under tensile creep are presented in Figure 4.9 (a - d).

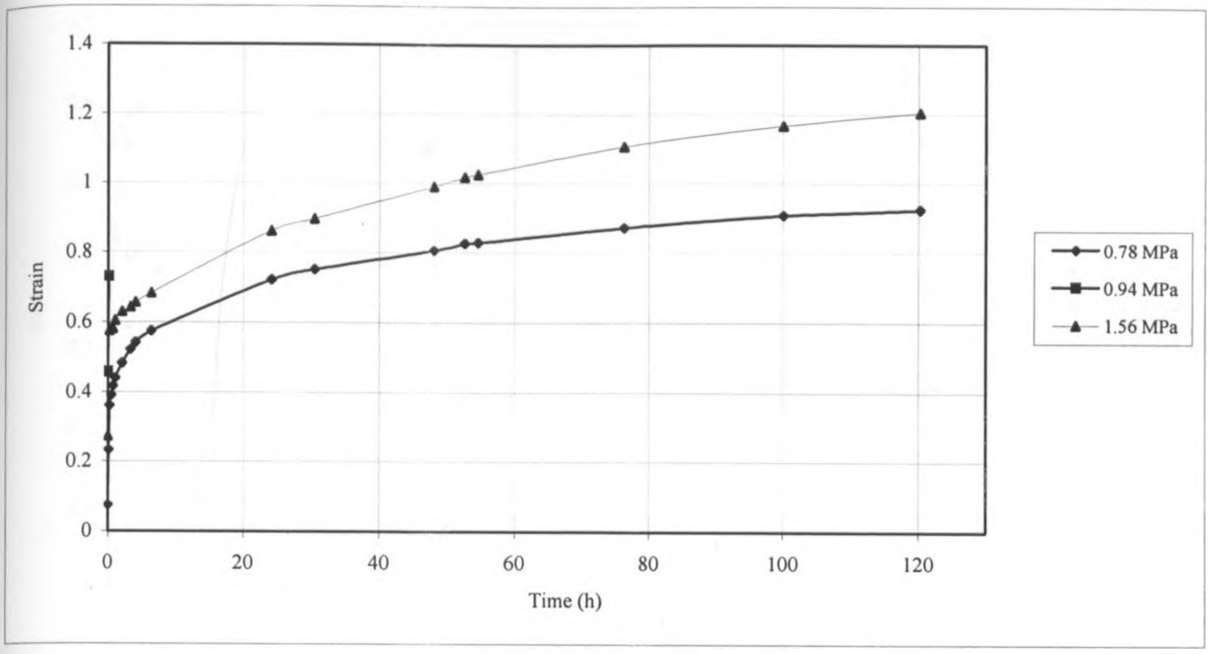

Figure 4.9 (a): Constant temperature field welded naturally degraded (7 years) creep curves at 30°c

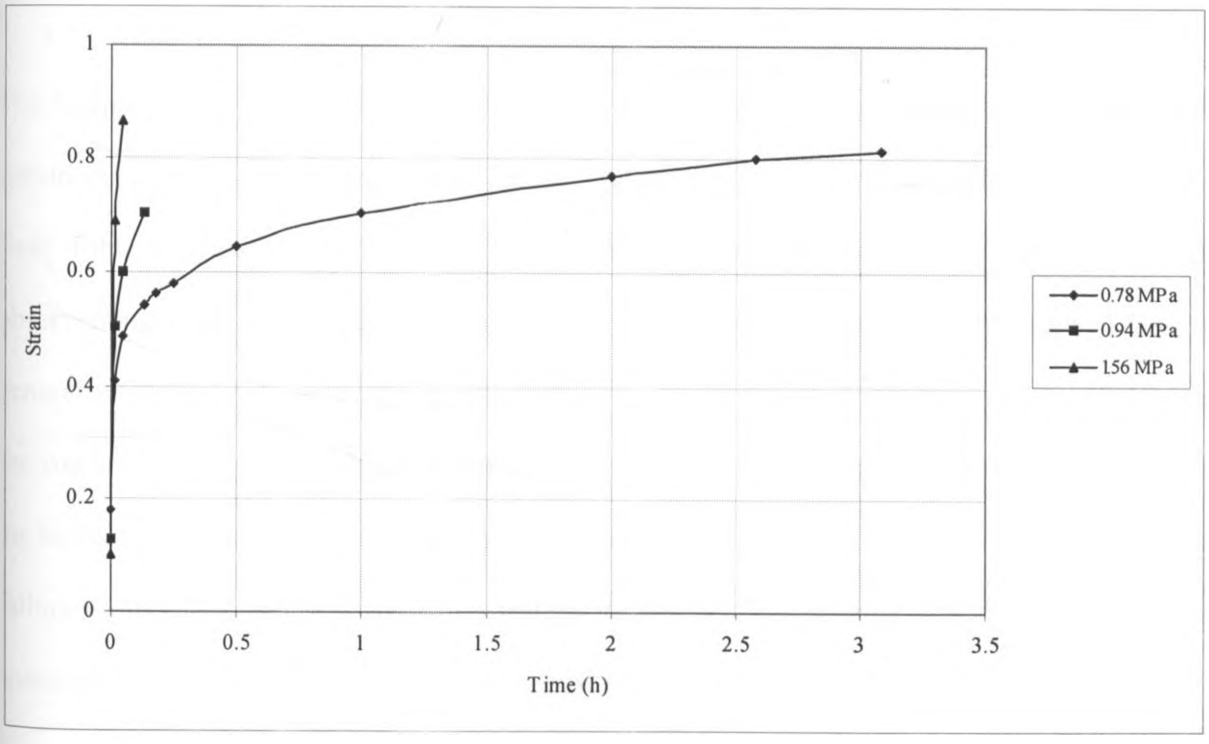

Figure 4.9 (b): Field welded fresh specimen creep curves at 40°C

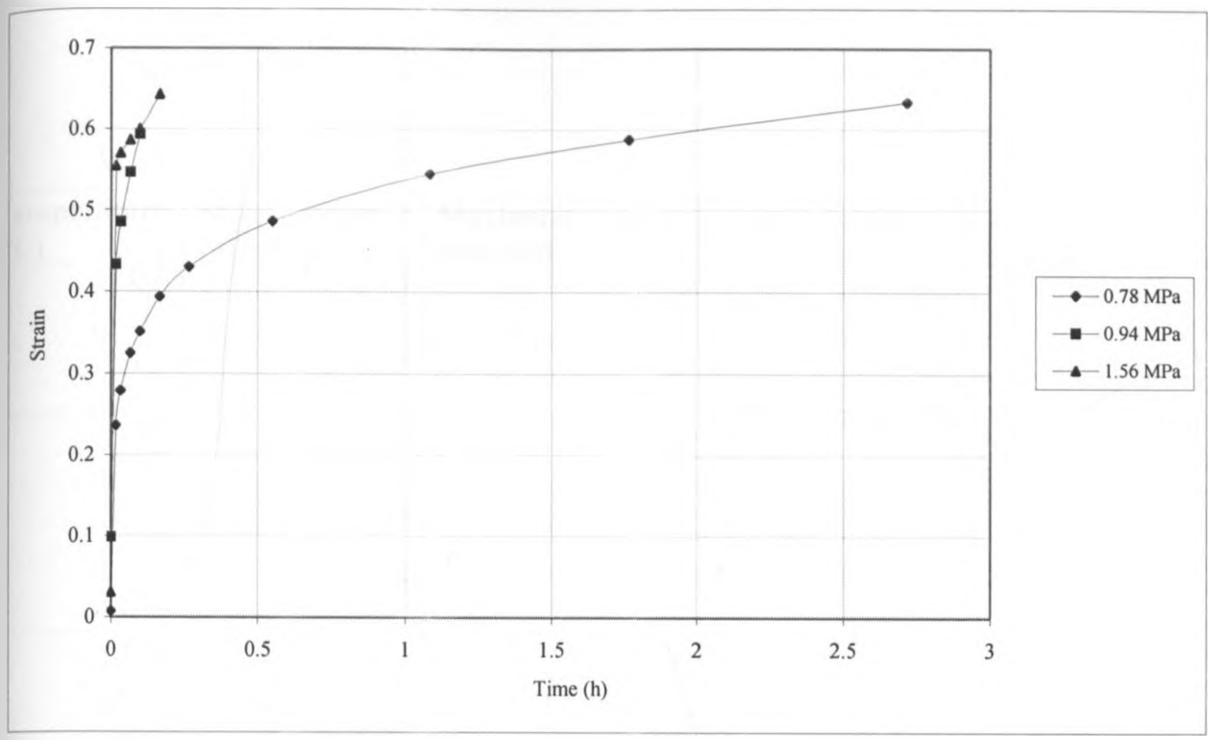

Figure 4.9 (c): Field welded fresh specimen creep curves at 50°C

The figures 4.9 (a – c) represent creep curves for specimens degraded naturally for 7 years, fresh specimens at 40°C and fresh specimens at 50°C respectively, all of which had been welded in the field. Table 4.5 gives a summary of the results obtained from figures 4.9 (a – c) as well as visual observations made. It was observed in all cases considered (Table 4.5) that the welded joint is generally a weak point. In all the experiments done, it was observed that the specimens failed on the welded joint and in much shorter times than in other experiments with clear specimens, with the highest time recorded being 120 hours and many of the specimens failing below 3 hours. The failure in all cases was in shear at the welded joint. This was an indication that in most of the specimens, complete fusion had not been attained during the initial welding.

Table 4.5: Summary of shift factors, gradients and y-intercepts from the constant temperature master curves

Temperature (°C)	Stress applied (MPa)	Maximum strain obtained	Time to failure (h)	Point of failure
30	0.78	0.9	120	Welded joint
	1.56	1.2	120	Welded joint
40	0.78	0.8	3.1	Welded joint
	0.94	0.7	0.2	Welded joint
	1.56	0.9	0.1	Welded joint
50	0.78	0.6	2.7	Welded joint
	0.94	0.6	0.1	Welded joint
	1.56	0.6	0.2	Welded joint

In all the curves, failure in welded specimens was seen likely to occur as the applied stress was increased. In all the curves, those specimens that were stressed at 0.78MPa persisted much longer than those loaded at higher stresses. The highest strain level attained for any welded specimen was 1.2. When this strain level (see dotted line in Figure 4.8 (d)) was superimposed on the master curves it was found that the material would fail at a maximum of 1 year (10,000 hours) when loaded at 0.78 MPa and a minimum of less than one hour when loaded at 1.56 MPa. It is clear that the welded joint is definitely a weak point in the installed dam liner exposed to tensile stresses.

With such high failure rates in welded joints, an alternative joining method was sought. But from literature (section 2.1.10) it was seen that it is even more difficult to join HDPE by adhesives than by welding due to the non-polar nature of polyethylene. Polyethylene is in fact listed in many sources as one of several plastics that cannot easily be joined by adhesives.

Since sources such as Aithani *et al* (2006) point to strengths of up to 80% in the welded joints, it seems that the reason for such low strains in samples obtained from the field is poor workmanship that resulted in weak welded joints. The feasible remedy is therefore factory welding of the dam liner before transportation to the field for installation. Alternatively, field welding may be done under controlled conditions particularly with regard to the welding temperature to ensure that the material is in a semi-molten state during the operation, the time and magnitude of pressure applied. It was also noted that the width of the welded joints obtained from the field was relatively small, about 1.3 cm. This had been listed by Aithani *et al.* (2006) as another constraining factor on the strength of the welded joint apart from welding temperature, applied pressure and pressure dwell time.

Further tests were done in an attempt to find the conditions under which the strongest weld may be attained in HDPE. In the tests, the following parameters, earlier investigated by other researchers and found not to be significant beyond certain reasonable levels were held constant:

- Rate of heat application at 1cm/s for a width of 2.6 cm. and length of 10 cm. for hot knife welding and 10 s. of heating of the surfaces to be welded in the oven for hot air welding.
- Magnitude of pressure applied at 0.3 MPa. Pressure higher than 0.3 MPa was observed to deform the specimen.

- Dwell time of the applied pressure at 60 seconds followed by natural cooling to room temperature.

The results for hot air welding while holding the width of the weld, applied pressure and dwell time of the pressure constant at 2.6cm, 0.3 MPa and 60 s. respectively are presented in Table 4.6.

Table 4.6: Effect of temperature on the strength of hot air welded joints

Temperature (°C)	**Peel test result (Failure strength and description)**	**Conclusion**
135	0.5 MPa - Readily failed at the welded lap joint in shear	Despite being the welding point, a weak weld is formed with incomplete fusion. There is need to increase temperature.
150	1 MPa - Readily failed at the welded lap joint in shear	Weak weld with incomplete fusion
160	1 MPa - Readily failed at the welded lap joint in shear	Weak weld with incomplete fusion, slightly stronger than previous welds
165	2 MPa - Readily failed at the welded lap joint in shear	Weak weld with incomplete fusion, still stronger than previous welds
170	5 MPa - Failed at the welded lap joint in shear	Strong weld but still with almost complete fusion
175	9 MPa - Failed at the welded joint in shear	Strong weld but still with almost complete fusion. There was now need to increase the temperature by units of 1 °C
176	11 MPa - Failure outside the welded joint, while the welded joint remained intact for five specimens tested	Complete fusion was attained at this temperature
177	The exposed section of the material melted very fast and was easily distorted. No readings were taken from the damaged specimen.	It was difficult to obtain a weld at this temperature
178	The exposed section of the material melted very fast and was easily distorted	Any further increase in temperature would only cause distortion in the material structure due to excess heat and the tests were stopped

In hot air welding, particular attention was given to the width of the weld, which was doubled to 2.6 cm. It was also necessary to find the temperature of air that would cause the material to melt. Temperature was progressively increased from 135 °C (the average melting point of HDPE) upwards with very weak welds obtained up to 176 °C. At 176 °C, it was found that there formed enough welded material to form a strong joint within at the constant conditions specified. This was higher than the melting point of the plastic, (135 °C) to supply latent heat required for melting in a relatively short time of 10 s. and due to the inefficiency of convection heat transfer from the hot air to the plastic. Any temperature below 176°C was not capable of melting enough material to obtain the required fusion at the specified constant conditions. The simple peel test suggested by Aithani et al (2006) was used to determine whether the joint formed was strong enough. Failure (peeling) at the welded joint suggested a weak joint and failure away from the welded joint denoted a strong joint where complete fusion had occurred. In all the tested specimens prepared by hot air fusion at 176°C, failure occurred outside the welded joint.

The hot knife welding technique was also tested. The detailed results for the tests on the hot air welding technique are presented in Table 4.7. A flat bar of width 2.6 cm was heated in an oven to a constant temperature and used to weld two flaps of the lap joint together by sliding the flat bat between them at high temperature. The flat bar was incubated in an oven to acquire the required working temperature before being used for welding. It was found that at temperatures below 350°C of the flat bar, it was not possible to obtain a well fused joint at the constant conditions, since the degree of melt and quantity of molten material yielded was not adequate to create a strong joint as determined by the peel test.

Table 4.7: Effect of temperature on the strength of hot knife welded joints

Temperature (°C)	Peel test result (MPa)	Important observations	Conclusion
135(mp)- 350	1.5 (Average)	Readily failed at the welded joint in shear. Almost no melting of the material. The knife tended to stick to the material and caused distortion.	While the knife has been heated to the material melting point, a lot of the heat is lost to raise the temperature of the material from room temperature to its melting point. The knife must be significantly hotter than the melting point of the material.
360	2	Failed at the welded lap joint in shear Stickiness of the knife still experienced	Weak weld with incomplete fusion
370	2	Failed at the welded lap joint in shear Stickiness of the knife still experienced	Weak weld with incomplete fusion
380	5	Failed at the welded lap joint in shear Stickiness of the knife still experienced	Weak weld with incomplete fusion
390	8	Failed at the welded lap joint in shear slight stickiness experienced	Strong weld with almost complete fusion. There was now need to increase the temperature by units of 1 °C
400	11	Failed outside the lap joint. No stickiness of the knife experienced	Failure outside the welded joint indicates a strong weld. This was the best result that was obtained.
401	-	Beyond 400 °C the material began to burn and the surface was too damaged to be welded	It was not possible to obtain a results beyond 400 °C

Another problem at temperatures below 350°C was the fact that the hot bar tended to stick to the material, making it difficult to obtain a joint with even dimensions. This indicated that the heat energy stored by the hot knife was not adequate to maintain the material in the molten state long enough. The material therefore solidified and adhered to the knife. Temperatures between 350°C and 400°C may be described as transitory since there was still stickiness of the knife and the joints were not completely fused but the joints formed were much stronger than those formed

below 350°C. However, when the bar was heated at 400°C, the sticking of the bar was no longer experienced instead the material melted readily and produced adequate melt to sustain a strong joint. Heating the flat bar beyond 400°C, resulted in the material burning and puncturing as the flat bar was slid through the joint. This indicates a need for good temperature control during welding.

The results of tensile tests on specimens made by the hot knife welding method are presented in Table 4.1 alongside other tensile test results and the creep test in Figure 4.9 (d).

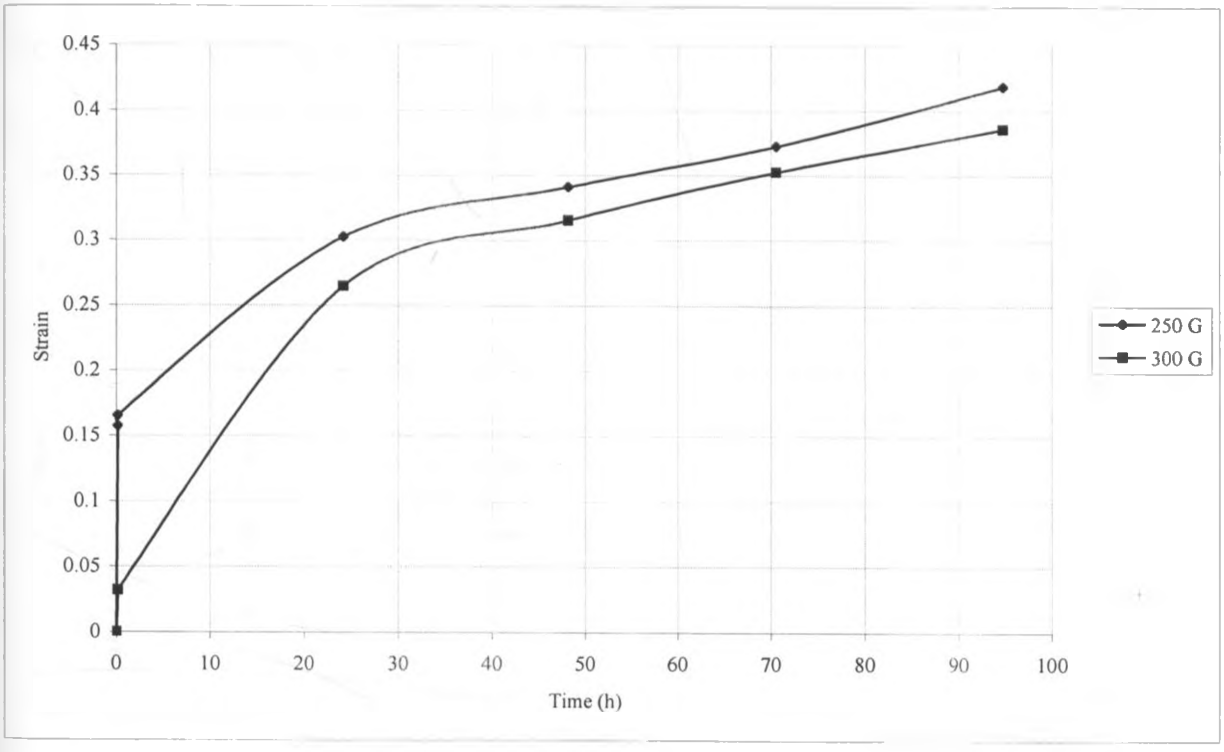

Figure 4.9 (d): Laboratory welded fresh specimen creep curves at room temperature

The strains in Figure 4.9 and Table 4.1 for welded joints are relatively lower than other results in the same table as a result of the increased thickness of the welded specimen (almost twice) the as

a result of the lap joint. The shape of the creep curve at the beginning of the creep test in Figure 4.9 is also not as steep as the other curves due to the increased specimen thickness. It was concluded from these results that to obtain a strong joint, the temperature that will cause adequate melting by conduction or convection must be met by the agent causing melting. It was also observed that stronger joints are obtained with larger widths of the welded joint.

4.10 Alternating Temperature TTSP for Fresh Specimens

Figure 4.10 (a – d) represent the creep curve for the three levels of stress with temperature being alternated between 20°C and 30°C, between 30°C and 40°C, between 40°C and 50°C and between 50°C and 60°C respectively.

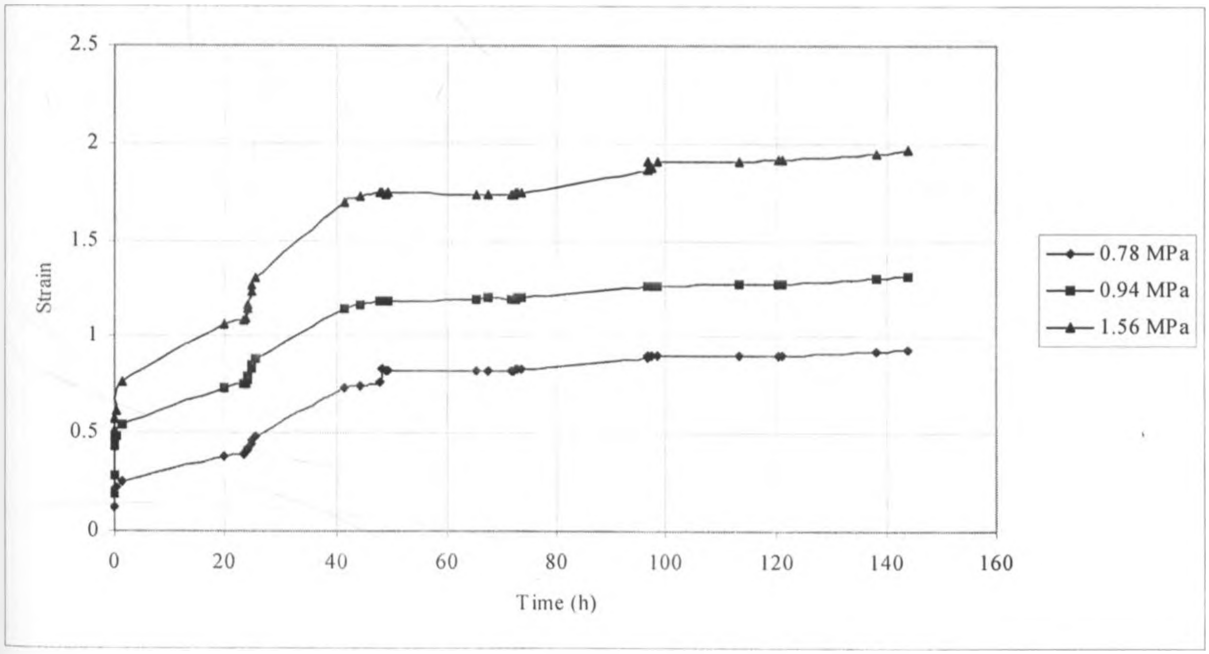

Figure 4.10 (a): Creep curve for alternating temperature between 20°C and 30°C

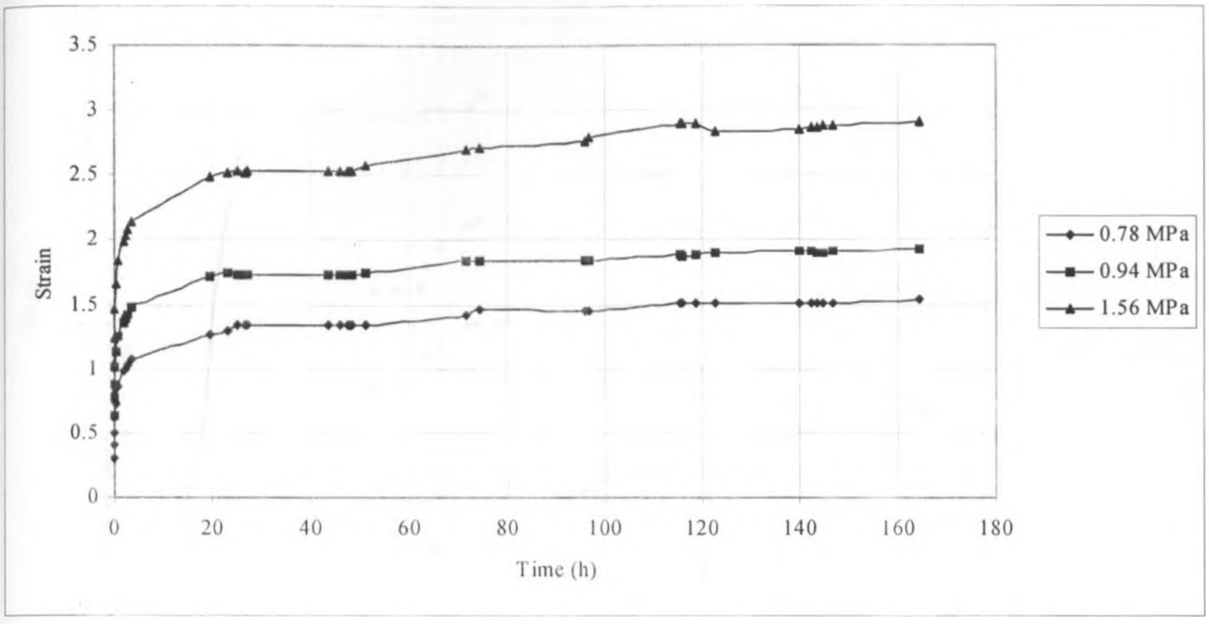

Figure 4.10 (b): Creep curve for alternating temperature between 30°C and 40°C

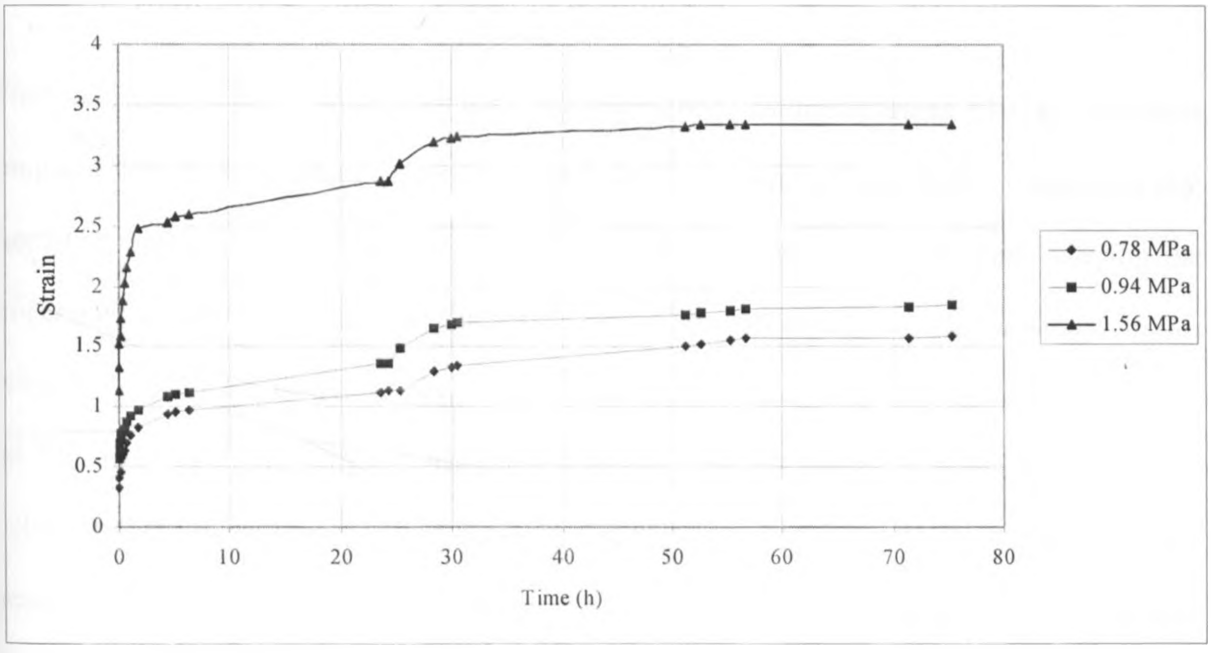

Figure 4.10 (c): Creep curve for alternating temperature between 30°C and 40°C

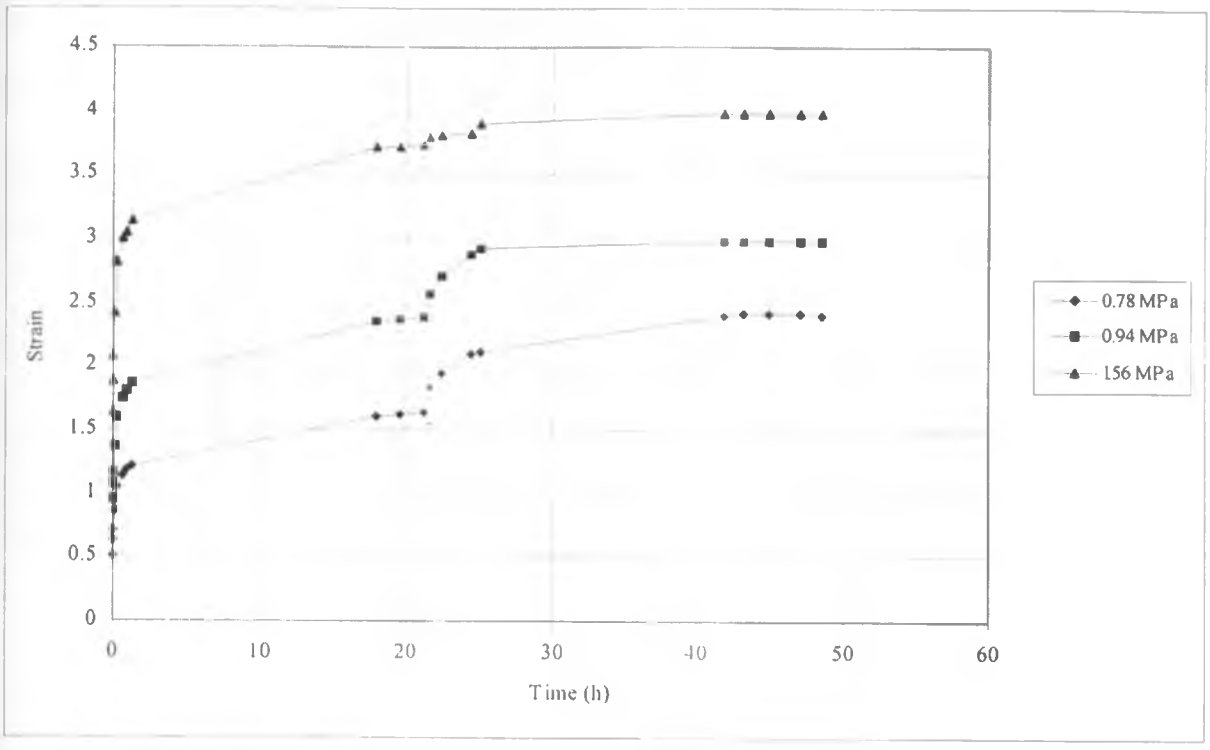

Figure 4.10 (d): Creep curve for alternating temperature between 50°C and 60°C

When the values of creep strains attained at alternating temperatures (Figures 4.10 (a) – (c)) were compared with those obtained at constant temperature (Figures 4.5 (a) – (c)) , it was clear that alternating temperature during loading resulted in greater values of strain than keeping the temperature constant. For example, in Table 4.4, it was observed that the maximum strains recorded at 30°C were almost similar to those obtained by cycling the temperature between 20°C and 30°C over a 24 hour period. It had been expected that since there would be decreased strain at 20°C, then the overall strain would decrease. The essence of this experiment was to answer the question as to whether the alternating tropical temperatures (high temperatures in the day and low temperatures at night) had a greater effect on material properties than just elevated temperature. From Table 4.5, it was observed that in most of the temperatures at which testing

was done, the tests at alternating temperature had bigger strains than those carried out at constant temperature at similar stress levels in tensile creep.

Table 4.6: Comparison of strains obtained at constant temperature with those obtained under alternating temperature

Constant Temperature				**Alternating Temperature**			
Applied stress (MPa)	0.78	0.94	1.56	Applied stress (MPa)	0.78	0.94	1.56
Temp (°c)	Maximum strain			Temp (°c)	Maximum strain		
30	0.9	1.4	1.8	30 (average between 20 – 40)	1.2	1.6	2.4
40	1.7	1.9	2.4	40 (average between 30 – 50)	1.6	1.9	3.1
50	1.9	2.5	3.0	5 (average between 50 – 60)	2.0	2.5	3.6

After creep experiment, the specimens that had been stressed were monitored to get readings for recovery. These are presented for specimens subjected to stress at constant temperature and those stressed at alternating temperature. The results are presented in Figures 4.11 (a) and (b).

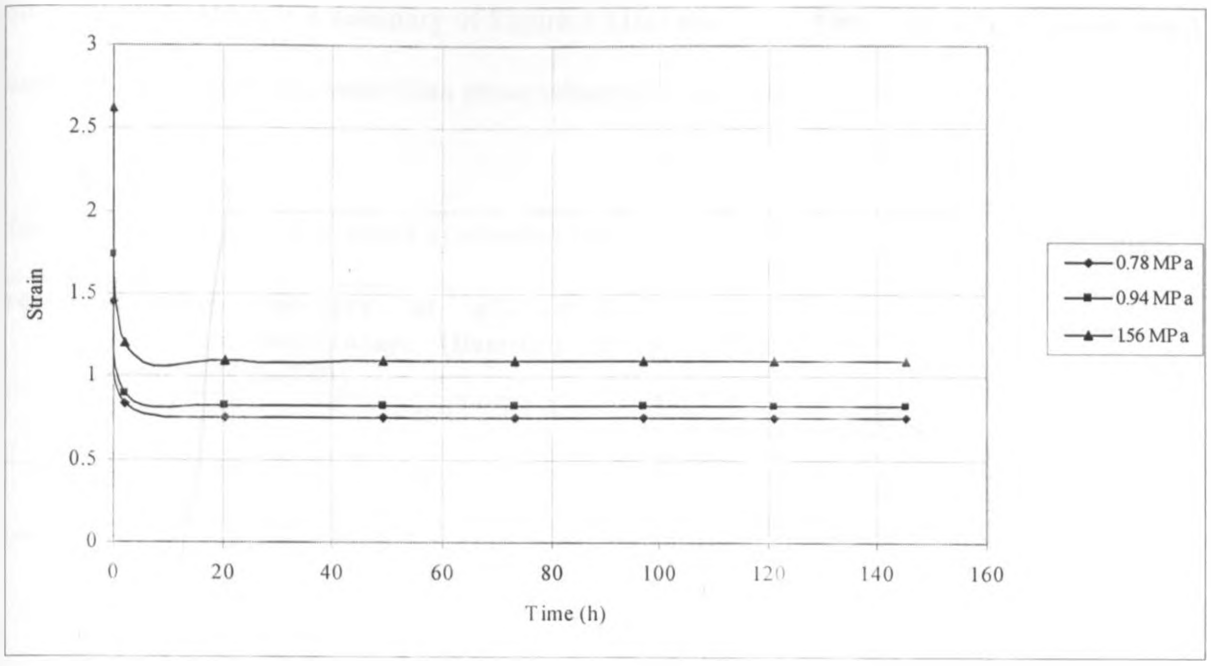

Figure 4.11 (a): Creep recovery for fresh specimens stressed at 30°C

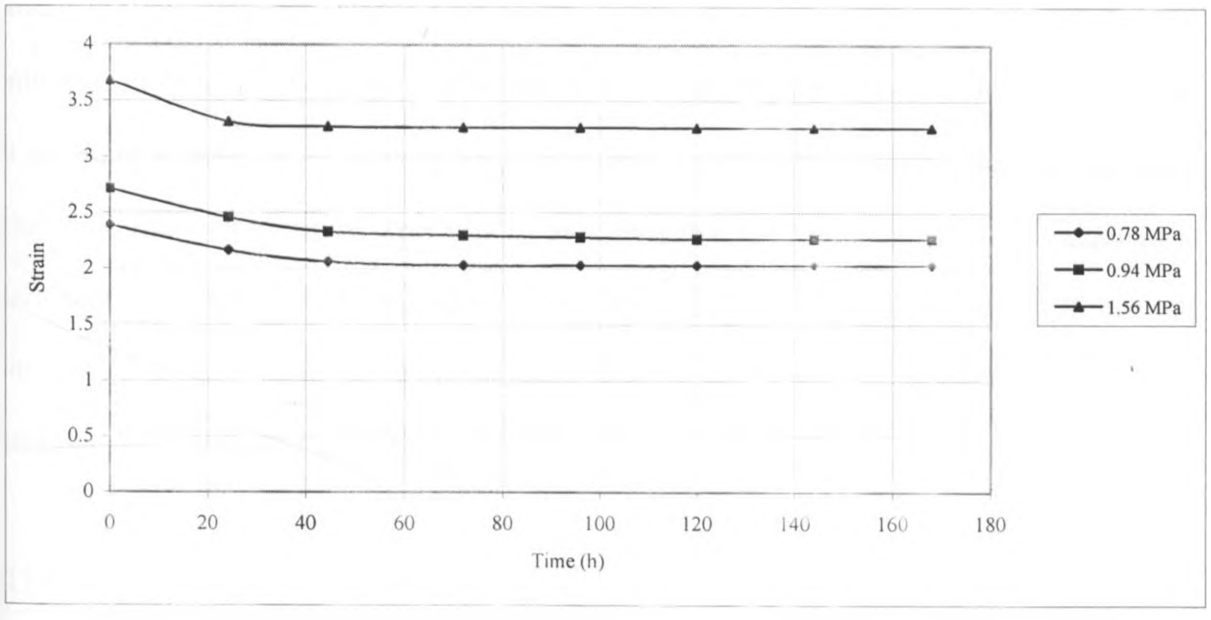

Figure 4.11 (b): Creep recovery for fresh specimens stressed at alternating temperature between 30°C and 40°C

From Table 4.7 (which is a summary of Figure 4.11(a) and (b)) the recovery of specimens tested at constant temperature is greater than those subjected to alternating temperature.

Table 4.7: Comparison of recovery at constant temperature and under alternating temperature

Stress level (MPa)	**Recovery at alternating temperature (Between 30 and 40)**	**Recovery at constant temperature (30 °C)**
0.78	0.3	0.7
0.94	0.4	0.9
1.56	0.4	1.4

The net result of the observations is that: alternating temperature results in higher creep strain and lower recovery than constant temperature when the load is removed is that there is more damage in the specimens exposed to alternating temperature. In practical terms, after the application of equal levels of creep stress and both specimens allowed sufficient time to recover, the specimen exposed to alternating temperature was observed to be longer than the specimen tested at constant temperature. This was an indication that the specimen which was exposed to alternating temperature had undergone more plastic than elastic deformation. It may be concluded that alternating temperature resulted in more damage to the plastic lining' than operation at constant temperature.

4.11 Constant Temperature TTSP for Naturally Degraded Specimens

The resulting creep curves for experiments on naturally degraded specimens are presented in Figures 4.12 (a - c). For purposes of comparison, creep curves of fresh specimens are superimposed on the curves.

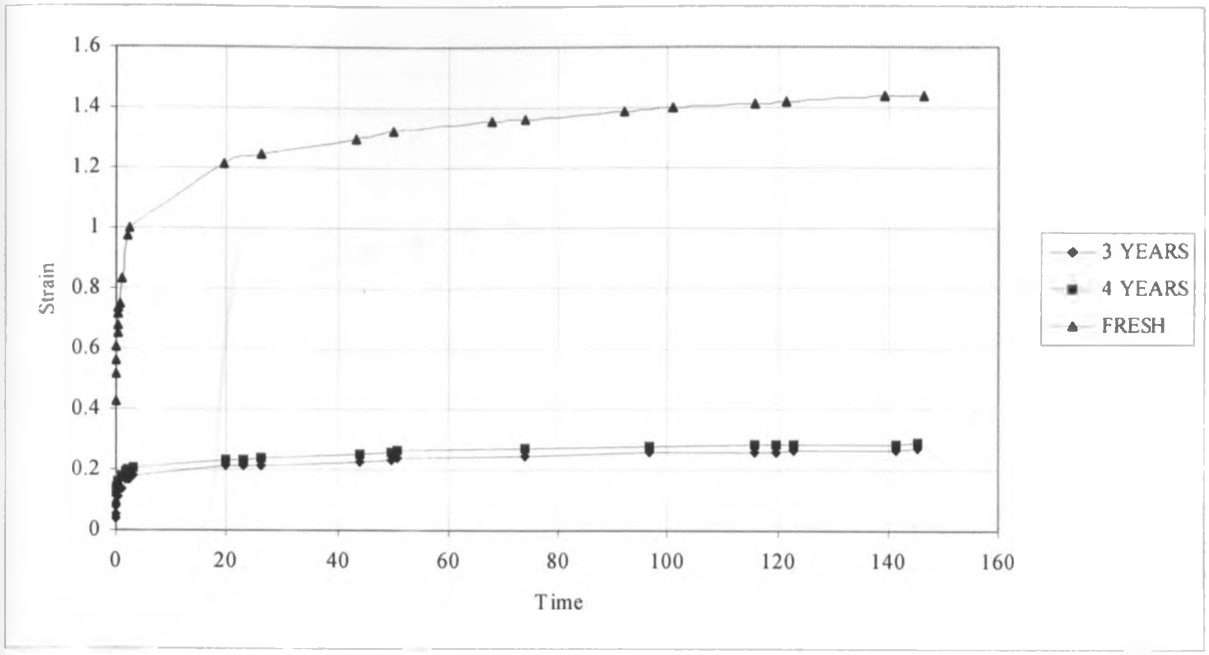

Figure 4.12 (a): Constant temperature creep curves for caturally degraded specimens, 30°C and 0.94 MPa

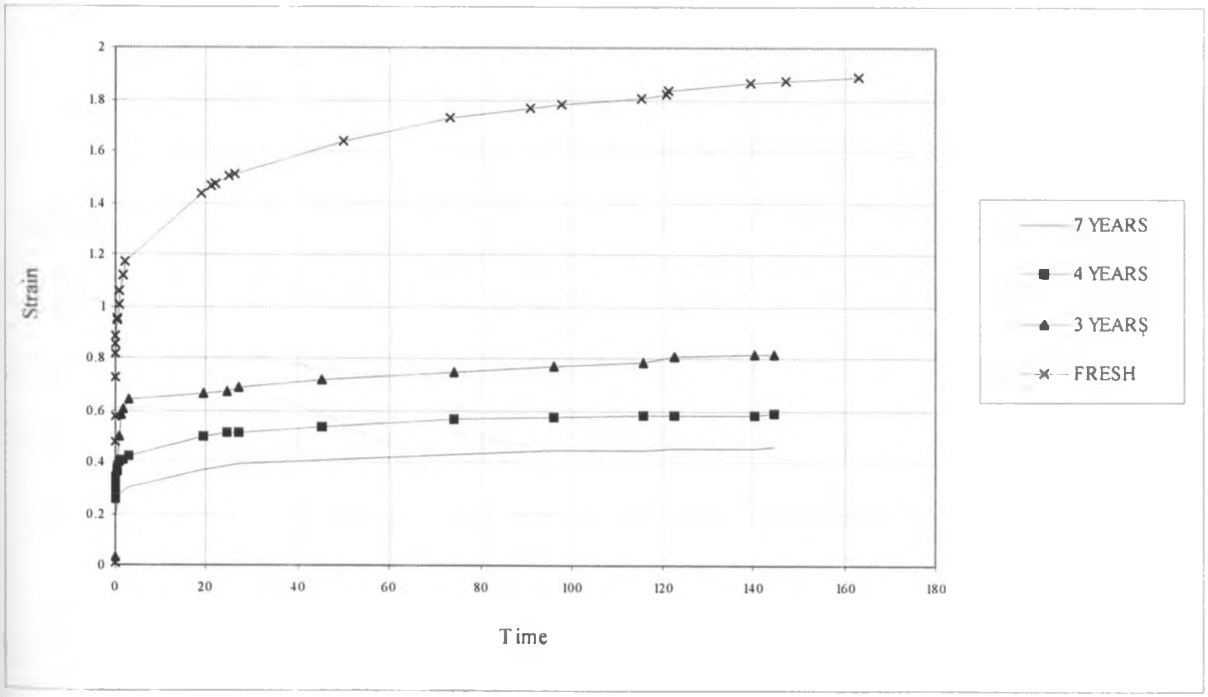

Figure 4.12 (b): Constant temperature creep curves for naturally degraded specimens, 40°C and 0.94 MPa

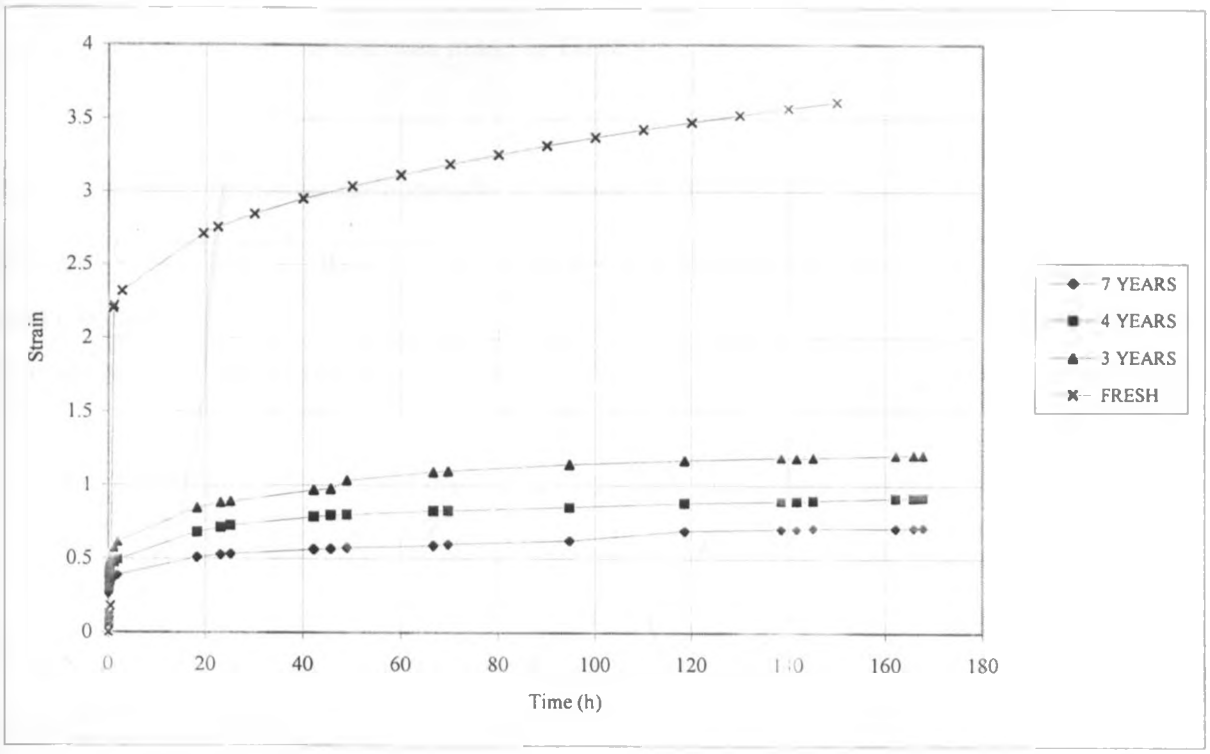

Figure 4.12 (c): Constant temperature creep curves for naturally degraded specimens, 50°C and 0.94 MPa

It is clear from the creep curves that the fresh specimens attained much higher strain values than specimens already exposed to natural degradation. It is also noted that natural degradation is high between 0 and 3 years and then slows down thereafter, in a manner very similar to exponential decay. This can be concluded from the fact that the difference in the strain attained for fresh specimen and the 3-year specimen is much higher than the strain attained between the 4-year and 7-year specimen.

In an attempt to find a relationship between the strain in naturally degraded specimens and the years of natural degradation, the results of the creep test were considered after 140 hours of

testing when the rate of deformation was deemed to be stable. The summary of the strains achieved by the various specimens was made in Table 4.8.

Table 4.8: Summary of strains for naturally degraded specimens after 140 hours of creep

Duration of exposure (years)	**0**	**3**	**4**	7
Temperature	Strain recorded after 140 hours of testing			
30	1.42	0.30	0.28	
40	1.90	0.80	0.60	0.43
50	3.51	1.25	0.90	0.70

In Figure 4.12 (d), duration of time over which the specimen had been exposed to natural degradation was designated t_d and the strain (ε_t) against which it was plotted is the total strain. That is, the strain from which the initial strain (ε_o) was not subtracted.

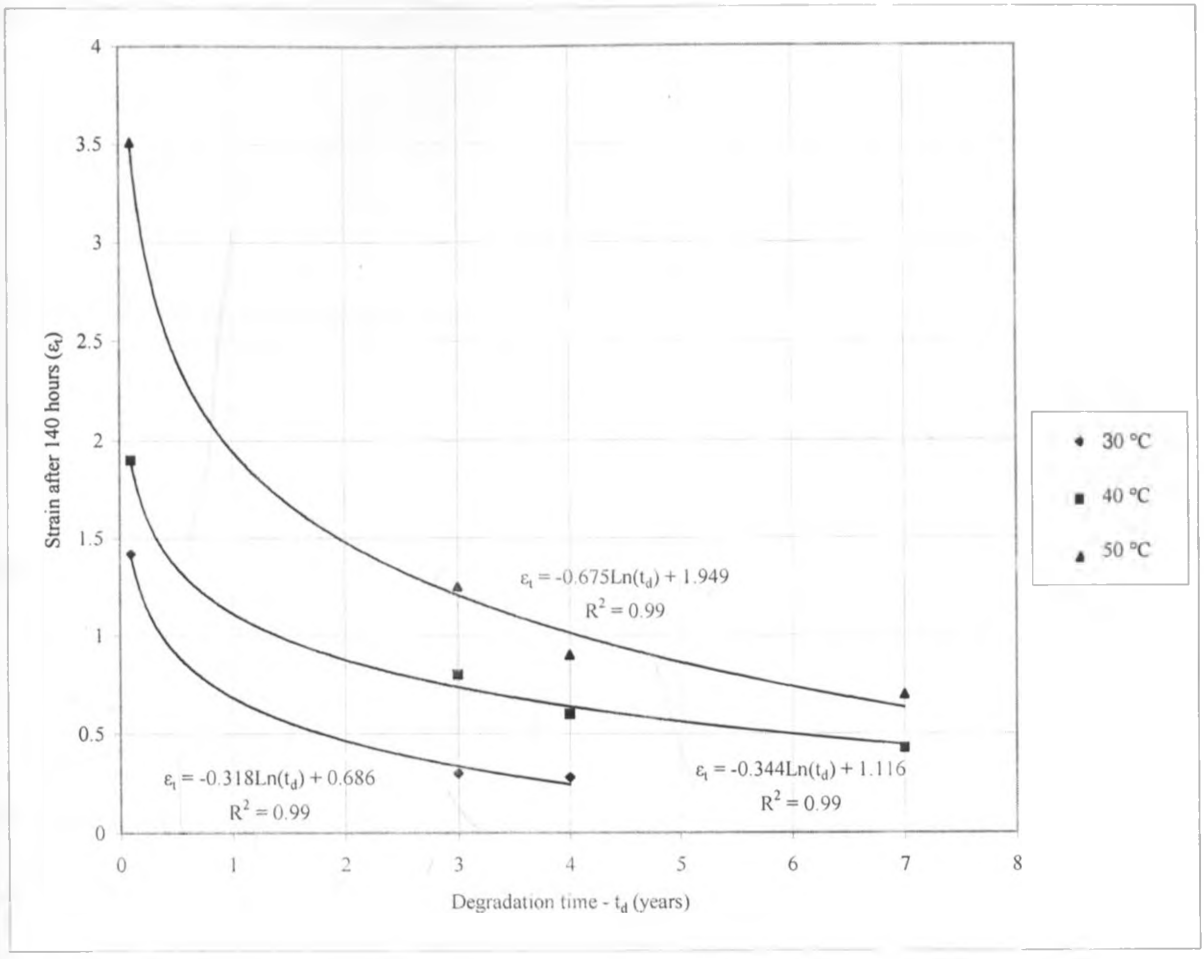

Figure 4.12 (d): The strains of naturally degraded specimens after 140 hours of tensile creep test at different temperatures

The curves obtained were fitted using a logarithmic relationship that can be rearranged to form an exponential decay relationship between the strain and the degradation time. For example, the logarithmic relationship obtained at 40° was:

$$\varepsilon_t = -0.344\ln(t_d) + 1.116 \qquad \text{.....[4.1]}$$

Where the parameters in equation [4.1] may be generalized to read:

$$\varepsilon_t = n_d \ln(t_d) + m_d \quad \text{.....[4.2]}$$

Equation [4.2] may be rearranged to read:

$$t_d = Ce^{\frac{\varepsilon_t}{n_d}} \quad \text{.....[4.3]}$$

Where:

$$C = e^{\frac{-m_d}{n_d}} \quad \text{.....[4.4]}$$

From Equation [4.3] it is possible to predict the expected lifetime of the plastic reservoir after setting the limits for ε_t. The limiting ε_t is the maximum strain in the tensile test for specimens that do not have welded joints (obtained from Table 4.1) and the limit in welded joints is the maximum strain in welded joints (obtained from Figures 4.9 (a) – (c)). From Figure 4.12(d), the values of n_d and m_d were summarized in Table 4.9 for ease of extrapolation.

Table 4.9: Summary of values of n_d and m_d for use in extrapolation between temperatures (for 140 hours)

Temperature	n_d	m_d
30	-0.318	0.686
40	-0.344	1.116
50	-0.675	1.949

Curves with similar decay equations were obtained at 80, 100 and 120 hours. Equation [4.3] is therefore proposed for use to predict the service life (t_d) of the HDPE dam liner. A similar curve was also obtained by plotting maximum strain values obtained from Table 4.1 against the time naturally degraded specimens were exposed to the natural environment and yielded a high value of R^2 presented in Figure 4.12 (e).

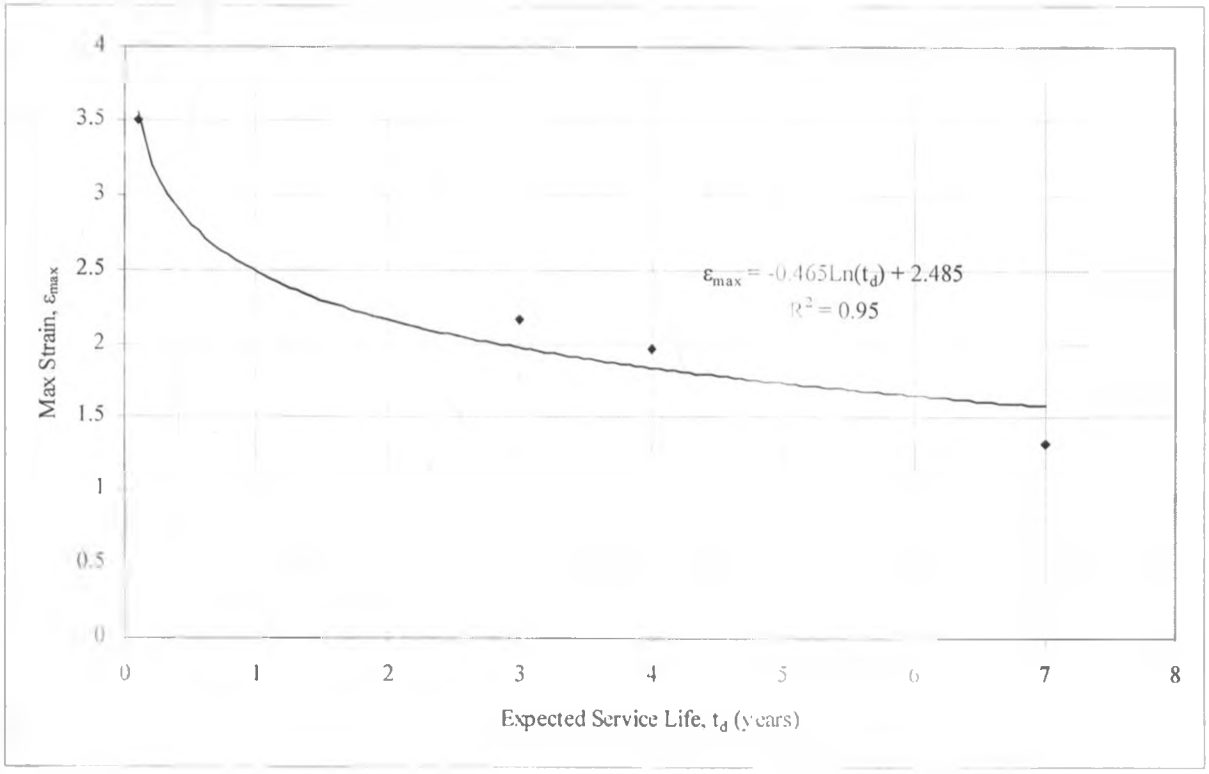

Figure 4.12 (e): The maximum strains of naturally degraded specimens in tensile test at room temperatures

Equation [4.3] can be considered to be a generalized relationship that combines the effect of all the degradation factors to which the material was exposed. It therefore encompasses all the degradation agents identified in Chapter 2 including elevated temperature, hydrolytic degradation, alternating temperature and UV radiation. A recommendation is made to segregate

the effect of the individual degrading agents acting simultaneously using the principle that decay by two or more modes may be represented by the general decay law as presented in literature.

A quantity may decay via two or more different processes simultaneously. In general, these processes often called "decay modes", "decay channels", "decay routes" have different probabilities of occurring, and thus occur at different rates in parallel. The total decay rate is given by the sum of the decay routes; thus, in the case of two processes or more processes, Equation [4.3] may be adapted to read:

$$t_d = Ce^{\frac{\varepsilon_t}{n_d}} = Ce^{(\frac{\varepsilon_{d1}}{n_{d1}} + \frac{\varepsilon_{d2}}{n_{d2}} + \ldots\ldots + \frac{\varepsilon_{dn}}{n_{dn}})} \quad \ldots\ldots\ldots [4.5]$$

Equation [4.5] applies for n different degrading agents and C may be expanded appropriately. Such an equation would predict the expected lifetime of HDPE lining under different conditions.

CHAPTER 5: CONCLUSIONS AND RECOMMENDATIONS

5.1 Conclusions

The following conclusions were made from the study. It was concluded that:

1. The tensile strength of the material increases with time of exposure to natural degradation, while the density and the maximum tensile strain decreases with time of exposure to natural degradation.
2. At constant stress over long periods of time, failure of the material results from the inability of the material to creep and not from inadequate strength.
3. The onset of the tertiary stage of creep in the material increases with temperature
4. The short and long term creep properties are accurately predicted by the Findley Power Law and Time-Temperature Superposition (TTSP)
5. Exposing the liner to alternating temperature results in higher degradation than exposing the liner to constant temperature.
6. Degradation of the liner is most active during the first few months of installation.
7. The welded joint of samples collected from the field is the weakest point in the liner. The strength of the welded joint may be improved by correct selection of welding parameters (width of welded joint, joining pressure, dwell time of the pressure and temperature).

5.2 Recommendations

While the research answered some questions regarding the mode of degradation of HDPE plastic liner and its service life, there are several issues that still need to be addressed so as to achieve better understanding of the material. It was observed during the course of this project that the liner shrinks substantially when exposed to the natural degradation agents. It is recommended

that research should be undertaken in this line so as to determine the rate of shrinkage and its causes.

It is also recommended to conduct further research to breakdown the exponential decay law proposed in Equation 4.5 to determine the effect of each degrading agent and to find out which is the most destructive. This would help to determine where most preventive care needs to be applied.

It is recommended for more research to be conducted with regard to developing welding devices that can satisfy the optimum conditions demonstrated in the laboratory during field welding, particularly with regard to temperature and pressure control.

REFERENCES

Aithani, D., H. Lockhart, R. Auras and K. Tanprasert, 2006. Predicting the Strongest Peelable Seal for 'Easy-Open' Packaging Applications, Journal of Plastic Film & Sheeting, Vol. 22, Pp 247-263, October 2006

Alwis, K. G. N. C. and C. J. Burgoyne, 2006. Time-Temperature Superposition to determine the Stress-Rupture of Aramid Fibres, Preprint, University of Cambridge, United Kingdom.

ASTM D1693-2007a. Standard Test Method for Environmental Stress-Cracking of Ethylene Plastics, ASTM International, West Conshohocken, PA, www.astm.org.

ASTM D2990-1995. Tensile Compressive and Flexural Creep and Creep Rupture of Plastics, ASTM International, West Conshohocken, PA, www.astm.org.

ASTM D638-2003 Standard Test Method for Tensile Properties of Plastics, ASTM International, West Conshohocken, PA, www.astm.org.

Baragiola, R. A., 1999. Class Notes, Materials Science, University of Virginia, http:// www.virginia.edu / bohr /mse102.

Barbero, E. J. and J. J. Michael, 2003. Time-Temperature-Age Viscoelastic Behavior of Commercial Polymer Blends and Felt Filled Polymers, www.mae.wvu.edu/barbero/pdf (Accessed in January 2008).

Beckmann, J., G.B. McKenna, B.G. Landes, D.H. Bank and R.A. Bubeck, 1997. Physical Aging Kinetics of Syniotactic Polystyrene as Determined from Creep Behaviour, Polymer Engineering and Science, Vol. 37, No. 9, Pp 1459-1468, September 1997.

Beijer, J.G.J. and J.L. Spoormaker, 1997. Viscoelastic Behaviour of HDPE Under Tensile Loading, Proceedings of the Yield and Fracture of Polymers Conference, Cambridge, U.K.

British Plastics Federation, 1981. Weathering of Plastic Materials in the Tropics - Part 6: Further Evaluation of a Solar Radiation Concentrating Device (EMMA) as a means of Accelerating the Weathering of Plastics, Propellants, Explosives and Rocket Motor Establishment, Joint Committee on Behaviour of Plastics Materials under Tropical Conditions, Waltham Abbey, Essex

Chung, T.J., 1988. Continuum Mechanics, Prentice Hall, New Jersey, U.S.A.

Corneliussen, R. D., 2002. Properties - High Density Polyethylene (HDPE), Http://Www.Maropolymeronline.Com / Properties (Accessed On 8-1-2008)

Crawford, R.J., 1998. Plastics Engineering, Elsevier, Butterworth Heinemann, UK.

Dally, J.W. and W.F. Riley, 1985. Experimental Stress Analysis. McGraw Hill Book Company, Tokyo.

Donald, A. M., 2004. Viscoelasticity, www.polymerfsg.tripod.com/pdf/viscoelasticity.pdf (Accessed on 8-1-2006).

Earthodyssey, 2007. Recycling Symbols, http://www.earthodyssey.com/symbols.html (Accessed in January 2008)

Eleni, Z., 1998. Investigation of Ageing Factors on Polymers and Composites, www.mae.wvu.edu / barbero /pdf (Accessed in January 2008)

Feller, R.L., 1994. Accelerated Aging: Photochemical and Thermal aspects, Edwards Bros., Ann Arbor, Michigan, USA.

Fung, Y. C., 1972. Stress Strain History Relations of Soft Tissues in Simple Elongation, in Biomechanics, its Foundations and Objectives, ed. Fung, Y. C., Perrone, N. and Anliker, M., Prentice Hall, Englewood Cliffs, NJ.

Gates, T. S. and M. A. Grayson, 1998. On the Use of Accelerated Aging Methods For Screening

High Temperature Polymeric Composite Materials, American Institute of Aeronautics and Astronautics: 99-1296, Pp. 925-935, Vol. 2

Grassie, N. and G. Scott, 1985. Polymer Degradation and Stabilization, Cambridge University Press, London.

Gumbe, L.O., 1993. An Introduction to the Mechanical Properties of Building Materials. Text Book Manuscript, Department of Environmental and Biosystems Engineering, University of Nairobi.

Hsuan, Y. G., 2003. Protocol for 100 Years Service Life of Corrugated High Density Polyethylene Pipes: PART II - Stress Crack Resistance, Oxidation Resistance and Viscoelastic Properties of Finished Corrugated Pipes, Florida Department of Transportation.

Idol, J. D. and R.L. Lehman, 2004. Polymers (Chapter 12) in The CRC Handbook of Mechanical Engineering, 2nd Ed. Edited by F. Kreith and Y. Goswami, CRC Press. London.

Illinois Tool Works, 2007. Plexus Guide to Bonding Plastics, Composites and Metals, www.itwplexus.com (Accessed in May 2008)

Johnson, G. A., G. A. Livesay, S. L-Y. Woo and K. R. Rajagopal, 1996. A Single Integral Finite Strain Viscoelastic Model of Ligaments and Tendons, ASME Journal of Biomechanical Engineering, Vol. 118, pp. 221-226.

Kay, D., E. Blond and J. Mlynarek, 2007. Geosynthetics Durability: A Polymer Chemistry Issue, 57th Canadian Geotechnical Conference Proceedings.

Kenya Rainwater Association, 2004. Progress Report on Ndeiya Karai Project, Kenya Rainwater Association .

Kolarik, J., A. Pegoretti, L. Fambri and A. Penati, 2003. Prediction of Nonlinear Long-Term

Creep of Heterogeneous Blends: Rubber Toughened Polypropylene – Poly(styrene-co-acrylonitrile), Journal of Applied Polymer Science, Vol. 88, 641-651, Wiley Periodicals.

Kwan, M. K., T. H.C., Lin, and S. L.Y. Woo, 1993, On the Viscoelastic Properties of the Anteromedial Bundle of the Anterior Cruciate Ligament, Journal of Biomechanics, Vol. 26, pp. 447-452.

Lai, J. and A. Bakker, 1995. Creep and Relaxation of Nonlinear Viscoelastic Materials, Polymer Engineering Science, No. 35, Pp1339-1347.

Lee, A. and G. B. McKenna, 1997. Anomalous Aging in Two-Phase Systems: Creep and Stress Relaxation Differences in Rubber-Toughened Epoxies, Journal of Polymer Science, B: Polymer Physics, 35: 1167–1174, 1997, John Wiley & Sons Inc.

Mase, G.E., 1990. Theory and Problems of Continuum Mechanics, Schaums Outline Series, McGraw Hill, New York, USA.

Morgan, R., C. Dunn and C. Edwards, 2003. Effects of Creep and Relaxation in Gap Analysis for Durability of Fiber Reinforced Polymer Composites in Civil Infrastructure 6 (1). Characterization of Polyethylene with Differential Scanning Calorimetry, (DSC) and Dynamic Mechanical Analysis (DMA) Www.Benelux-Scientific.Com/Foto/Netzsch-09-2005-03.Pdf (Accessed On 8-1-2008)

Netzsch Applications Laboratory Newsletter, 2005. Characterization of Polyethylene with Differential Scanning Calorimetry, netzsch.co.kr/admin/board. (Accessed in August 2006)

O'Connell, P. A. and G. B. Mckenna, 1997. Large Deformation Response of Polycarbonate: Time-Temperature, Time-Aging Time, and Time-Strain Superposition, Polymer Engineering and Science, September 1997, Vol. 37, No. 9.

Onyango, D.M., 2003. Women at the Source of Life: The Experience of Kenya Rainwater Association, FAO Dimitra Newsletter, No. 8, October 2003, Brussels, Belgium.

Peggs, I.D. and M.F., Kanninen, 1995. HDPE Geosynthetics: Premature Failures and their Prediction, *Geosynthetics International*, Vol. 2, No. 1, pp. 327-339.

Pioletti, D. P., L. R. Rakotomanana, J. F. Benvenuti, P. F. Leyvraz, 1998. Viscoelastic Constitutive Law in Large Deformations: Application to Human Knee Ligaments and Tendons. J Biomech, 31(8):753-757.

Plastics Pipe Institute, 2008. Handbook of PE Pipe, http://plasticpipe.org / publications / pe handbook. html (Accessed in January 2008).

Reddy, D. V. and J. Fluet, Jr., 1995. The Effect of Compressive Creep on the Structural Integrity and Drainage Capacity of Landfill Lining Systems, Florida Atlantic University Publication.

Reed, P.H., 2003, Creep Response of FIRE and Other Burning Plasma Experiments, Proceedings of Symposium on Fusion Engineering, Atlantic City.

Rowe, G.M., M.J. Sharrock, M.G. Bouldin and R.N. Dongré, 2003. Advanced Techniques to Develop Asphalt Master Curves from the Bending Beam Rheometer, Petroleum and Coal, Vol. 43, No.1, Pp 54-59.

Salerni, C., 2007. Adhesive Technologies For the Assembly of Hard-to-Bond Plastics, Technical Briefs - Issue No.4, www.akd-tools.gr /xmsAssets/ File/ Catalogues/ USA/ Hard-To_Bond_Plastics.pdf (Accessed in May 2008)

Sigmaaldrich, 2008. Aldrich Polymer Products Applicaton & Reference Information, www.Sigmaaldrich.Com / Img/ Assets/ 3900/ Thermal Transitions of Homopolymers.Pdf (Accessed On 8-1-2008)

Smith, K.J., 2005. Compression Creep of a Pultruded E-Glass/Polyester Composite at Elevated Service Temperatures, M. Sc. Thesis, Georgia Institute of Technology.

Thermal Analysis and Rheology, 2007. Application of Time-Temperature Superposition Principles to DMA, Thermal Analysis Application Brief, Number TA-144, http://www.tainst.com (Accessed in January 2008).

Thornton, G. M., A. Oliynyk, C. B. Frank, and N. G. Shrive, 1997, Ligament Creep Cannot be Predicted from Stress Relaxation at Low Stress: A Biomechanical Study of the Rabbit Medial Collateral Ligament, J. Orthop. Research., Vol. 15, pp. 652-656.

Timoshenko, S.P. and J.N. Goodier, 1983. Theory of Elasticity, McGrawHill, New York.

Tolba, M.K., O.A. El -Kholy, E.EL-Hinnawi, M.W. Holdgate, D.F. McMichael and R.E Munn, 1992. The World Environmental 1972-1992 (pp158-182, pp247-280) UNEP, Chapman & Hall, London.

UNEP, 2003. Water – 2 Billon People are Dying for it, United Nations Environmental Programme, http://www.unep.org / wed / 2003 / keyfacts.htm (Accessed in June 2006)

Veazie, D.R. and T.S. Gates, 2004. Physical Effects on the Compressive Linear Viscoelastic Creep of IM7/K3B Composite, Langley Research Centre, Hampton, Virginia, www.nasa.org.

Wu, C., 2000. Long Term Performance of Polymers, www.me.umn.edu / divisions/ design/ composites/ Projects/ Polymer

APPENDIX 1

Illustration of the use of the lifespan predictive equations

Given an outdoor application of the HDPE plastic liner at a temperature of 45°C and the maximum expected strain is 1, the expected lifetime may be computed as follows:

From Table 4.9, obtain interpolated values of n_d and m_d as -0.5095 and 1.5325 respectively. Then find the value of the constant C from equation 4.4 as:

$$C = e^{\frac{-1.5325}{-0.5095}} = 20.2438$$

Then from equation 4.3, the expected lifetime t_d may be calculated from equation 4.3 using $\varepsilon_t = 1$ and $n_d = -0.5095$ as follows:

$$t_d = Ce^{\frac{\varepsilon_t}{n_d}} = 20.2438 \times e^{\frac{1}{-0.5095}} = 2.8 years$$

This value may be confirmed from the curves in Figure 4.12 (d). If there was more than one variable then equation 4 5 would be used in a similar manner.